AD-A089 314 ARMY MATERIEL SYSTEMS ANALYSIS ACTIVITY ABERDEEN PROV--ETC F/G 12/1
PROCEEDINGS OF THE MEETING OF THE SPECIAL INTEREST GROUP ON CON--ETC(U)
MAY 80 H E COHEN

UNCLASSIFIED NL

1 OF 2
AD A089314

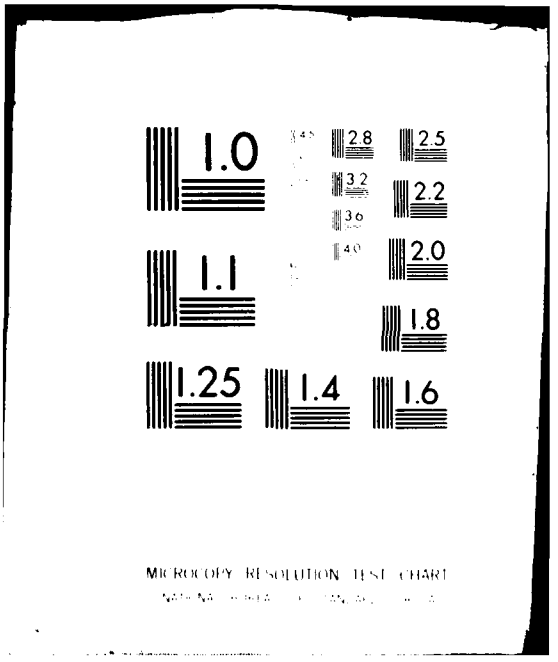
1.0
2.8
2.5
3.2
2.2
3.6
4.0
2.0
1.1
1.8
1.25
1.4
1.6
MICROCOPY RESOLUTION TEST CHART

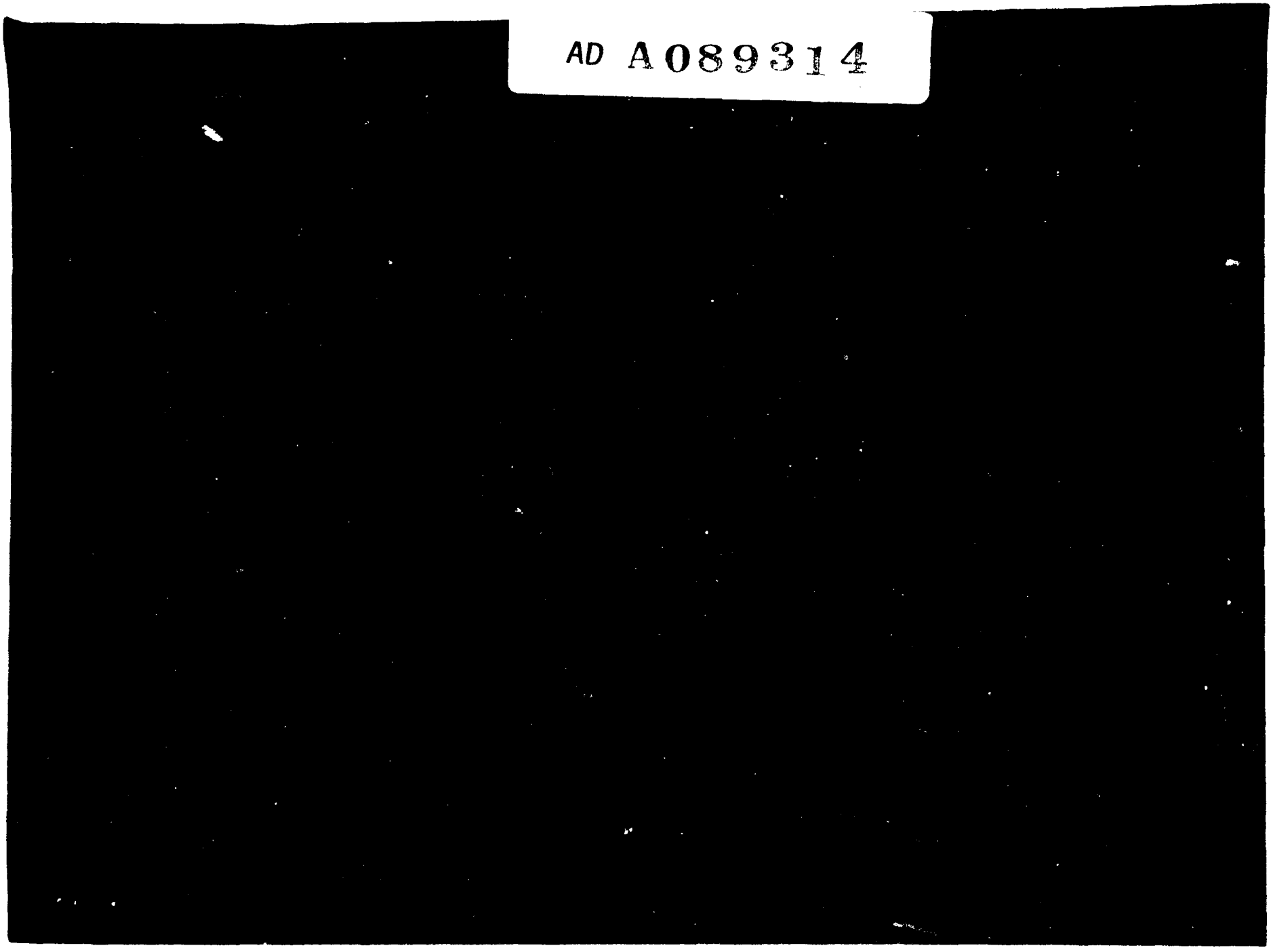

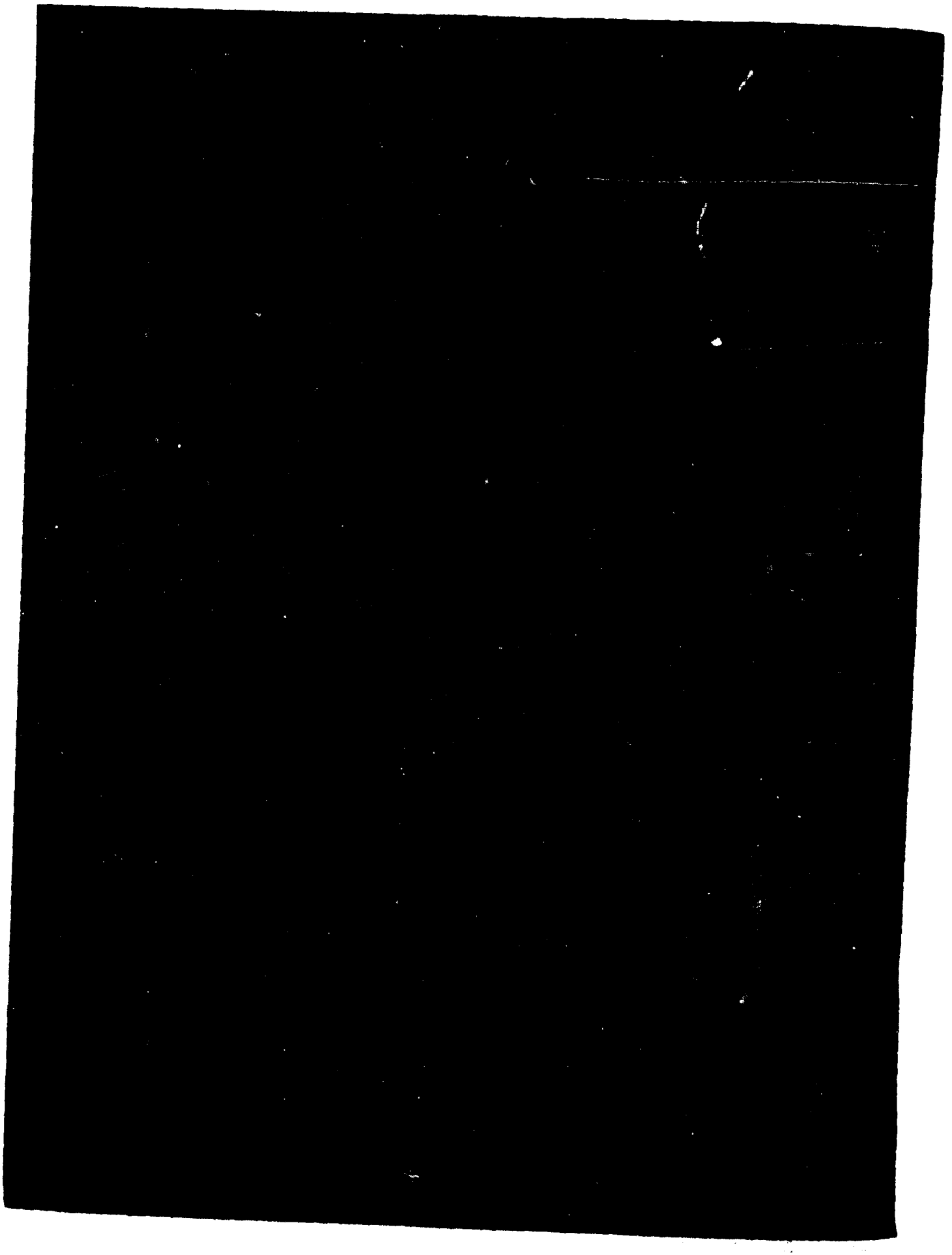

UNCLASSIFIED

SECURITY CLASSIFICATION OF THIS PAGE *(When Data Entered)*

REPORT DOCUMENTATION PAGE	READ INSTRUCTIONS BEFORE COMPLETING FORM
1. REPORT NUMBER	2. GOVT ACCESSION NO. AD-A089 314 / 3. RECIPIENT'S CATALOG NUMBER
4. TITLE *(and Subtitle)* Proceeding of the First Meeting of the Special Interest Group on Control Theory (22 May 80) Aberdeen Proving Ground, MD	5. TYPE OF REPORT & PERIOD COVERED Conference / 6. PERFORMING ORG. REPORT NUMBER
7. AUTHOR(s) H. Cohen (Chairman)	8. CONTRACT OR GRANT NUMBER(s)
9. PERFORMING ORGANIZATION NAME AND ADDRESS Director US Army Materiel Systems Analysis Activity Aberdeen Proving Ground, MD 21005	10. PROGRAM ELEMENT, PROJECT, TASK AREA & WORK UNIT NUMBERS DA Project No. 1R665706M541
11. CONTROLLING OFFICE NAME AND ADDRESS Director US Army Materiel Systems Analysis Activity ATTN: DRXSY-MP Aberdeen Proving Ground, MD 21005	12. REPORT DATE May 1980 / 13. NUMBER OF PAGES 129
14. MONITORING AGENCY NAME & ADDRESS *(if different from Controlling Office)* Cdr, US Army Materiel Development & Readiness Comd, 5001 Eisenhower Avenue, Alexandria, VA 22333	15. SECURITY CLASS. *(of this report)* UNCLASSIFIED / 15a. DECLASSIFICATION DOWNGRADING SCHEDULE

16. DISTRIBUTION STATEMENT *(of this Report)*

Approved for public release; distribution unlimited.

17. DISTRIBUTION STATEMENT *(of the abstract entered in Block 20, if different from Report)*

18. SUPPLEMENTARY NOTES

19. KEY WORDS *(Continue on reverse side if necessary and identify by block number)*

Control Theory, Kalman Filtering, Man-Model, Maneuvering Target, Fire Control, Missile Guidance and Control

20 ABSTRACT *(Continue on reverse side if necessary and identify by block number)*

Report documents papers presented at first meeting of special interest group on control theory with emphasis on military systems and recommendations of participants.

DD FORM 1 JAN 73 1473 EDITION OF 1 NOV 65 IS OBSOLETE

UNCLASSIFIED

SECURITY CLASSIFICATION OF THIS PAGE *(When Data Entered)*

TABLE OF CONTENTS

FIRST MEETING

SPECIAL INTEREST GROUP ON CONTROL THEORY

22 May 1980

MTD Bldg 400
APG, MD 21005

AGENDA

1 WELCOMING STATEMENT - Keith A. Myers
Assistant Director, US Army Materiel Systems Analysis Activity, APG, MD

2 Research for US Army Advanced G&C System
by Dr. William C. Kelley
Guidance & Control Directorate
US Army Missile Laboratory
Redstone Arsneal, AL

3 Sub-Optimal State Estimation as Related to Predictive Fire Control System Design
by T. R. Perkins
Combat Support Division
US Army Materiel Systems Analysis Activity
Aberdeen Proving Ground, MD

4 Detection and Initiation of Firing Command for an Acceleration Predictory Fire Control System Engaging Maneuvering Targets
by H. H. Burke
Combat Support Division
US Army Materiel Systems Analysis Activity
Aberdeen Proving Ground, MD

5 Hybrid Computer Simulation of Combat Tank Driven Reticle Fire Control
by John Groff
Ground Warfare Division
US Army Materiel Systems Analysis Activity
Aberdeen Proving Ground, MD

6 Robust Autoregressive Models for Predicting Aircraft Motor From Noisy Data
by Walter Dziwak
US Army Armament Research & Development Command
Dover, NJ

7 A Design Methodology for Estimators and Predictors in Fire Control System
by James F. Leathrum
Consultant to AMSAA

8 Design & Implementation of Modern Control Concept to Improve the XM97 Helicopter Turret System
Doo J. Lee
US Army Armament Research & Development Command
Dover, NJ (Paper not available at this time)

9 Future Plans - Discussion
Herbert E. Cohen
DARCOM Mathematics Program Office
US Army Materiel Systems Analysis Activity
Aberdeen Proving Ground, MD

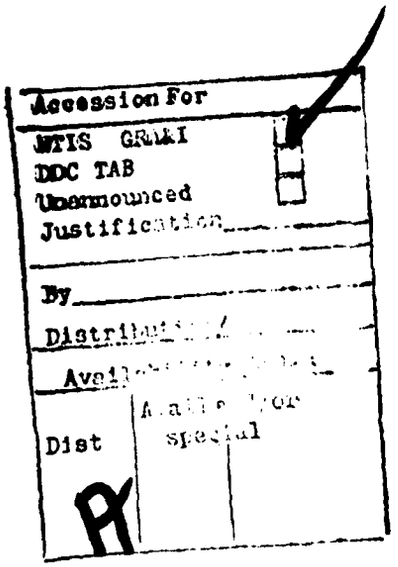

DISCUSSION AND SUMMARY

The chairman of the special interest group on control theory solicited from those attending their views on the following issues, namely,

a. How can we trigger a greater DARCOM-wide participation to this important subject to the Army.

b. Was this first meeting constructive and useful. Was there a need for another meeting. If so, when, where and who should attend.

All participants considered the first meeting very useful addressing significant problem areas in fire control and missile guidance. There was unanimous agreement to hold a second meeting in early FY81 (Nov/Dec 80) at APG and general agreement to invite the Navy and Air Force to participate. Recommendation was made and favorably indorsed by all to change the name of the group to "Coordinating Group on Modern Control Theory" to emphasize the application of "modern control theory and techniques" to military problems as compared to classical control theory techniques. Suggestion was made that the chairman explore the feasibility of using the JTCG/ME by which the Navy and Air Force could participate.

It was strongly felt that travel funds severely limited number of participants and that DARCOM HQ support should be solicited to encourage subordinate commands to actively participate in this coordinating group.

Next page is blank.

RESEARCH FOR US ARMY ADVANCED G&C SYSTEM

Dr. Harold L. Pastrick
Guidance & Control Directorate
US Army Missile Laboratory
Redstone Arsenal, Alabama 35809

Abstract

In 1978 the US Army Missile Command embarked upon a task to develop an advanced guidance and control system for future missiles. It was intended to "leapfrog" systems currently under development in order to meet the stringent demands and constraints imposed by targets with predicted characteristics of the 1990s and beyond and by the predicated battlefield environment of that time.

In this paper the problem is redefined and the latest development program presented. Results that have been achieved to date are described, particularly in the areas of mathematical models of the missiles and their guidance and control (G&C) systems being used for analyses and simulations; aerodynamics; propulsion; guidance laws being developed and analyzed; status of development of Disturbance Accommodating Control; signal processing to locate and track the target(s); and digital design tool development. The paper is concluded with a section of future plans, to include contractor support.

I. Introduction

The US Army Missile Command (MICOM) recently began a task to develop an advanced G&C system for future Army Modular Missiles. The intent is to "leapfrog" systems currently under development. The purpose of this paper is to describe the work that has been completed within this new task and to provide an indication of future efforts that are now planned.

The first step in implementing this task was to conduct a literature survey to establish a technology base starting point. Following this survey, guidance laws were placed in five categories and defined mathematically. The implementation and predicted performance of each category was then investigated and compared in light of current and predicted hardware and software capabilities.[1] This work was subsequently updated in 1979.[2]

The program objectives are three-fold:

- To develop and prove a G&C system that is capable of guiding and controlling future US Army missiles (generally defined as air defense and surface-to-surface general support) to destroy prescribed lines of future targets. This must be accomplished under the predicted severe battlefield environment of the future.
- To "leapfrog" systems under current development.
- To broaden and deepen the existing G&C system technology and design base within the G&C Directorate of MICOM.

In the sequel the expected threat and its characteristics will be summarized. This is followed by a description of the development plan for the advanced G&C system. The progress to date is presented, and the paper is concluded with a section on future plans.

II. Expected Threat

Theater defense typically is provided by a mixture of ground-based and airborne defense systems supported by radars, command and control systems, electronic warfare equipment, and passive measures such as camouflage, decoys, and equipment dispersion. The air defense objective of ground based systems is to limit the opponent's effectiveness by attacking his critical assets so that land forces may maneuver with a minimum of interference from the enemy air weaponry.

For many years now, the enemy doctrine has emphasized large mass and brute force, and his air attacks will provide no exception. It is entirely feasible to assume that an attack in the Central Europe area will be accompanied by several thousand combat aircraft.[3] In addition, his doctrine calls for the massing of large quantities of artillery fire on a section selected for a tank-led breakthrough. It is unlikely that NATO forces either now or in the near future will match the Warsaw Pact forces in terms of numbers of weapons, nor is it the intent to aim toward that end. Rather, it is important to optimize the effectiveness of our smaller force to meet the anticipated threat.

The Army is attempting to maximize the effectiveness of its current family of air defense weapons while concurrently developing a new family to meet the threat of the 1990's. In the near term, there will be continued modification of current systems as necessary, and while still feasible, to overcome qualitative and quantitative deficiencies. Longer-term replacements continue in development or procurement for all the major field army air defense systems. Examples of this strategy include the following: high to medium altitude missile systems - PATRIOT for MIKE HERCULES and HAWK; short range missile systms - U. S. ROLAND for CHAPARRAL; manportable missiles - STINGER for REDEYE; mobile gun systems - DIVAD given to VULCAN. The systems will provide the effective aerial umbrella needed by our forces to not only survive, but to fight effectively.

For security reasons, it is impossible in this forum to describe specifically the air threat that will be encountered in the scenario described above. However, in order to quantify the problem somewhat, we shall attempt to attribute vehicle characteristics to the enemy based on our current technology in the field of air defense targets. The Targets Management Office, US Army Missile Command since

---

*This paper is declared a work of the US Government and therefore is in the public domain.

**Consulting Engineer, Associate Fellow, AIAA.

1964 has published an extensive library of target program reports. In particular, they have classified a variety of aerial targets as test and evaluation (T&E) targets used for air defense weapon systems. Needless to say, targets used for this purpose must exercise an air defense weapon system to the limits of its capabilities. [5]

A particularly interesting target is known as HAHST, an acronym for High Altitude High Speed Target. It is designed to achieve speeds up to Mach 4 at altitudes up to 100,000 feet. Additional performance characteristics for HAHST and other existing targets are given in References 2 and 5.

The effectiveness of any missile system is conditioned on its ability to function in an Electronic Countermeasures environment. Stand off jammers, barrage jammers and even dispensed chaff will be used to deny the air defense tracking radars the capabilities needed to be effective in their sector. The jammers are intended to reduce the acquisition range of the radars and, if perfected, will eliminate accurate tracking entirely. Additionally, the threat, aircraft and missiles will be fabricated to present the smallest possible radar cross section. The state-of-the-art in this field is beyond the scope of presentation in this paper.

From a defensive viewpoint, the effect of enemy jamming of the air defense radars and the minimization of enemy attack aircraft radar cross sections have a profound impact on the air defense missile system. The rationale is reasonable and straightforward. If the enemy does indeed have aircraft and attack missiles and remote pilotless vehicles (RPVs) either with or better than the characteristics attributed to them via the method above, and if the enemy minimizes his radar cross section to the current state-of-the-art, his attack vehicles will be extremely difficult to acquire at long range. The effect of the combined high speed and high agility (i.e., high g-maneuver capability) with low radar cross section yields precious little reaction time to the air defense system. The close-in acquisition will seriously degrade the existing air defense missile's G&C system's performance, since most are based on a proportional navigation and guidance (PNG) law. An environment such as presented above, however, can be better addressed in terms of guidance laws explicitly tailored to this type of threat. Thus, the optimally guided and controlled, highly maneuvering, defensive missile using terminal guidance sensors chosen from across a wide range of the frequency spectrum must be initiated into the development cycle. As a necessary first step, the research described in the sequel addresses that problem.

III. Development Program Plan

From an overall systems viewpoint, this program shall address the issue of creating new theory in the G&C area to meet the high performance threat of the future as one of the leading technology items. Closely associated with it and in parallel with the G&C effort, weapon system work shall be undertaken to modify airframe and propulsion to be capable of engaging the threat of the 1990's. General support weapons shall be viewed initially as a subset of the air defense system(s), whereas previously, these two classes of weapons were developed independently. This research shall attempt to view them as potentially similar systems that utilize different modules such as propulsion, guidance, warhead, etc.

A program plan initiated by the G&C Directorate, MICOM, was undertaken approximately two years ago with the program objectives enumerated above. The program plan contains six intermediate objectives, the end of which each constitutes a program milestone. They are:

- Define overall program;
- Collect elements that will form the candidate G&C systems;
- Define candidate G&C systems;
- Evaluate the candidate G&C systems: select best system;
- Design and fabricate the selected system;
- Demonstrate "Proof-of-Concept" of the selected system.

These separate program elements (or intermediate) objectives are described below in more detail. An accompanying milestone chart is provided as Fig. 1.

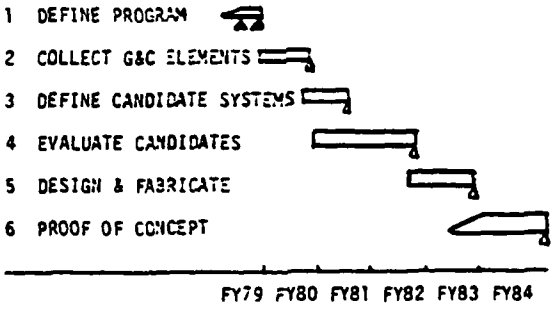

Figure 1. Program Milestone Chart.

Task 1. Define Overall Program

In this first task it is necessary to define the program objectives, goals, and constraints. This is followed by a survey of representative missile plants and the characteristics of sensors and effectors that might be used (either available or under development). Target dynamics and initial conditions must be defined, as must missions for the missile system(s) using the advanced G&C systems that emanates from this program. Also included in the first program element is the beginning of coordination with other missile-developing agencies and services. Finally, the time frame predicted usage of the G&C system must be defined. As described in this paper, most of Task 1 has been completed.

Task 2. Collect Elements for Candidate G&C Systems

In this task detailed definitions of the characteristics of candidate guidance laws, candidate autopilots (control laws), state estimation techniques, state truncation techniques, and Disturbance Accommodation Control (DAC) shall be accomplished. [5] Further, characteristics of all

expected disturbances, both external (to the missile) and internal, must be collected and evaluated. The need for DAC and for state estimation will be evaluated. Characteristics of all expected significant system nonlinearities will be collected and their dynamic importance evaluated.

Task 3. Define Candidate G&C Systems

The components and subsystems that have been identified in the earlier tasks will now be combined into candidate G&C systems. Missile structural dynamics will be determined (if not already completed within the plant definition of the earlier tasks) or refined, as necessary. The simulation program objectives will be defined; the simulation program will then be defined; and finally, development of the final system simulation will begin. Investigations of the dynamics of the candidate G&C systems will begin using both mathematical analysis and computer simulation. A figure of merit (cost functional) will be developed during this task, as will model error effects and criteria.

Task 4. Evaluate Candidate G&C Systems

The development of the system simulation and the investigation of the candidate G&C systems, begun in Task 3, will be completed. The candidate G&C systems then will be evaluated with respect to the Figure of Merit developed in Task 3, using mathematical analysis and computer simulation. The strengths and weaknesses of distributed versus centralized controllers will be assessed, probably as enhanced by the use of microcomputers. Finally, the best G&C system will be selected and integrated into a missile airframe.

Task 5. Design and Fabrication

A detailed design of the selected G&C system will be performed. The testbed(s) selected for use in the Proof-of-Concept phase will be fabricated and/or assembled.

Task 5. Proof-of-Concept

The Proof-of-Concept will be demonstrated with hardware firings during this task. These firings will be augmented by simulations (computer and hardware-in-the-loop as deemed necessary) and analyses as necessary.

IV. Progress to Date

The accomplishments to date have been achieved by elements of MICOM and through the use of research contracts. It has been supplemented through coordination with the US Air Force Armaments Laboratory at Eglin Air Force Base, the US Army Ballistic Missile Defense Systems Command at Huntsville, Alabama, and the Office of the Under Secretary of Defense. This coordination has been and will continue to be carried out to eliminate duplicated development effort on similar projects within the Department of Defense. To augment the in-house research and engineering capability, several research contracts have been initiated in specialized areas currently including: the Computer Sciences Corporation, Huntsville, Alabama; the Dynamic Systems Research and Training Corporation, Huntsville, Alabama; the University of Florida; Western Kentucky University; and the Control Dynamics Company, Huntsville, Alabama. Additional contracts with other organizations are anticipated as the scope of the program grows.

The technical work comprising Tasks 1 and 2 has been apportioned to various members of the MICOM and contractor team. As indicated, most of Task 1 has been completed, and effort on Task 2 work is underway.

A. Target Definition

A comprehensive investigation of predicted future targets and their dynamics has been completed. This investigation included reviewing and discussing material available within the sources of the US Army and US Air Force and included inputs from several industrial organizations. Finally, the collected information was discussed with elements of the Office of the Under Secretary of Defense, Research and Engineering. While most of the collected information is classified for security reasons, the results of this most important phase of the study lead to emphasizing targets in three categories: highly maneuverable aircraft, cruise missiles, and tactical ballistic missiles. Not addressed in this study are RPV's and surface targets. It is felt that use of a sophisticated missile system to engage numerous RPV's would not be cost effective and that missiles currently under development will be able to combat surface targets. Except for periodic updating, this subtask is now complete.

B. Missile Plant Characteristics

In order to get the other subtasks underway, standard equations of motion for missile bodies with some structural flexibility have been used. The missiles are assumed to be acted upon by the usual aerodynamic forces and torques. Currently, variations of the SPRINT missile family are among the principal contenders for the airframe and propulsion system.

C. Aerodynamics

A detailed plan is being generated for future actions in gathering and generating aerodynamic data to be used in this program. Novel aerodynamic shapes are under consideration and evaluation for use in developing control authority for missiles using advanced G&C systems. These include missiles using configurations shown in Table 1 (along with their characteristics).

D. Error Sources

Expected error sources have been categorized into five detailed groups, to include predicted mean and standard deviation values. Several are presented as representative of the groups. These will, of course, change as the choices are narrowed and the program develops.

1. Missile. Included in this group are parameter uncertainties such as thrust magnitude and misalignment, C.G. location and offset, mass, and transverse and axial moments of inertia.

2. Aerodynamic. Normal and axial forces; pitch, yaw, and roll moments; pitch and yaw damping derivatives; roll damping coefficient due to fin deflection; and axial drag are factors.

Table 1. Aerodynamic Configurations and Characteristics.

Configuration	Advantages	Disadvantages	Mach No.	Altitude (ft.)	Maneuverability (g's)
1. Deployable wings with all-moveable tails	a. Simple controls b. Good roll control	a. Control force in opposite direction from maneuver b. High angle of attack	2-4	0-100 K	10-15
2. Low aspect ratio, long-chord delta wing with tab controls	a. Simple controls b. Good roll control	a. Control force in opposite direction from maneuver b. High angle of attack	4-7	0-140 K	20-30
3. Flared skirt-stabilized missile with all moveable wings	a. Control force in direction of maneuver b. Lower angle of attack	Possible higher drag and hinge moment	4-7	0-140 K	20-30
4. Reentry body shape with moveable wedge controls *	a. Simple shape b. Good roll control	Roll control surfaces separate from maneuvering controls	5-10	?	?
5. Lifting body *	a. Lower angle of attack b. Control force in direction of maneuver	Complicated aerodynamic shape	3-6	0-90 K	10

* Comment. Must use bank-to-turn guidance.

3. Instruments

• Accelerometers - scale factor stability, bias stability, non-orthogonality, "g^2" - scale factor, third-order scale factor, cross-axis sensitivity, cross-coupling, scale factor asymmetry, and rectification error.

• Gyroscopes - scale factor stability; bias stability; non-orthogonality; anisoelastic drift; drift rates in pitch, yaw, and roll due to input axis and spin axis accelerations as well as those (rates) independent of acceleration, due to torquer nonlinearities, and due to electronic noise; and mass unbalance.

• Porro-prism azimuth alignment.

• Laser inertial measurement unit misalignment with respect to missile body axes.

• Accelerometer triad origin displacement.

• Uplink/downlink bias and calibration errors.

• Optical correlator errors.

• Radar - range track and angle track noise and accuracy, ground clutter noise, and target glint noise.

4. External. Wind magnitude and direction (initial azimuth, elevation, and roll alignment of the missile; target velocity and illumination jitter; semiactive laser pointing accuracy and beam divergence; gravity bias; atmospheric effects (e.g., upon radio range).

5. Subsystems

• Common nonlinearities - saturation, coulomb (and other) friction, backlash, and bang-bang with dead zone.

• Computer - quantization, truncation, and fixed word length.

• Seeker - boresight error (in pitch and yaw) due to servo noise; channel crosscoupling; coupling between the seeker head and the airframe; effects of the radome and irdome on angle linearity; angle bias (the electrical equivalent of mechanical BSE); gain stability; angle noise; and boresight error in pitch and yaw due to clutter, receiver, and jamming noise.

• Autopilot - bias errors, time delays, and gain stability.

• Guidance - errors in initial position, velocity, and acceleration.

As the program progresses, these error sources will be analyzed further to determine which might be amenable to cancellation by appropriate disturbance accommodation design theory and techniques.

E. Guidance Laws

This is a major thrust area within the program. As indicated above, an extensive literature search has been completed and documented. This was followed by placing guidance laws in five categories and describing each mathematically. The implementation and predicted performance of each category has been initially reported in Reference 1 and subsequently updated in Reference 2. A summary of the latter is shown in Table 2.

Investigations continue into areas of optimal guidance, in particular, emphasizing digital aspects in anticipation of the expected use of on-board digital controllers. Constant effort is made to reduce implementation complexity, where complexity is defined as requirements for hardware and software. Other innovative techniques are under investigation. They include assessing the potential application of Singular Perturbation Theory, Disturbance Accommodating Theory, and means of determining or predicting the very important (for optimal applications) quantity, time-to-go, i.e., remaining time of flight at any instant (see Table 3).

1. Optimal Control. A conventional implementation of Linear-Quadratic Optimal Control is portrayed graphically in Figure 2. The optimal control authority, u^o_{LQ}, is selected to be

$$u^o_{LQ} = -R^{-1}B^T K_x \hat{x} \quad . \tag{1}$$

The matric Riccati equation is solved to obtain the control gain, $K_x(t)$, while minimizing a quadratic performance index.

2. Disturbance Accommodating Control. The Disturbance Accommodating Control (DAC) theory is described for the continuous-time domain in Reference 6. The general nature of the DAC controller is to generate a real-time on-line estimate of the actual (instantaneous) disturbance waveform and create a special control action that exactly

Table 2. Conventional Guidance

Approach	Advantages	Limitations
1. Attitude Pursuit	a. Simplest implementation b. Fixed targets	Sensitive to target velocity, disturbances
2. Velocity Pursuit	a. Simple implementation b. Non-maneuvering targets	Sensitive to target acceleration, disturbances
3. Proportional Navigation Guidance (PNG)	a. Simple implementation b. Maneuvering targets	Sensitive to high end game maneuvers

Table 3. New Guidance Approaches

Approach	Advantages	Limitations
1. Linear Quadratic (LQ) Regulator	Better than PNG against maneuvering target	a. T_{GO} estimate required b. Must compute time-varying control gain (K_x) c. Disturbances ignored
2. Linear Quadratic Gaussian (LQG) Regulator	Better than LQ against noise-type disturbances	a. T_{GO} estimate required b. Must compute time-varying control gain (K_x) c. Must comoute Kalman gain for estimator
3. Disturbance-Utilizing Control (DUC)	Better than LQ or LQG against waveform-type disturbances	a. T_{GO} estimate required b. Must compute 2 time-varying control gains (K_x, K_{xz})
4. Singular Perturbations	Computational efficiency	An approximation to optimal control

cancels-out the disturbance effect on the missile. The DAC theory will be extended into a discrete-time domain. To date, the class of systems and disturbances amenable to a discrete-time version of DAC have been defined. Work is underway on a description of the state-reconstructor that will be associated with a digital DAC controller. Also under consideration is the possibility of applying DAC to various missile subsystem or component outputs, such as sensors, whose normal outputs have been modified by the influence of the disturbances upon the sensors.

An innovative modification of DAC is Disturbance-Utilizing Optimal Control (DUC)[7]. In this case waveform-type disturbances are exploited optimally. Examples of such disturbances are drag, target maneuvers, wind gusts, any effects of the gravitational field. A graphical portrayal of DUC implementation is shown in Figure 3. In this case, the optimal control authority is specified as

$$u^o_{DUC} = -R^{-1}B^T(K_x\hat{x} + K_{xz}\hat{z}) \ , \qquad (2)$$

where $K_x(t)$ is found by solving a matric Riccati equation, and $K_{xz}(t)$ is found by solving a linear differential equation. To date, computer simulations have shown DUC to be quite effective when compared to the performance achieved by using conventional LQ controllers.

3. Singular Perturbations. Application of Singular Perturbation Theory to missile control may be attractive if it is deemed necessary for the control law to account for high order model terms.[8] The standard approach is to approximate the model with relatively lower order equations. However, the neglected higher order terms may be dynamically significant. Because their inclusion might create computational problems, a possible alternative might be the application of Singular Perturbation Theory. The application is particularly amenable to controller design where the open-loop plant has a wide eigenvalue dispersion, slow and fast modes, or parasitic parameters.

F. Sensor Characteristics

Various existing and predicted sensors have been characterized. Trade studies to aid in their selection have been identified. It now appears that a sensor using some form of pattern recognition may be required. The problem is to find or begin developing a sensor that can provide a guidance signal with a superior signal-to-noise ratio from data that has been deliberately modified, for example, by high powered jamming equipment.

G. Computer-Aided Design Tools

A number of computer programs are available (such as root locus and other frequency domain

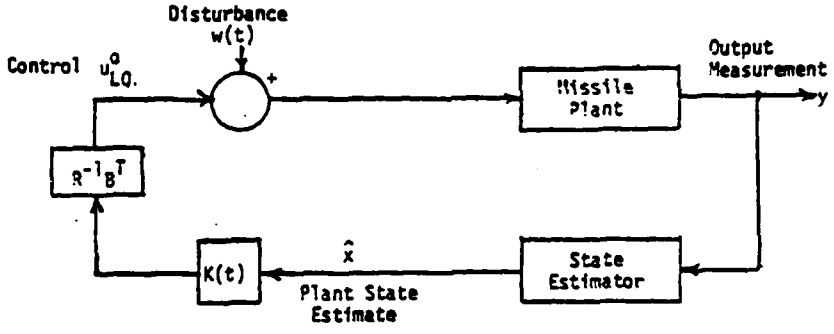

Figure 2. Conventional Linear Quadratic Optimal Control.

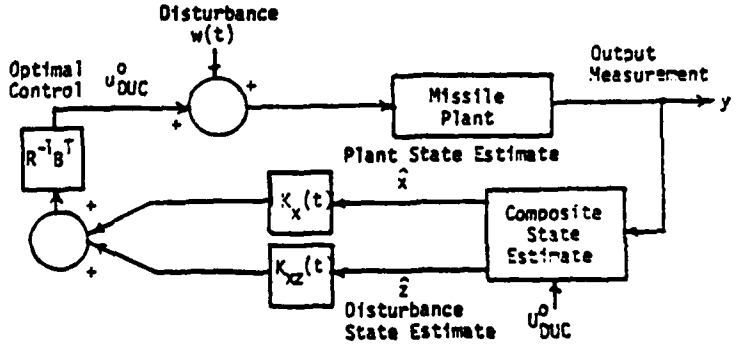

Figure 3. Disturbance-Utilizing Optimal Control.

techniques) to aid in design of control systems. Most of them are in the continuous-time domain, although there does exist a z-transform manipulation program. An executive routine currently is being coded to manipulate these programs efficiently.

H. Microcomputer State-of-the-Art

A continuing assessment of microcomputer state-of-the-art has been instigated within this program. Microcomputers will become an integral part of advanced G&C systems, with their small size, light weight, and relatively low cost. Presently, microcomputers software capabilities are being investigated with a Tektronix 8002 Microprocessor Laboratory. This investigation will be followed by an analysis of the computational capability to meet the requirements imposed by an advanced G&C system.

I. Digital Design Tool Development

The probability that an advanced G&C system will be implemented digitally seems to be nearly assured. It is for this reason that the foregoing work has been oriented strongly in the direction of digital implementation and its consequences. A review of analysis and design tools available to the G&C system designer is being conducted. Where the need for a new tool appears to be warranted, it will be developed within this program when possible. Emphasis is placed on both simplicity of application and being able to draw on practising engineers existing engineering training and experience.

One example of such a tool is "SAM" (acronym for Systematic Analytical Method). SAM provides an alternative to the use of signal flow graphs and the application of Mason's Gain Rule to determine selected states of the missile.[9] The technique is particularly useful for analysis of complicated sampled-data control systems. An advantage of using SAM is that the cumbersome application of Mason's Gain Formula can be avoided. Further, the entire method of constructing signal flow graphs may be circumvented. Since only the equations describing the system are needed for SAM, even the customary block diagram is not needed. The technique is analytical in nature and makes use of a systematic manipulation of the system algebraic equations. These manipulations follow prescribed rules set forth in the technique.

A second simplified technique is the determination of digital control system response by cross-multiplication.[10] This technique permits the analyst to obtain the response (at the sampling instants) of any system state from its closed-loop transfer function expressed in the complex z-domain. If it is desired to know the response between sampling instants, either the submultiple method or the modified z-transform method may be adapted to the cross-multiplication technique.

A third, more sophisticated technique is the Parameter Space Method. It is being developed for determining the stability and dynamic characteristics of a digital control system in terms of several selected system parameters.[11] The method requires that the system characteristic equation be available in the complex z-domain. Although not necessary, its application is facilitated by augmenting the analytical results with graphical portrayals in a selected multiparameter space. The method is based on analysis and synthesis methods for linear and nonlinear control system design which are amply described in Siljak's excellent monograph on the subject.[12] In essence, the parameter space method permits the designer to evaluate graphically the effects of the locations of the roots of the characteristic equation. Hence, he may design the control system in terms of his selected performance criteria; e.g., absolute stability, damping ratio, settling time. He is able to see the effects on the characteristic equation roots (and hence on system dynamics) of changing several adjustable parameters. The method has been extended to portray the effect of varying the sampling period, thereby permitting one to observe the effect of the choice of various values assigned to the sampling period on absolute and relative stability. Also, simple recursive formulas have been derived so that the resulting formulation is deliberately cast in a form particularly amenable to solution by a digital computer or a desk calculator, emphasizing the interplay between analysis and computing machines.

J. Documentation

A major portion of the progress reported above has been documented in a comprehensive US Army Missile Command report.[13]

V. Future Plans

Plans for the next fiscal year revolve primarily about implementating Task 3 (define candidate G&C systems) of the development program as well as completing any partially-completed portions of Task 2 now underway. Close communication will be maintained with the intelligence community to become aware of any changes to the presently predicted targets as contrasted to the attribution mentioned above. Detailed analytical models of the missile plant(s), effectors, and autopilot(s) will be developed. The possibility of modifying plant characteristics by making innovative use of aerodynamics is to be investigated. Projected advances in the field of propulsion will also be investigated. The comparison of various digitally-implemented guidance laws will be continued, including those that incorporate DAC. Applications (other than to guidance laws) of DAC theory to improve system performance will be investigated. Development of a modular guidance simulation to implement this investigation has already begun. Trade studies concerning identified existing and future sensors will be conducted, with the possibility of developing a new sensor with capabilities not yet in existence. Advances in microcomputer state-of-the-art will be watched closely. Finally, tools to aid the G&C system designer to handle digital implementation will continue to be both assessed and developed.

VI. Conclusions

As indicated within this paper, there is a clear need for the development of an advanced G&C system for US Army future tactical missiles. This need is dictated by the predicted targets of the future, the anticipated battlefield of the future, and the characteristics of tactical missiles that are either in the inventory or under development at this time. The nature of the future G&C system will be digital so that the overall missile system may be availed of present and predicted advantages that are implicit in digital controllers. The form of

the guidance law probably will be optimal, since the performance criteria that must be minimized must take more into account than miss distance.

VII. References

[1]Pastrick, H. L.; Seltzer, S. M.; and Warren, M. E., "Guidance Laws for Short Range Tactical Missiles," AIAA Paper No. 79-0059, 17th Annual Aerospace Sciences Meeting, New Orleans, Louisiana, 15-17 January 1979.

[2]Pastrick, H. L. and Seltzer, S. M., "Future US Army Missile G&C Systems," AIAA Paper No. 79-1749, AIAA Guidance and Control Conference, Boulder, Colorado, August 6-8, 1979.

[3]Pierre, Percy A. and Keith, Donald R., Equipping the United States Army, A Statement on the FY80 Army RDTE and Procurement Appropriation to the Committee on Armed Services, House of Representatives - First Session, 96th Congress, 5 March 1979.

[4]Brown, Harold, Department of Defense Annual Report, Fiscal Year 1979, Washington, D.C., 2 February 1978.

[5]Accardi, Roy R., Target Programs, US Army Missile Material Readiness Command, Redstone Arsenal, Alabama, 18 July 1978.

[6]Leondes, C. T., ed., Control and Dynamics Systems: Advances in Theory and Applications, Vol. 12, Chapter by C. D. Johnson entitled "Theory of Disturbance-Accommodating Controllers," Academic Press, Inc., 1976.

[7]Kelly, W. C., "Theory of Disturbance-Utilizing Control with Application to Missile Intercept Problems," Ph.D. dissertation, University of Alabama in Huntsville, October 1979.

[8]Sannuti, P. and Kokotovic, P., "Near Optimal Design of Linear Systems by a Singular Perturbation Method," IEEE Trans. on Automatic Control, Vol. AC-14, pp. 15-22, February 1969.

[9]Seltzer, S. M., SAM: An Alternative to Sampled-Data Signal Flow Graphs, US Army Missile Research and Development Command, Technical Report TR T-79-49, 10 May 1979.

[10]Seltzer, S. M., Determination of Digital Control System Response by Cross-Multiplication, US Army Missile Research and Development Command, Technical Report TR T-79-58, 29 May 1979.

[11]Seltzer, S. M., Sampled-Data Analysis in Parameter Space, US Army Missile Command, Technical Report T-79-64, June 1979.

[12]Siljak, D. D., Nonlinear Systems, Wiley, New York, 1969.

[13]US Army Missile Laboratory, Advanced Analysis for Future Missiles, US Army Missile Command, Technical Report TR-RG-80-8, 21 November 1979.

Acknowledgements

The following people are gratefully acknowledged as having contributed heavily to this program:

MICOM: Mssrs. J. Derrick, R. Gambill, L. Isom; Dr. W. Kelly; Mssrs. R. Maples, W. McCowan, J. McLean, L. Murdock; J. Thacker, D. Washington, C. Wills.

Dynamic Systems Research and Training Corporation: Dr. C. D. Johnson.

University of Florida: Professor M. Warren.

Western Kentucky University: Professor R. York.

Control Dynamics Company: Dr. S. M. Seltzer.

FOR PRESENTATION TO

SPECIAL INTEREST GROUP ON CONTROL THEORY

SUB-OPTIMAL STATE ESTIMATION AS RELATED TO PREDICTIVE FIRE CONTROL SYSTEM DESIGN

T. R. Perkins
US Army Materiel Systems Analysis Activity
Aberdeen Proving Ground, MD 21005

ABSTRACT

The engagement of maneuvering land vehicles with gun systems place extreme performance requirements on the fire control system designs. The effectiveness of a gun fire control system depends on the capability to provide an accurate fire control solution, i.e. predict the future position of the target a projectile time-of-flight later. Non linear prediction is shown to not only improve performance but to also increase available time for firing against maneuvering targets. Sub-optimal, multi-variable, adaptive estimation approaches are shown to improve the affectiveness of predictive fire control systems.

Sensitivity analyses are presented that relate system induced errors and target motion induced errors to tracking noise and predictor order. Relationships between system stability and performance for two basic types of fire control systems are presented.

INTRODUCTION

This paper discusses the fire control system problem, the nature of land vehicle mobility and agility and the ability of predictive fire control systems to effectively engage maneuvering vehicles. Existing performance specification do not satisfactorily describe the level of maneuverability expected in a tactical situation. Rather, present specifications define performance requirements for fixed vehicle speed and heading movement which has resulted in the development of fire control system designs that are significantly degraded in a maneuvering target environment. The problem is addressed, in general, for the four cases of firing vehicle-target vehicle movements. The processes required in the fire control solution are identified and the sensitivity of system performance to the propagation of tracking errors is discussed. The stability and performance characteristics of two generic fire control system configurations are analyzed in some detail.

GUN FIRE CONTROL SYSTEM PROBLEM

The purpose of gun fire control systems is to have a projectile, that has been fired a time of flight previously, impact the target that was sighted a time of flight earlier. The critical motion parameters that degrade the performance of predictive fire control systems have been identified as cyclic oscillations exhibiting frequencies that are within the motion capabilities of tactical land vehicles (1). Tracking error, defined as the difference between target and reticle position, does not in itself cause the performance degradation. The inability of the fire control system to determine the motion derivatives of the line-of-sight (LOS) to the target, and predict the future position of the target are the two main factors that cause fire control systems degradation.

The error in the ability of a fire control system to cause the projectile to intercept the target a time of flight later is referred to as total gun pointing (TGP) error. TGP error is defined as the offset between the actual gun pointing direction at round exit and the location of the target centroid at round impact. The TGP error is the sum of the propagated system induced (SI) errors and target induced (TI) errors (i.e. TGP error = SI errors + TI errors). The SI errors, considered in this study, are the tracking error (difference between the tracker LOS and true LOS to the target) at the time of firing (lay error) and the estimation errors (difference between estimated LOS states and true LOS states). The SI errors propagated through a projectile time of flight result in a kinematic lead error. The TI error is caused by the target motion during the time of flight of the projectile. It is dependent on the order of the lead solution in the fire control system. For a first order lead system the TI error is the difference between the actual LOS movement during a projectile time of flight and the propagated LOS movement assuming perfect LOS rate at the

time of fire. The first order predictor system TI error ignores the presence of actual target acceleration at time of firing and during projectile flight time. For a second order lead system the TI error is the difference between the actual LOS motion during a projectile time of flight and the propagated LOS movement assuming perfect LOS rate and acceleration at the time of firing. The second order predictor system TI error accounts for target acceleration at time of firing but ignores the actual target acceleration during projectile flight time. This distribution of errors is shown in Figure 1. The ballsitic flight characteristics of the projectile are ignored.

The fire control solution occurs during a short time interval which is related to the time of flight of the projectile. The motion conditions of both the firer and the target are needed to understand and solve the fire control system problem. Four motion conditions exist: stationary firer-stationary target, stationary firer-moving target, moving firer-stationary target, and moving firer-moving target. The stationary firer-stationary target is the least dynamic situation and is the least complex case, and the moving firer-moving target is the most complex case. For each of the cases, the LOS between the firer and target is the key to which of the four fire control processes are being called upon in a demanding manner.

FIRE CONTROL SYSTEM PROCESSES

A fire control system may be broken down into four distinct processes. Each of these processes are present in all types of fire control systems. They are: tracking, estimation, prediction, and gun pointing. In specific designs these four processes are accomplished in different manners.

The tracking process is important in all four cases. For the moving firer cases, tracking becomes more critical because the base motion of the firer must be compensated and it may be affected in a secondary manner by target motion. Tracking is usually accomplished manually and is concerned with the alignment of the sight reticle with the target. The gunner is involved directly at this stage and accuracy of tracking will be a characterization of the ability of any given gunner to perform the task. Test data obtained from experimental investigations can be used to determine tracking error means, standard deviations, and correlation time constants useful for building models of the tracking errors.

The estimation process is the intermediate stage between the tracking process and the prediction process and its configuration is dependent upon the order of the prediction process. Estimation is the process of filtering the tracking data to provide the necessary target motion information required in the prediction process. The accuracy of the tracking data will influence the performance of the estimation process. The system error induced by the estimation process decreases with improvement in tracking accuracy.

Prediction of target future position to obtain intercept between projectile and target is dependent upon an estimate of the present motion of the target and time of flight of the projectile. The output of the estimator is not a complete description of the present motion of the threat, therefore, the predictor does not have the necessary information to calculate the threat's future position exactly. If restrictions are placed on the allowable threat motions, then the predictor's ability to determine its future position is improved. Oversimplification of allowable threat motions has placed unrealistically simplified requirements on the operation of the estimation and prediction processes. Realistic threat motions are determined by the mobility capabilities of tactical vehicles. In the past, the majority of threats that have been studied have been nonaccelerating. The requirements of an estimator and a predictor for this type of motion are to combine the apparent threat velocity estimate and projectile time of flight for the lead solution. The required lead is constant and can be realized after some settling time. The existence of accelerating targets requires the estimator and predictor to develop constantly changing lead angles, hence, the need for nonlinear prediction.

An important point to observe is that for the stationary firer-moving target case, the prediction process is required to provide gun command orders that orient the gun to account for target motion during the projectile's time of flight, whereas in the moving firer-stationary target case this prediction process is not required because the LOS existing between the firer and target at instant of firing does not move during the projectile's time of flight. For the moving firer-moving target, LOS also moves after projectile firing.

The gun pointing process is required to align and stabilize the gun along the predicted LOS to the target. The stabilization and response of the gun pointing loop is a major concern for fire control system performance against maneuvering targets. Stabilization of the gun pointing process could have an adverse effect on overall system performance. The moving firer cases will stress the gun pointing process most severely but it is possible that the gun pointing process will be equally stressed for the stationary firer-moving target case with non linear prediction.

FIRE CONTROL SYSTEM CONFIGURATIONS

The three currently used fire control configurations are known as manual or iron sight, disturbed reticle and stabilized sight-director systems. A fourth method called closed loop refers to projectile spotting to adjust the fire control solution and is not considered in this discussion. The manual fire control system uses the brute force approach and concentrates on stabilizing the gun position exclusively. In this system the lead is introduced manually, therefore, there is no automation of the fire control estimation and prediction process. The disturbed reticle system stabilizes the gun position and disturbs the position of the tracking reticle from the gun line position. In this scheme the tracking, estimation and prediction processes are inseparable and the fire control solution is automated. The rejection of firer vehicle base motion is difficult to accomplish in this type of system. The last system to be considered is the stabilized sight-director system. The tracking process is accomplished by a tracker which is rotated from a stabilized base that has signals applied to isolate firer vehicle base movement. The resulting LOS orientation is referenced to interial space, as contrasted to the gun line for disturbed reticle systems. The estimation process is the intermediate link between the tracking process and the prediction process. The prediction process uses the estimation process outputs combined with projectile time of flight to determine the gun pointing commands. The gun pointing process uses the estimated LOS to the target summed with the calculated lead offset of the gun from the tracker LOS to position the gun line.

How well a fire control system configuration performs is a function of target movement, firer movement and fire control system design. The analytical methodology required to study this problem should be constrained to real time solution mechanisms. Another way to say this is: post data analysis techniques using data obtained from field tests will not provide the insight that is required to obtain an understanding of the relative performance of different fire control systems. Probability of hit information is useful for an assessment of systems that have been fielded but is not applicable for trade off studies of the type required in this study. Analytical methodologies such as servo mechanism synthesis and modern filtering technology are required to study this problem.

MANEUVERING TARGET DESCRIPTION

A quantitative description of the threat is required to evaluate the performance of fire control systems operating against maneuvering targets. To develop this description, it is necessary to consider the mobility and agility characteristics of threat vehicles in a realistic combat environment. A thorough description of anticipated maneuvering seems to defy identification because threat maneuvers constitute a large set of possibilities even when constrained by tactical doctrine, driver policy, terrain and vehicle capabilities. Two approaches, analytical and empirical, are available for consideration in the attempt to identify the maneuver characteristics of land vehicles. An analytic approach would view each maneuver as being composed of elements from an idealized group of movements. An empirical approach would view the maneuvers as having actually occurred during limited tests for different types of maneuvering vehicles. Neither of these approaches provide a complete maneuver description, but a combination of these two approaches offers some advantages and is the rationale adopted. The analytic approach will partially overcome the incompleteness of the empirical data base while the empirical data will offset the mathematical idealizations of the analytic methodology.

Empirical Approach

When using empirical data to demonstrate the performance of a gun fire control system, baseline performance can be determined with no concerns arising from idealization of the maneuvers. Since the number of maneuvers will be rather small, they neither provide sufficient information about the robustness of a fire control design methodology nor the pathology when the fire control system begins to degrade. When demonstrating the performance of a fire control system against experimental data, caution must be exercised to assure that the empirical data is properly inputted to the fire control system model. Matching of the data rates and noise levels often requires some preprocessing of experimental data to prepare it for use in simulation studies.

Analytic Approach

As a supplement to the empirical approach the analytic approach is used to investigate sensitivity effects for a larger group of movements. Simulating new or pathological maneuvers require that the analytic capability superimpose maneuvers arising from random disturbances and intentional, voluntary vehicle driver commands. The random disturbances may be represented in terms of time histories or power spectral densities. The time history approach is based on the development of a mathematical model of vehicle movement influenced by terrain effects and arbitrary driving habits of individual drivers. It is assumed that for no random effects

caused by terrain irregularities or driver input, the vehicle would follow a straight line-constant speed path. Maneuvers are viewed as perturbations on this straight line-constant speed path. Apparent acceleration, a (t), which is correlated in time, accounts for the vehicle's deviation from a straight line path. Maneuver capability is expressed by three quantities: the variance, or magnitude of a (t), the cyclic maneuver frequency and the time constant of the maneuver.

Intentional, voluntary vehicle driver commanded motion of land vehicles over terrain is a complicated subject in itself and will not be investigated in this study. It is recognized however, that an interaction between vehicle horsepower, weight, suspension, and locomotion concepts do combine with terrain over which it is moving to provide different levels of mobility with respect to a fixed reference frame. Therefore, different vehicle designs will have different mobility levels defined in terms of motion and derivatives of motion. Agility is closely related to mobility and yet it is a slightly different description of intentional vehicle motion. Where mobility describes the movement of a vehicle from one location to another location in a given period of time, agility describes the vehicle's ability to alter its mean path.

SENSITIVITY OF FIRE CONTROL PROCESSES

Degradation in gun pointing accuracy results from two major error sources, system and target induced errors. The target induced errors are caused by the motion of the target during the time-of-flight of the projectile. Since the target has the capability to maneuver within constraints of the terrain, vehicle characteristics and driver policy during a projectile's time-of-flight, there is no such thing as a correct (perfect) lead solution. The lead solution is based on the projected target position using the present target states and projectile time-of-flight. Therefore, the target induced error, in general, cannot be reduced to zero for a maneuvering target. However, it can easily be shown that the prediction process is capable of reducing the gun pointing error due to target motion.

The system induced errors are made up of biss and random errors emanating from specific components and subsystems. The propagation of these errors degrade the performance of the fire control system. The system induced errors of major concern are those occurring in the tracking process. Sensitivity analyses have been performed to evaluate the degradation of gun pointing commands to tracking process errors.

The analysis considers the fire control system processes to be interfaced in tandem with no feedback of outputs to a previous process. The analysis is further limited to a segment of a maneuvering target path which was generated by a maneuvering target path simulation program. This analytically generated path provides an exact time history of the target states (position, velocity and acceleration).

The tracking process is modelled by summing random errors of known variance with the output of a perfect LOS sensor. The output of the tracking process is, by definition, in LOS coordinates, however, cartesian coordinates are used, by choice and not a limitation of the methodology, in the estimation processes. For simplication, the transformation from LOS to cartesian coordinates is accomplished prior to adding tracking noise.

A sub-optimal, adaptive Kalman filter (KF) is used for the estimation process in the generic fire control system under consideration. The noisy tracking process signal is processed by the KF to provide a "best" estimate of the target states (position, velocity and acceleration). The estimation errors are minimized by providing the filter with the correct variance of the observation noise. In practice, this perfect match of noise variance is not achieveable but can be approached with detailed error analysis of the tracking process or with software methodology to estimate the noise. The latter is probably desirable and necessary because the variance of the tracking process error is not time invariant in a combat environment. The KF is the generic fire control system. The KF equations and theory are well known and are presented elsewhere (2,3). However, the adaptive feature of the designed KF, which requires on-line computation of the filter's gain, is outlined (4). The adaptive, time varying gain is obtained by changing the variance of the uncertainty of the embedded target dynamics, as a function of the estimated path geometry. The forcing function for the target dynamics is modelled as a random (Gaussian noise) rate of change of acceleration. The variance of u is defined in the body coordinates of the target as constant, diagonal elements of the Q matrix. The Q matrix is rotated as the target maneuvers to provide a time varying Q matrix in the filter's coordinate system.

The sensitivity of the estimates to the tracking process noise is evaluated for a typical maneuvering target path. The ground track of the maneuver is shown in Figure 2. The maximum speed and lateral acceleration are 10 m/sec and 2 m/sec^2, respectively. Figure 3 shows the degradation in velocity estimates as the standard deviation of the tracking process noise on the assumed position observation is increased from 0.05 meter to 1.0 meter. The degrada-

tion in the estimates of lateral acceleration for the same noise levels is shown in Figure 4. A comparison of these two figures shows that the velocity estimates are not as sensitive to the propagation of tracking noise as the acceleration estimates.

The prediction process provides the command for pointing the gun to the predicted target position. The estimated future position of the target depends on the order of the prediction process. Ideally, one would like to forecast the target position so that a projectile fired a time-of-flight earlier would arrive at a point in space simultaneously with the target. Unfortunately, only the present states, which are never known exactly, are available for use in computing future target position.

With knowledge of the true future position of the target, available from the target motion model, the degradation in the gun pointing commands can be evaluated for different tracking errors. Target induced errors and the propagation of the tracking process noise are analyzed to evaluate their effect on gun pointing commands.

The target induced errors are functions of target maneuver characteristics, projectile time of flight and prediction order. For a given prediction order and with perfect knowledge of the present target states and time of flight, the resulting target induced errors are lower bound prediction errors. Effects of time of flight and order of prediction are shown in Figure 5 for a maneuvering target whose maximum speed and lateral acceleration is 10 m/sec and 3.5 m/sec^2. Prediction errors are improved for decreases in time-of-flight and higher order of prediction.

First order prediction is linear and requires only accurate estimates of velocity to approach the lower bounds of prediction error. Second order prediction requires not only accurate velocity but also acceleration estimates to minimize the prediction errors. Figure 6 shows the standard deviation of prediction error for the target maneuver shown in Fig. 2 as a function of time-of-flight and variances of tracking process noise for first order prediction. These results indicate that the degradation in prediction error is minimized as the quality of tracking improves. However, the existence of the lower bound curve for second order prediction provides additional improvement, not realized by first order prediction. Assuming position observations (input to the KF) with a 1σ noise of 1.0 meter, Figures 6 and 7 show that there is no large difference between first and second order prediction. However, second order prediction with a reduction in the tracking process error to 0.05 meter (25 microradians at a range of 2000 meters) provides a significant improvement in the lead solution. Unlike first order prediction, second order prediction is not only more sensitive to the tracking process noise but also to the observation state. Figure 7 shows that improvements are realized if the observations are rates rather than position. If tracking accuracies of 0.04 m/sec (20 microradian/sec at 2000 meters) are achieved, the prediction error is within about ten percent of the lower bound for second order prediction.

The lead errors discussed above are the differences between the predicted and actual target positions for an estimated time-of-flight. Targets are not point sources and a more meaningful criteria for evaluating the system processes is the percent time on target for a specified engagement time. Assuming a target size of 2.3 meters X 2.3 meters, independent of target orientation, the percent time on target for the same tracking accuracy in Figure 7 is depicted in Figure 8 for times of flight between 1.0 seconds and 2.5 seconds.

STABILITY ANALYSIS OF GENERIC FIRE CONTROL SYSTEMS

General Discussion

The three basic fire control configurations in existence: manual, disturbed reticle and stabilized sight-director have been identified in terms of how the fire control processes are mechanized. All existing operational systems utilize the human operator to null the difference between the observed target and the reticle position. The degree of participation of the human in each of the three types of fire control systems is considerably different. Concern about the stability of the closed loop man-machine system is an important consideration in determining performance and is one of the primary distinguishing features that characterizes the effectiveness of the three types of fire control systems. In the manual system, the tracking, estimation and prediction processes, are performed by the man and the machine serves only to orient the gun line in accordance with the information provided by man. The tracking is performed by the man in the disturbed reticle and stabilized sight-director systems, however it is accomplished differently. The estimation and prediction processes are also mechanized differently in these two types of fire control systems. One of the important inherent advantages of a stabilized sight-director system compared to a disturbed reticle system is the decoupling of the tracking process from the estimation and prediction processes. The turret and gun position serve as the reference from which the reticle is distrubed in the disturbed reticle system. Involvement of the human gunner in the turret loop for the distrubed reticle system and his absence from the turret loop for the

stabilized sight-director system is a distinguishing feature of the systems. The tracking process is therefore more isolated from the estimation, prediction, and gun pointing processes in the stabilized sight-director system.

Disturbed Reticle Fire Control System

One fire control configuration in current use is the disturbed reticle concept. The following discussion is intended to describe in detail the functioning of the disturbed reticle fire control system and identify the four processes, showing how each is related to the other. Figure 9 describes the signal flow in such a system and the four major processes have been identified in terms of where in the system each is accomplished.

The input to the system is the LOS from the target to the reticle of the tracking system. The human operator, present in most current systems, moves the handle bar controller to align the reticle of the tracking system to be coincident with the target. The ability of any human controller to accomplish this task defines the quality of the tracking process. Handle bar controller output, which is directly related to the LOS rate, is used to drive two independent subsystems. The first is the turret servo which is commanded to rotate at a rate directly proportional to the handle bar controller deflection. The second subsystem driven by the handle bar controller is a lead screw servo and reticle system. The displacement of the lead screw servo is directly proportional to the filtered handle bar controller deflection multiplied by the projectile time of flight. The lead screw displacement is used to position the reticle of the tracking system.

These are two distinct feedback signal paths in the disturbed reticle configuration and the human is a series subsystem in both paths. Another important observation is to note that the signal loop made by the turret servo-man-handle bar controller is a degenerative feedback loop because of the negative summing junction. The signal loop made by the filter-time of flight lead servo-reticle servo-man handle bar controller is a regenerative feedback loop because of two negative summing junctions. During normal operation of the disturbed reticle system, the performance of these two feedback paths give rise to a dynamical system that exhibits some undesirable performance characteristics. Without further crossfeed compensation, the closed loop performance of the disturbed reticle system is at best marginally stable and at worst unstable. To overcome this condition, compensation signal paths are added. The basic compensation is a tachometer generator signal from the lead screw servo which is combined with the turret servo error signal. This composite signal is fed to the turret servo and the reticle servo to compensate for the dynamical mismatch that occurs in the reticle and turret servos. However, there is no such thing as a perfect compensation and the undesirable performance characteristics alluded to earlier can never be completely nullified, not to mention the potentially precarious situation that might occur if any failure or shift occurs in the compensation paths.

The important thing to observe about the root locations in the figures 10 and 11 is that there are numerator roots in the right half of the S plant. This arises from the basic disturbed reticle configuration and must be considered a fixed element phenomenon in this type of system. The poles or denominator roots describe the system operating point for a system gain of zero. The zeros or numerator roots describe the system operating point for a system gain of infinity. The dotted trajectories connecting these two extremes are a pictorial description of the operating point loci for all intermediate gains. These systems exhibit conditional stability because of the presence of positive feedback in the equivalent transfer function between B and A. These are different closures than exist for a negative feedback that occurs when both the reticle and turret crossfeeds are present as shown in Figure 12. The existence of these simultaneous crossfeeds from the lead screw servo and turret servo error to the turret servo and reticle servo tend to offset the non-minimum phase root condition shown in Figures 10 and 11.

In summary, it is the location of the operating points that determine the system stability characteristics. The frequency content of the tracking error is directly related to the operating points, but equally important is the magnitude of the tracking error which is influenced by the location of the numerator roots of the closed loop transfer function. These effects are interrelated, but the fundamental underlying requirement is to achieve an adequate stability margin of the closed loop system. This stability consideration is important for fire control system performance and the designers must take these factors into account. The end result is system performance which may be acceptable or not acceptable.

It can be asked why so much concern about this situation because disturbed reticle systems have performed satisfactorily in the past. Perhaps this is so, but with the introduction of maneuvering targets, the performance of this type of system may be adversely affected. When the target LOS, θ_{in}, shown in Figure 9 moves at a constant rate, the human operator is required to move the handlebar controller a nominal fixed amount. The turret servo develops a fixed nominal rate and the lead screw servo assumes a fixed nominal position. It then

becomes the task of the human to perturbate the handle bar controller about this nominal position in order to minimize the tracking error. When the target LOS rate is not constant, which is the situation for maneuvering targets, the handle bar controller must be moved consistent with the changing target LOS rate. The nominal handle bar controller position is not the only difference in the system operation for maneuvering targets. The turret servo accelerates and decelerates and the lead screw servo is constantly being driven to a new position. The position of the reticle is a result of these two signals paths. The dynamic performance mismatches are guaranteed to be greater than for the non-maneuvering targets and the tracking performance will be degraded. This degradation occurs from the inability of the closed loop system to accurately null the constantly changing target LOS rate. The extent of this degradation may not be immediately obvious to the casual analyst, but the oscillatory nature of this degradation will be observed once a sufficiently close survey of the tracking error is made. It is imperative that the resulting stability margin of the closed man-machine system be large to insure acceptable performance against maneuvering targets.

Recent work has shown that tactical targets can execute maneuvers of such a nature that when projectile times of flight of 1.5-2.0 sec are considered, target induced motion after projectile firing will cause excessive miss distances when linear predictor fire control systems are assumed and more over these miss distances can be significantly reduced when nonlinear or higher order predictor fire control systems are employed. These observations indicate lower boundary miss distances are possible for non linear lead systems. When this situation is presented to the fire control designer, his inclination will be to consider the possibility of including nonlinear prediction in the fire control system. In the disturbed reticle configuration shown in Figure 9, this may be a design impossibility because of the level of tracking performance obtainable from the operation of the disturbed reticle systems. To be more specific, the tracking error to develop usable target accelerations for nonlinear prediction is required to be smaller than the tracking error for first order prediction. The trade-off between the propagated system induced tracking errors for the nonlinear estimation process must be offset by the target induced prediction error improvements realized by the higher order prediction. The key ingredient for this situation to exist in a fire control system is to have high quality tracking errors.

If the human tracker is replaced by an automatic tracker the performance limitations imposed by the loop structures in a disturbed reticle system may negate the potential improvement attainable from the improved tracking. It is the coupled nature of the tracking, estimation, prediction, and stabilization process occurring in the disturbed reticle configuration that restrict its growth to better fire control system performance, especially against maneuvering targets.

Stabilized Sight-Director Fire Control System

A stabilized sight-director fire control system, shown in Figure 13 is actually two distinct systems that are brought together to accomplish the tracking, estimation and prediction processes of a fire control system. Stabilization of the tracking system is independent from stabilization of the turret. The stabilized sight is decoupled from turret and hull motion by the reverse torquing of the outer gimbal of the tracker to account for distrubances of the tracker base which is mounted on the turret. This decoupling enhances the ability of the tracker to maintain coincidence between the sight reticle and the target LOS. The stabilized reticle position can utilize both position and rate feedback to augment the stability of the sight. The orientation of the sight reticle is therefore an independent process from the turret motion.

Position and rate of the LOS are fed to a filter or estimation process to determine the necessary information about the LOS to the target that will be needed to offset the turret servo from the stabilized tracker. Multi-variable, sub-optimal technology can be applied to further improve the quality of tracking that can be realized from the stabilized sight-tracker. Therefore either linear or non linear estimates of LOS movement can be considered as possibilities. If LOS accelerations are to be estimated, the appropriate modeling of target dynamics and tracker uncertainties will be required to insure that the degree of suboptimality is not excessive. One very significant plus that couples the estimation and tracking process in a favorable manner is the utilization of sight line rate aiding feedback to the tracker obtained from estimation of the target rates and acceleration. This concept relaxes the task of the human tracker or auto-tracker and will improve the minimization of tracking error.

Output of the target state estimator is used in two separate paths. The first path uses $\dot{\theta}_T$ and $\ddot{\theta}_T$ to drive the turret servo as a director to follow the tracker LOS. The second signal path combines target state estimates with projectile time of flight and offsets the gun from the tracker LOS by the appropriate value to permit intercept of projectile and target a time of flight later.

Performance of the stabilized sight-director system should not be compromised by maneuvering targets to the extent that the disturbed reticle system is compromised. The basic reason for this is that the tracking system is essentially decoupled from the lead prediction system. However, there are some inherent stabilization problems that can occur in this configuration and they are accentuated by the temptation to obtain high preformance of the gun pointing process. The argument goes as follows: with increased tracker performance, the gun stabilization servo can be made to perform more rapidly, thereby increasing the overall capability of the system. However, with increased performance being required of the turret servo to follow the turret commands, the stability of the turret servo may be compromised because of the high gains in the director-follower loop. Experience with similar types of systems has shown that because of non-rigid gun tube and hull structures, the follower loop system must be phase stabilized and not gain stabilized, as is the case for less responsive systems such as disturbed reticle systems. This requires sophisticated compensation circuits to overcome system instabilities.

The stabilized sight is identified between the target input and the sight output in Figure 13. It in turn drives the gun turret servos which are used to position the base of the stabilized sight. The signal flow diagram and root loci for the stabilized sight-director system is shown in Figure 14. This is the same basic root locus obtained in the disturbed reticle system when the cross feeds were included. The dotted lines show the movement of the stability as the gain is increased. The addition of series compensation circuits in the tracker transfer function; such as $\frac{T_1 S+1}{T_2 S+1}$, which can easily be added in a straight-forward manner will alter the shape of the loci to obtain an optimized operating point, which would be difficult in the disturbed reticle system. The fundamental purpose of the tracking process is to align θ_S with θ_T. Simultaneously any disturbances on the stabilized sight are compensated by orientation of the sight base thereby simplifying the tracking task.

CONCLUSIONS

The inherent ability of a stabilized sight-director fire control system to decouple the tracking estimation, prediction and gun pointing processes may be exploited to improve effectiveness when engaging maneuvering targets. Accurate tracking is necessary for non linear prediction and multi-variable, sub-optimal design technology is required to achieve the needed accuracy of the target state estimates for mechanizing nonlinear prediction. Further studies are required to identify the specific details of the resulting system design. A complementary methodology employing stability and performance analyses will assist in this quest.

ACKNOWLEDGEMENT

The authors thank Mr. Warren Muehlberger for drawing the figures and Ms. Sharon Taylor for typing the manuscript.

REFERENCES

1. Burke, Harold, "Fire Control System Performance Degradation When A Tank Gun Engages A Maneuvering Threat" XVII US Army Operations Research Symposium, Ft. Lee, VA 6-9 Nov 1978.

2. Leathrum, Dr. James F., "An Approach To Fire Control System Computations and Simulations", US Army Materiel Systems Analysis Activity Technical Report No. 126, April 1975.

3. Gelb, Arthur, "Applied Optimal Estimation", MIT Press, 1974.

4. Burke, Harold H., Perkins, Tony R., Leathrum, James F., "State Estimation of Maneuvering Vehicles Via Kalman Filtering", US Army Materiel Systems Analysis Activity Technical Report No. 186, October 1976.

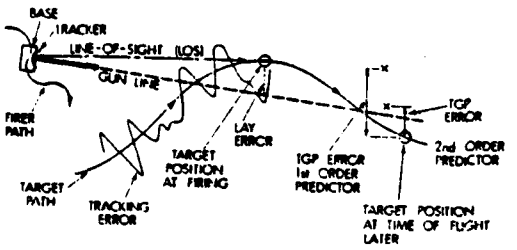

Figure 1 Fire Control System Error Sources.

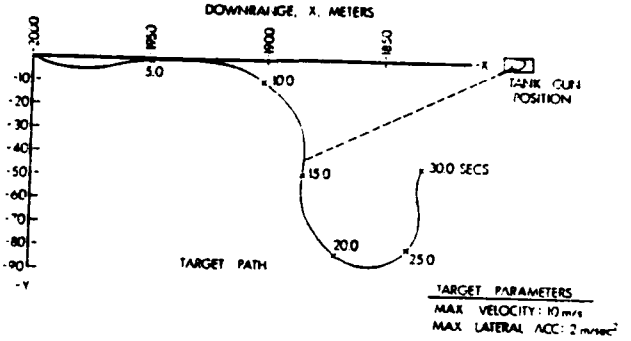

Figure 2. Typical Maneuvering Target Path.

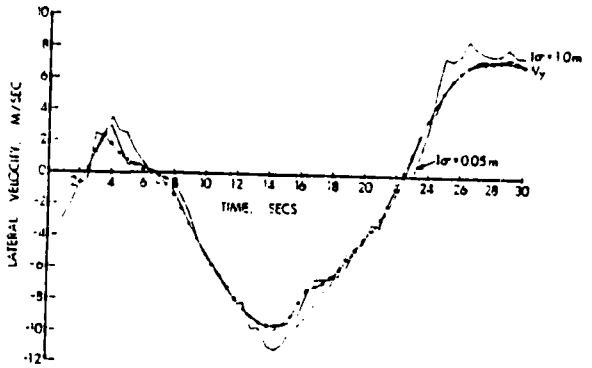

Figure 3. Sensitivity of Velocity Estimates to Observation Noise.

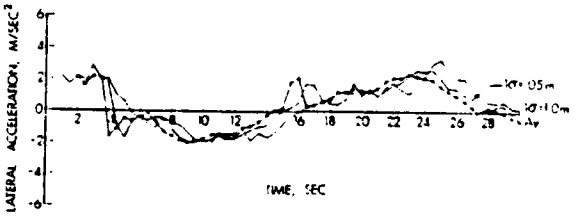

Figure 4 Sensitivity of Acceleration Estimates to Observation Noise.

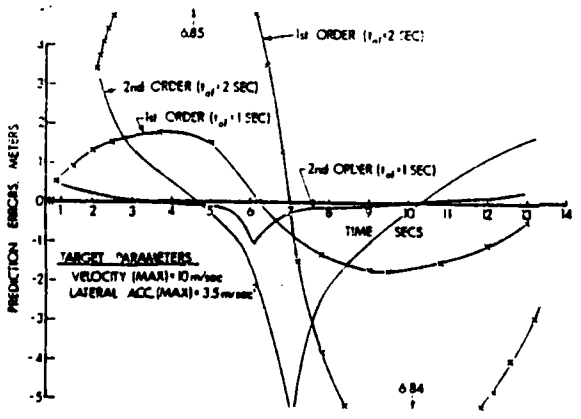

Figure 5. Effects of Time-of-Flight on Prediction.

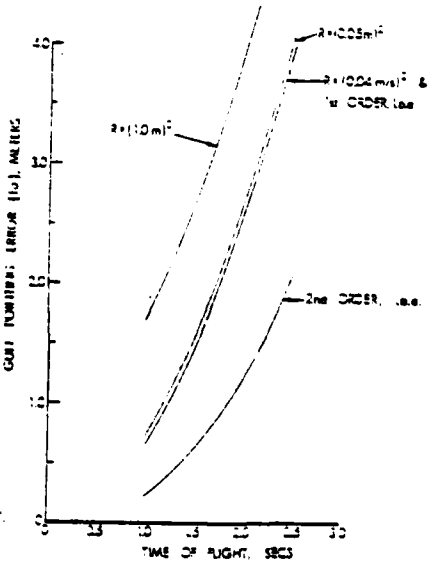

Figure 6. First Order Prediction Errors

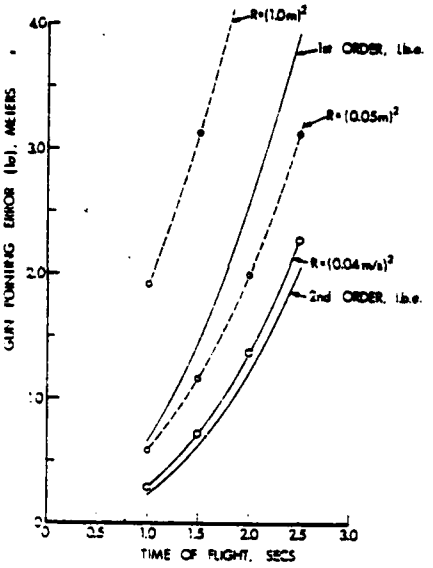

Figure 7 Second Order Prediction Errors.

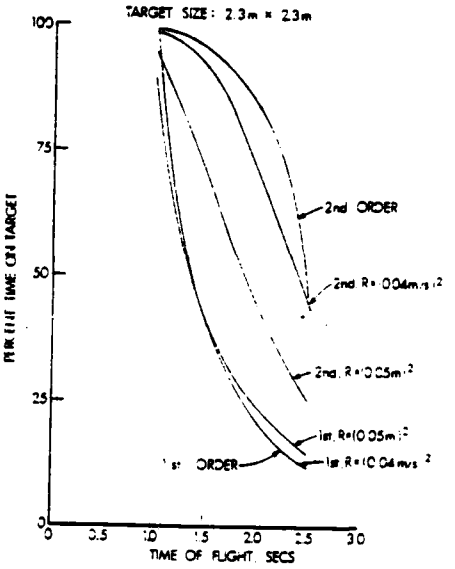

Figure 8. Time on Target.

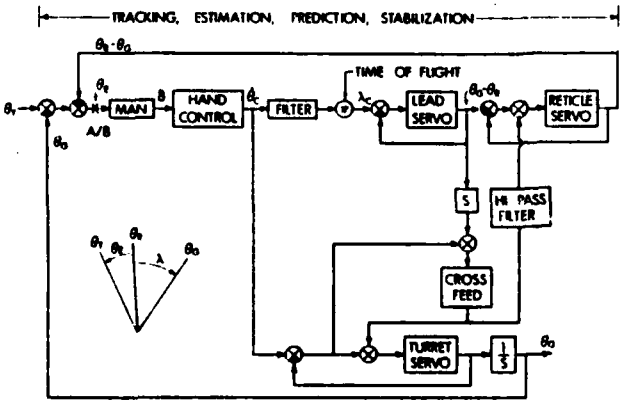

Figure 9 Disturbed Reticle Fire Control System.

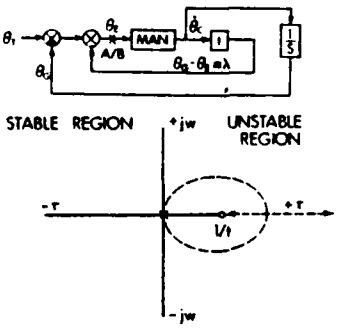

Figure 10 Disturbed Reticle Root Locus, Fixed Elements.

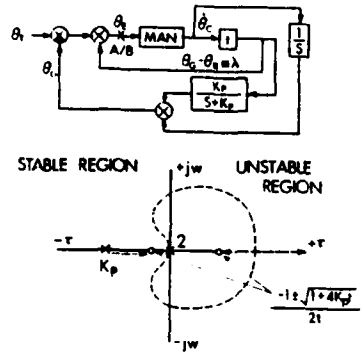

Figure 11. Disturbed Reticle Root Locus, Turret Servo Crossfeed.

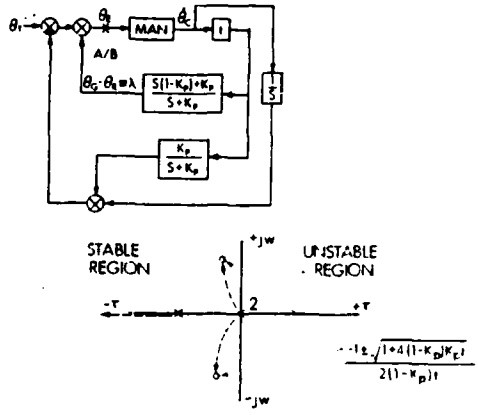

Figure 12. Disturbed Reticle Locus with Turret Servo and Reticle Crossfeeds

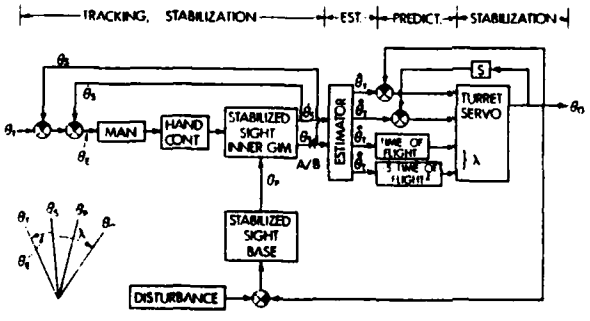

Figure 13. Stabilized Sight-Director Fire Control System

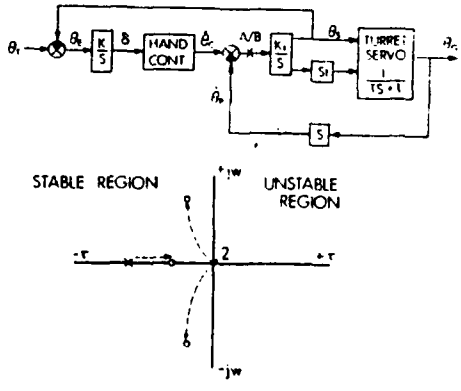

Figure 14. Stabilized Sight-Director Root Locus.

Next page is blank.

FOR PRESENTATION TO

SPECIAL INTEREST GROUP ON CONTROL THEORY

ABSTRACT

DETECTION AND INITIATION OF FIRING COMMAND FOR AN ACCELERATION PREDICTOR FIRE CONTROL SYSTEM ENGAGING MANEUVERING TARGETS

H. H. Burke - AMSAA

Maneuvering targets degrade the performance of all state of the art predictive fire control systems. Anti-aircraft guns, and tank guns are the two main weapon systems whose effectiveness is lessened by the presence of maneuvering targets. The application of the methodology described in this paper will significantly increase the performance for these systems, especially when the jinking or agile movement of the target increases.

A gun fire control system's function is to offset the gun line from the target line-of-sight to cause a projectile to intercept the target a time-of-flight after firing the gun. Two classifications of target motion occur; non-maneuvering and maneuvering. The projectile-target closest approach is a measure of miss distance and the performance of the gun fire control system. Non-maneuvering targets require a constant offset between the target line-of-sight and the gun line. The magnitude of the required offset is the product of the target velocity perpendicular to the line-of-sight and the projectile time-of-flight. Maneuvering targets require a time varying offset having a magnitude related to the non-maneuvering target offset plus an additional amount related to the target acceleration, acceleration rate, etc., perpendicular to the line-of-sight combined with the appropriate functions of projectile time-of-flight. The two most familiar fire control systems use (1) target velocity and (2) target velocity and acceleration combined with time-of-flight to determine the gun line offset. Recent application of sub-optimal estimation methodology, specifically Kalman filtering has resulted in the development of velocity plus acceleration controlled offsets that have significantly increased the performance of gun fire control systems when maneuvering targets are engaged. A penalty is associated with the estimation of accelerations. Whereas, it is relatively simple to estimate velocities, such is not the case for accelerations. As projectile flight times increase the benefits derived from acceleration estimates are penalized by the errors introduced in the offset calculation by the "noise". Current tactical mobility indicates that maneuvering targets require target acceleration estimates in addition to target velocity estimates to calculate effective gun line offsets. As projectile time-of-flight increases the benefit of this offset philosophy is degraded.

When the firing rate of gun is relatively low with respect to the cyclic motion of the maneuvering target, it is possible to correlate the firing times with the zero crossing of the velocity perpendicular to the line-of-sight. The closest approach of the projectile to the target a time-of-flight later crosses from a positive to a negative miss distance in this region and both velocity and

acceleration are used to determine the gun line offset. The LOS velocity zero crossing times can be sensed with rate gyros on fire control system. The apparent displacement, velocity and acceleration of a maneuvering target is viewed from a fire control system situated at some distance. The LOS rate zero crossings are detected by a rate gyro, causing the gun to fire a projectile. The closest approach miss distance between the target and projectile a time-of-flight later indicate the zero crossing character of the closest approach miss distance in this region. Burst fire will be more effective in this region.

DETECTION AND INITIATION OF FIRING COMMANDS FOR AN ACCELERATION PREDICTOR FIRE CONTROL SYSTEM ENGAGING MANEUVERING TARGETS

H. H. Burke - AMSAA

DEVELOPMENT OF A FIRE CONTROL SYSTEM CONCEPT TO IMPROVE PERFORMANCE AGAINST MANEUVERING TARGETS

An investigation of the performance of different order predictors for gun fire control systems engaging maneuvering targets was conducted in 1977 and reported on in Reference 1. The intent of that study was to demonstrate the theoretical reduction in miss distance that was obtainable, assumming perfect tracking of a maneuvering target. The notion that fire control systems should consider second order or acceleration terms in the prediction of the gun line was introduced as a possible alternative to the present first order or velocity term used in current fire control systems. In 1978 a paper presented at AORS XVII (Ref 2) extended this work and discussed progress in the technical area of analytical describing maneuvering targets for the purpose of studying fire control system performance. The three processes taking place in all fire control systems were identified as tracking, estimation and prediction (There is a fourth process, pointing which was added later). The three basic known types of fire control systems; manual, disturbed reticle, and stabilized sight-director were described and compared in a basic manner. Prediction characteristics of first and second order systems were discussed and the relative magnitude of fire control system errors from the tracking, estimation, and prediction processes were described. A brief mention of a firing doctrine utilizing second order prediction to maximum advantage was presented (This idea

(1) AMSAA TR 234, Aug 78.

(2) Given at XVII AORS, Nov 78.

was not exploited until recently and later in this paper it will be shown that the fundamental utilization of this firing doctrine is the concept that can be easily mechanized and applied to tank gun fire control systems, with results that offer major performance improvement over existing first order prediction concepts) A paper describing the application of sub-optimal state estimation design methodology to the development of improved fire control systems was the subject of Reference 3. Some of the earlier work was contained in this paper along with the introduction of the stability characteristics of the two main fire control concepts; disturbed reticle and stabilized sight-director. It was argued that the inherent performance of a stabilized sight was superior to a disturbed reticle because the tracking, estimation and prediction processes were more decoupled and therefore each process could be designed to function better. Some results presented in Reference 3 indicated that the so called "lower bound" performance for second order predictions was superior to first order predictors for an analytically generated path when tracking noise was introduced in the form of uncorrelated noise. This advantage decreased and for larger values of tracking noise an inversion in performance between the two prediction orders occurred. This trend was used to argue that the superior tracking performance of a stabilized sight-director system would enhance the benefit of second order prediction. Another method of deciding on the benefits of the two orders of predictors was offered; time on target. It was also shown that for the analytically modeled target motion being studied, that the basic shape of the prediction error for first and second order systems was different, and it was believed that this was the fundamental reason that the time on target indication showed that for low tracking errors, second order

3) Given at Univ of Pitt Modeling & Simulation Symposium, Apr 79.

prediction was superior to first order prediction. A separate AMSAA Interim Note (Reference 4) was written in May 79. The purpose of this paper was to more fully develop the argument that predictor orders were all improtant in determining the distribution of errors in a fire control system when maneuvering targets are engaged. The target induced errors were claimed to be much larger then the tracking and estimation errors in themselves, but it was admitted that the tracking and estimation errors had to be small to utilize the second order prediction, thereby reducing the target motion induced errors. It was believed and still is that the disturbed reticle fire control configuration can not meet the demands placed on it that second order prediction requires. This will have to be studied in detail before a positive conclusion can be reached.

Throughout the period of this work we have communicated with many different groups, both within and outside the government. One of the items we have shared with them is a data tape having six time histories of maneuvering targets. Initially our work centered on these paths but in order to remove the instrumentation noise (the data gathering system had no relationship to a fire control tracking process, but was rather a ranging system) the paths were smoothed to surpress the high frequency noise, leaving frequencies no greater than 1/8 HZ in most cases. These data were then used to determine the "lower bound" performance measures mentioned earlier. Based on these smoothed paths, the analytically generated maneuvering target generator was developed. For the fire control studies conducted, to determine the relative performance of first and second order predictors, the analytical generated paths were used.

---

(4) *AMSAA Interim Note C-82, May 79*

Some other groups, using the data types supplied them chose to operate directly on the data following the removal of some obvious data timing irregularities. This approach was more in keeping with real world data, in that there were certainly frequencies greater than 1/8 HZ in the data. The filtering algorithms used were therefore required to cope with correlated high frequency noise superimposed on the basic path motion that the analytically generated paths contained. The results obtained from these studies were not as favorable toward second order prediction as the AMSAA studies. In an attempt to sort out the reasons for this difference in reuslts and to determine the mechanism that causes the performance trends to shift when empirical data, such as the empirical data tapes, are used compared to the analytically generated paths, the same data were analyzed by us, using the optimal filtering designs we had developed using the maneuvering path generator. Before discussing the findings of this effort it should be mentioned that in Reference 1, for the "lower bound" studies, it was found that if the cyclic period of the target motion was twice as rapid as the time-of-flight of the projectile, an inversion between first and second order predictors occurred. Three of the paths reported on in Reference 1 had this characteristic and the results are described in Reference 1. It was argued that realistic maneuvering targets would not exhibit frequencies in this region (¼ HZ). The empirical data contained in the subject tapes supplied to the other researchers and now being studied by us probably exhibited such frequencies, not from actual vehicle movement, but from instrumentation imperfections. This was the basic reason for development of the analytical generator, but one of its short comings may

be that the correlated high frequency tracking errors are not realisticly represented. A counter argument to this idea is that the data contained on the tapes does not reflect the correlated tracking error signal for a given fire control system; be it a disturbed reticle or stabilized sight-director system.

However several of the paths studied by some of the other researchers have recently been processed by AMSAA using the same estimation model math developed using the analytical path generator. Some extremely interesting and exciting results have emerged. Initially, time-on-target was used as a figure of merit. Indeed, as some of the other investigators have pointed out, the second order predictor does worse than the first order in some regions and better in other regions of the paths. Where is the cue that controls this performance reversal? Inspection shows that as the cyclic movements referred to in Reference 1, are less than twice the flight time the second order system out performs the first order system and in periods where the cyclic motion becomes more prononunced at higher frequencies, (i.e. higher apparent accelerations) the first order system out performs the second order system. This explains the reversal of performance obtained using the empirical data. The smoothed data having only the basic path motion, with the instrumentation noise removed, did not exhibit a reversal (the frequencies in the data were such that the apparent periods were always greater than twice the time-of-flight.)

It was still believed that in spite of this turn of events, seen from analyzing the empirical tapes, that some advantageous trade-off existed for second order predictors over first order predictors using the empirical

path data. This was based on the fact that the miss distance time histories for the two predictors were entirely different for a given path. This trend is demonstrated graphically, in Figure 5 of Reference 3 for the analytical path generator studies and is repeated for all of the empirical data analyzed from the data tape mentioned. Examples of this are shown in Figure 1 and appendices 2 & 3. As discussed in Reference 3, the trend shown in Figure 1 is not as clear cut when larger values of noise are introducted, but it does still exist in practice theory according to the empirical paths we hava analyzed Thus far this trend does persist with suprisingly accurate timing. This situation speaks well for the model we are using for the sub-optimal estimator and for the fact that it was developed using an analytical path generator model rather than empirical data. The main effects described in Figure 5 of Reference 3 and Figure 1 of this paper are (1) the miss distance for a second order predictor passes through zero a time-of-flight increment after the apparent velocity sensed by the fire control system passes thru zero (2) the miss distance for a first order fire control system passes thru zero a time-of-flight after the apparent velocity passes thru its maximum value and (3) when the time-of-flight exceeds the time remaining before the apparent acceleration reverses direction, the miss distance errors for a second order predictor becomes very large.

These findings have been found to exist in the empirical data and can be utilized to develop a fire control system concept that will greatly improve performance against maneuvering targets, over existing fire control systems using no prediction or 1'st order prediction. The concept has the inherent built in ability to revert to first order automatically

and become second order when required. It is based on the firing doctrine concept mentioned in Reference 2 which was ignored by us for a long time in favor of the time on the target advantage that second predictor provided when analytical paths were studied. Noise detracts from the comparison. The cue or sensing device required is a rate gyro to sense LOS rate. As the LOS rate crosses zero, the fire control system will fire and the projectile will impact the target a time of flight later. The timing accuracy of these "firing windows" is very accurate, even when the empirical data tapes are used. In some cases there is less time interval in the "firing window" than others, but for the majority of opportunities, based on the logic of the LOS rate passing thru zero, the time intervals vary between 100 ms and 800 ms. When the firing rate is in the vicinity of 1 round/8 sec for tank guns, this rationale is reasonable, in that the best opportunity to hit the maneuvering target is determined by utilizing these "firing windows". When the target is not maneuvering too much, the accleration levels occurring at these regions where the LOS rate passes thru zero are not significant and do not corrupt the basic goodness of first order prediction. Analysis of the empirical data seems to indicate this effect.

It is believed that these findings justify the incorporation of second order prediction in fire control systems, and that instead of assuming a "fire hose" or arbitrary firing time to compare different predictors, that a firing doctrine similar to the one just described be adopted. This concept degrades gracefully to the manual offset or no predictor case ar the maneuver level lessens and both velocity and acceleration are small.

The inherently better tracking capability of a stabilized sight-director system will provide a more precise sensing of the "firing window" than can be obtained with a disturbed reticle system. Also this firing doctrine can be used to advantage for a rapid burst fire gun by firing the burst in this "firing window".

For cyclic frequencies (be they real maneuvering vehicle movements or tracking line-of-sight motion) there is a penalty for higher frequencies and extended time-of-flight as shown in appendix 1. This has implications on gunner sight line movement frequency characteristics and long engagement ranges if there is validity to the serpentine or cardoid model in representing real world vehicle maneuvering. The results of the analysis reported in appendices 2 & 3 for ATMT empricial paths 433 and 315 indicate there is such validity and a second order parabolic predictor can predict serpentine vehicle movement in this region of apparent velocity nulling (region 1) with errors described in appendix 1. When the first order predictor outperforms the second order predictor, close inspection of the region reveals that the cyclic frequencies are larger ($\geq$ ¼ HZ). It is believed that suppression of these tracking frequencies will be a minor problem to cope with by the fire control designer.

Harold Burke 4/21/80

HAROLD H. BURKE

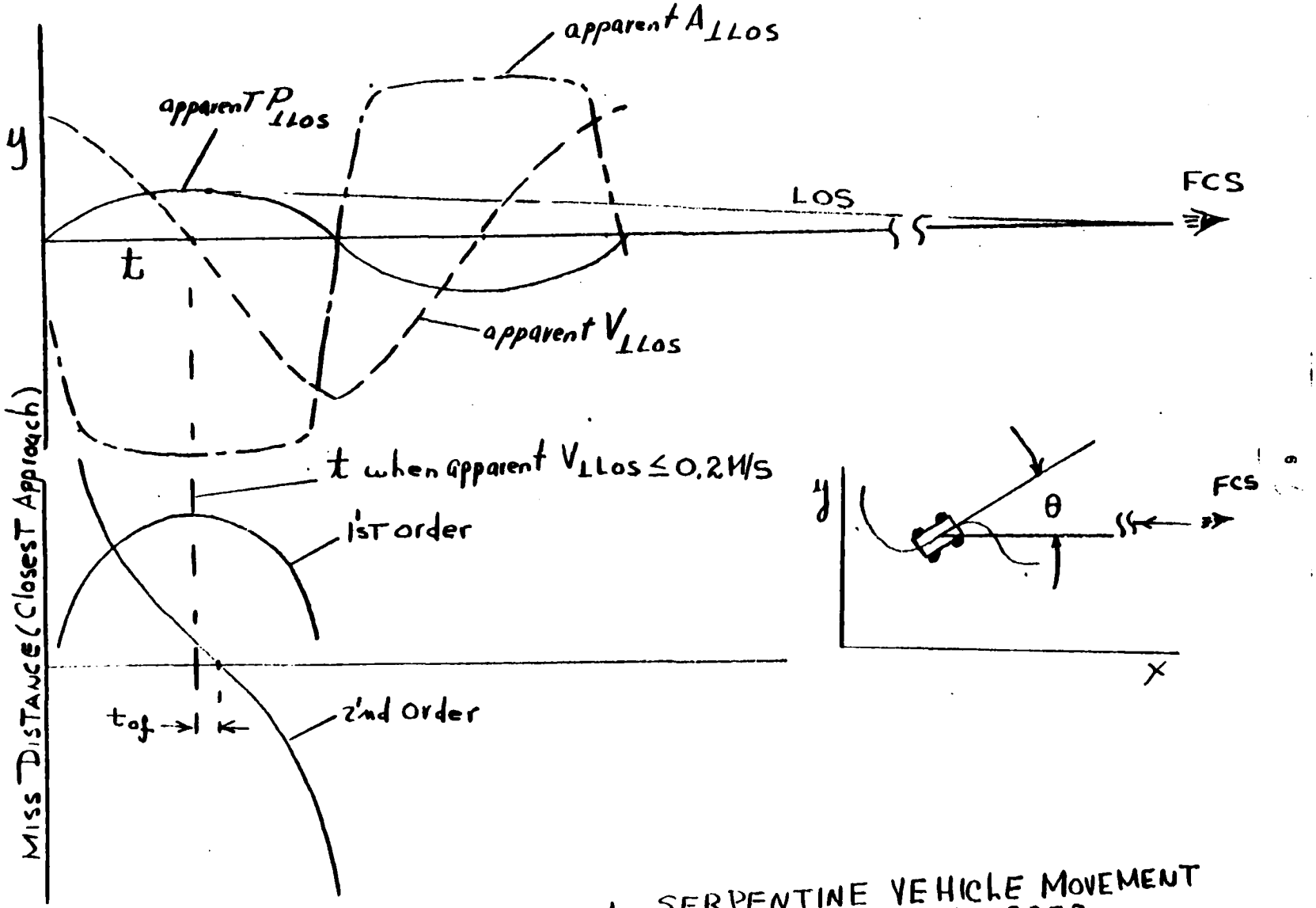

Figure 1- SERPENTINE VEHICLE MOVEMENT MODELED 1'ST/2'nd ORDER PREDICTOR MISS DISTANCE

3/13/80
H.B.

APPENDIX 1

2'nd ORDER PREDICTOR AND SERPENTINE MANEUVERING VEHICLE MOVEMENTS

The maneuvering path generator is built to generate movement of a maneuvering vehicle from point A to B as though the vehicle moves on arcs of circles interconnected by transition segments.

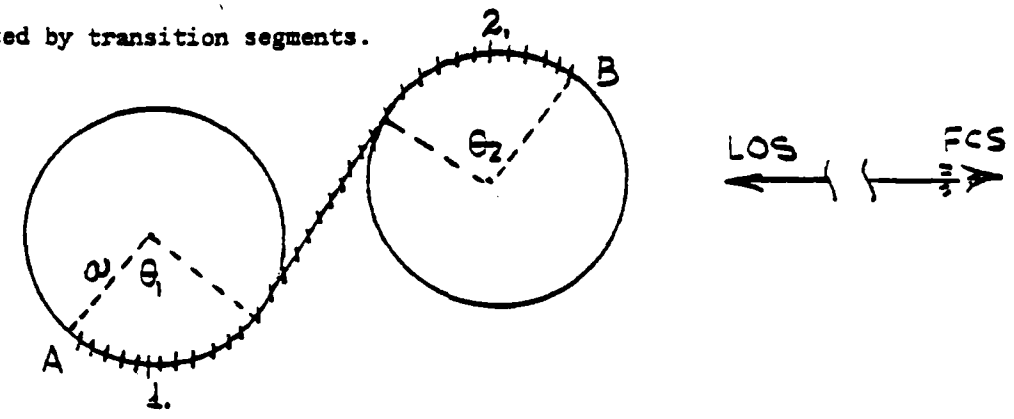

If this movement is viewed from a distance, such that it is approaching the FCS, and if the velocity of the vehicle is constant thru arcs θ_1 and θ_2, the apparent positions, velocities and accelerations perpendicular to the LOS can be assumed to be simple harmonic motion. Points 1 and 2 are the places where the apparent position reverses direction, apparent velocity crosses zero and apparent acceleration peaks. A detailed discussion of this set of conditions is contained in a paper delivered at AORS XVII, Nov 79. This "serpentine" math model has been in a sense validated by the fact that for the ATMT empirical data tapes, at least in the regions surrounding points 1 and 2, these apparent position, velocity and acceleration trends exist. The next question to address is how well does a second order or velocity plus acceleration offset predictor work for this region about 1 & 2. Assuming the analytic model of apparent vehicle motion from the maximum position point at t=0, the equation relating apparent movement to time is $y = -a - a\cos\omega t$

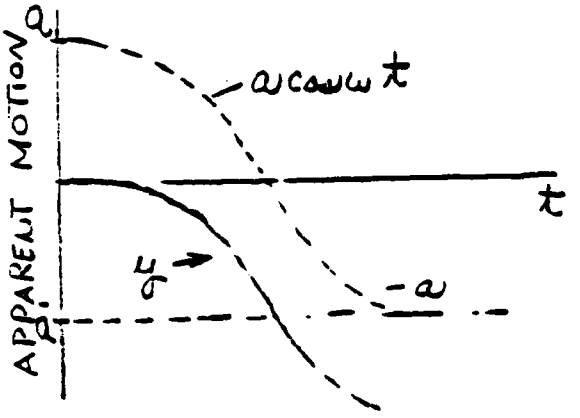

where a = amplitude or radius of circle

ω = cyclic frequency of movement

t = time

Representing cos ωt in a series, we have

$$\cos \omega t = 1 - \frac{(\omega t)^2}{2!} + \frac{(\omega t)^4}{4!} -$$

Then $y = -a + [a - \frac{a(\omega t)^2}{2!} + \frac{a(\omega t)^4}{4!}]$

or

$$y = -(a\omega^2)\frac{t^2}{2!} + \frac{a\omega^2 t^2}{2!}\frac{\omega^2 t^2}{12}$$

But $a\omega^2$ = magnitude of apparent acceleration at point 1 (A_{pp})

Then

$$y = -A_{app}\frac{t^2}{2} + A_{app}\frac{t^2}{2}\frac{\omega^2 t^2}{12}$$

or

$$y = -A_{app}\frac{t^2}{2}\left[1 - \frac{\omega^2 t^2}{12}\right]$$

The apparent movement of y for the serpentine math model of the path generator from point 1 (t=0) approximates the parabolic second order predictor concept, ie:

$$y = \dot{y}_{to} \cdot t - App \frac{t^2}{2}$$

But $\dot{y}_{to} = 0$
Then $y = -App \frac{t^2}{2}$

with the $\frac{\omega^2 t^2}{12}$ term representing the error between the simple harmonic and parabolic curves.

To obtain some insight into the magnitude of this error the following table shows the error term for various cyclic frequencies and times of flight

	$(\omega^2 t^2/12)$		
t (time of flight)	1 sec	1.5 sec	2.0 sec
ω = 1/4 HZ (1.5 r/s)	0.1875	0.421	0.75
ω = 1/8 HZ (.785 r/s)	0.05	0.078	0.21
ω = 1/10 HZ (.628 r/s)	0.033	0.049	0.13

Plotted, this demonstrates the degrading relationship that ω(cyclic frequency) has on the ability of a second order predictor to predict simple harmonic motion in this localized region (point 1).

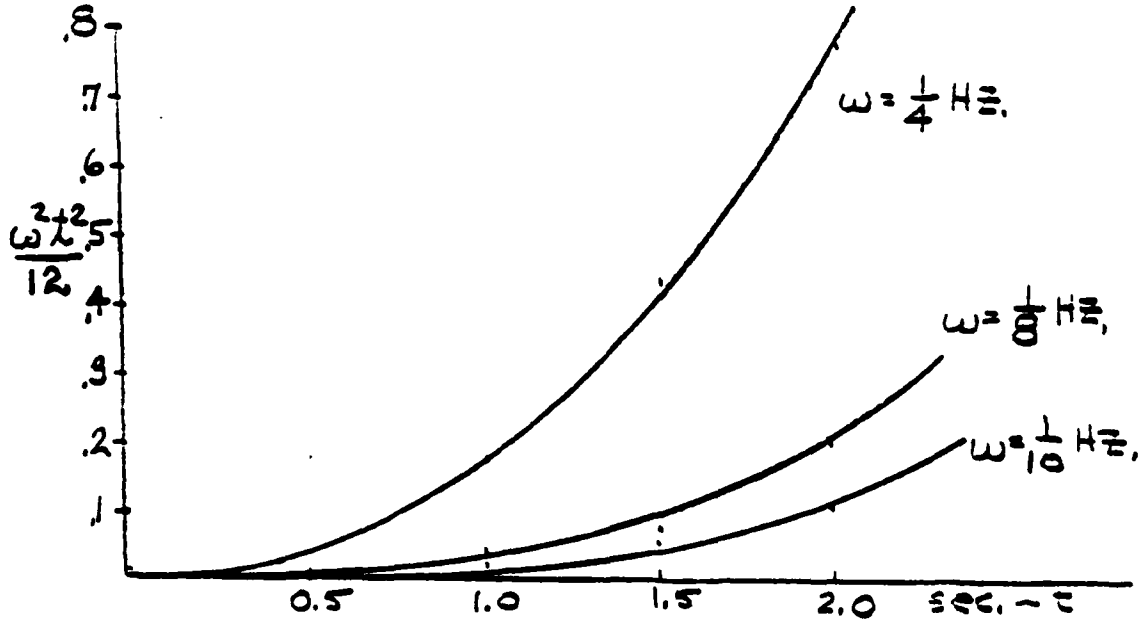

APPENDIX 2

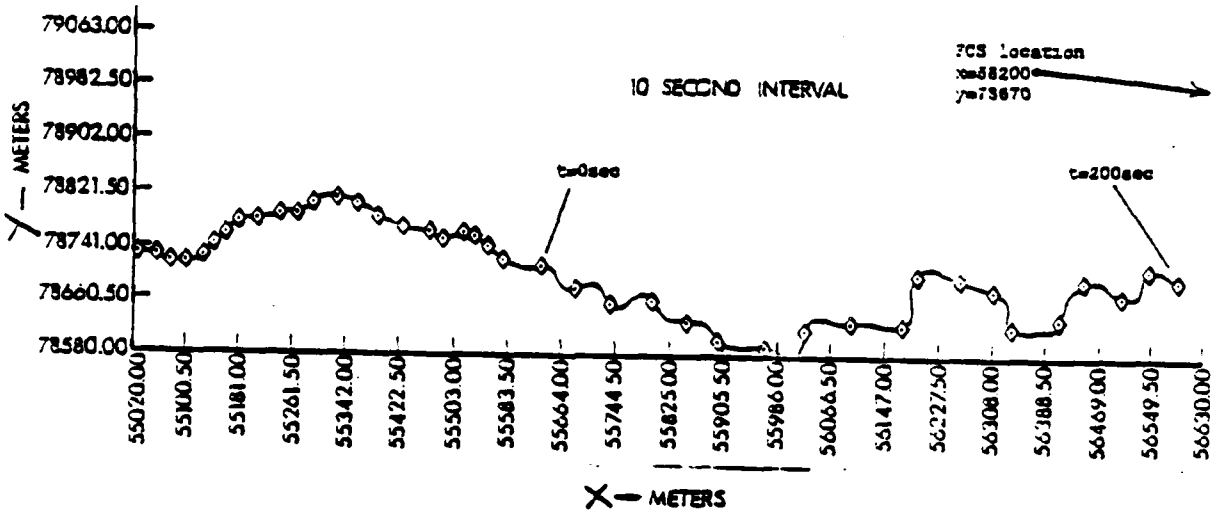

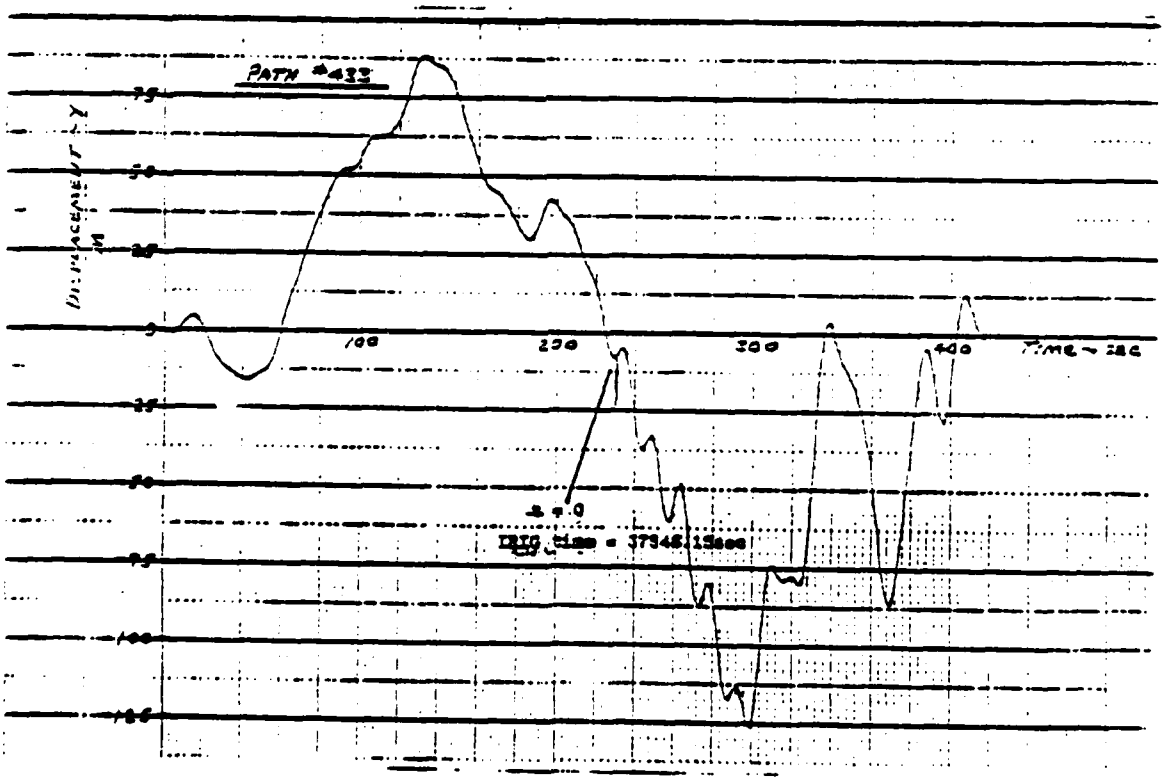

ATMT Path 433, M60 Vehicle

THIS PAGE IS [illegible]
FROM COPY FURNISHED TO DTIC

Inclosure 1a

ATMT Path 433

T_F = 1.5 sec.; Filter: Q = 6.,1., R = .01

(1)

Firing Occurs At	Miss Distance 2'nd Order (M)		Miss Distance 1st Order (M)
2.9s			
1.5tof	4.2	3.09	4.66
4.4s	4.3	1.62	3.98
	4.4	0.19	3.25
	4.5	-0.48	2.80
	4.6	-0.17	2.90
	4.7	-0.28	2.78

V_X=3.2 M/S

V_Y=4.3 M/S

$\theta = \tan^{-1} \frac{V_Y}{V_X} = 39.6^\circ$

(2)

Firing Occurs At			
	12.7		
	12.8	+0.196	-1.94
11.5s	12.9	- .484	-2.44
1.5tof	13.0	- .69	-2.55
13.0s	13.1	- .81	-2.59
	13.2	-1.23	-2.91
	13.3	-1.69	-3.26
	13.4	-1.94	-3.35

V_X=7.5

V_Y=2.2

$\theta = 16.3^\circ$

ATMT PATH 433

(3) Firing Occurs At	Miss Distance 2nd Order (M)		Miss Distance 1st Order (M)
16.2s			
1.5tof			
17.7s	17.4	- .338	2.81
	17.5	- .491	2.64
	17.6	-. 458	2.57
	17.7	- .253	2.85
	17.8	+ .148	3.17
	17.9	+ .766	3.52
	18.0	+ .846	3.57

V_X = 5.5

V_Y = 3.5

θ =32.5°

(4) Firing Occurs At			
24.8s	26.0	-4.891	-7.21
1.5tof	26.1	-4.692	-7.20
26.3s	26.2	-4.216	-6.95
	26.3	-2.12	-5.77
	26.4	- .072	-4.53
	26.5	+2.06	-3.17
	26.6	+3.66	-1.98

V_X = 6.6

V_Y = 6.4

θ = 44.1°

(5) Firing Occurs At			
30.0s	31.1	2.11	4.56
1.5tof	31.2	2.85	4.96
31.5s	31.3	2.12	4.58
	31.4	1.08	4.03
	31.5	.25	3.51
	31.6	- .56	2.94
	31.7	- .98	2.70
	31.8	-1.52	2.34
	31.9	-2.36	1.77

V_X = 4.7

V_Y = 4.5

θ = 43.8°

ATMT PATH 433

(6)
Firing Occurs At
39.3s
1.5tof
40.8s

(acceleration reversal during tof)

V_X = 5.3

V_Y = .121

θ = 1.3°

Miss Distance		
2nd Order (M)		1st Order (M)
40.2	-1.95	-3.25
40.3	-1.12	-2.84
40.4	.45	-1.96
40.5	1.50	-1.28
40.6	1.63	- .996
40.7	1.81	- .732
40.8	2.42	- .239
40.9	3.80	- .681

(7)
Firing Occurs At
40.7s
1.4tof
42.2s

V_X = 5.4

V_Y = .4

θ = 4.2°

41.8	+ .434	1.42
41.9	+ .169	.98
42.0	+ .197	8.54
42.1	- .041	.87
42.2	- .650	.74
42.3	-1.07	.32
42.4	-1.22	.00
42.5	-1.18	- .16
42.6	-1.01	- .19
42.7	-1.04	- .13

(8)
Firing Occurs At
57.8s
1.5tof
59.3s

V_X = 7.1

V_Y = 2.3

θ = 17.9°

58.9		
59.0	-2.85	-3.13
59.1	-2.50	-3.04
59.2	-2.40	-3.12
59.3	-1.81	-2.86
59.4	- .67	-2.27
59.5	+1.09	-1.22
59.6	+2.50	-2.55
59.7	-3.26	+ .343

ATMT PATH 433

(9)

Firing Occurs At
60.5s
1.5tof
62.0s

	Miss Distance 2nd Order (M)	1st Order (M)
61.6	.687	2.47
61.7	.17	2.16
61.8	.46	2.44
61.9	.13	2.32
62.0	− .26	2.13
62.1	− .34	2.07
62.2	− .11	2.17
62.3	+ .26	2.29
62.4	+ .75	2.54

$V_X = 6.7$

$V_Y = 2.3$

$\theta = 18.9^\circ$

(10)

Firing Occurs At
67.0s
1.5tof
68.5

68.1	-1.08	-3.89
68.2	-1.56	-4.19
68.3	-2.87	-4.98
68.4	-2.99	-5.24
68.5	-3.45	-5.63
68.6	-3.57	-5.73
68.7	-3.46	-5.84
68.8	-2.72	-5.70

$V_X = 6.7$

$V_Y = 2.3$

$\theta = 19.4^\circ$

(11)

Firing Occurs At
76.7s
1.5tof
78.2s

77.8	2.42	4.12
77.9	1.83	3.84
78.0	1.33	3.61
78.1	1.19	3.57
78.2	1.68	3.85
78.3	1.78	3.85
78.4	0.47	3.17
78.5	- .380	2.61
78.6	-1.15	1.95

$V_X = 8.2$

$V_Y = 3.2$

$\theta = 21.3^\circ$

ATMT PATH 433

(12)	Miss Distance	
Firing Occurs At	2nd Order	1st Order
81.2s	(M)	(M)
1.5tof	82.2 -1.89	-3.41
82.7s	82.3 -1.71	-3.36
	82.4 -1.38	-3.30
	82.5 - .44	-2.78
	82.6 + .23	-2.34
	82.7 .14	-2.50
	82.8 - .147	-2.70
	82.9 - .55	-3.26
	83.0 -1.67	-3.43
	83.1 -2.06	-3.51

$V_X = 6.9$

$V_Y = 3.6$

$\theta = 27.6^\circ$

(13)		
Firing Occurs At	85.4 .521	2.35
84.4s	85.5 - .360	1.88
1.5tof	85.6 -2.26	.771
85.9s	85.7 3.43	- .019
	85.8 3.03	- .174
(Velocity reversal during tof)	85.9 -2.55	.012
	86.0 1.195	.695
	86.1 .044	1.18
$V_X = 7.7$	86.2 1.028	1.69
	86.3 1.18	1.74

$V_Y = 1.4$

$\theta = 10.3^\circ$

(14)		
Firing Occurs At		
91.6s	92.8 - .74	-2.69
1.5tof	92.9 - .88	-2.75
93.1s	93.0 -1.52	-3.16
	93.1 -1.82	-3.35
	93.2 -1.66	-3.37
	93.3 -1.12	-3.14
	93.4 - .847	-3.04

$V_X = 8.3$

$V_Y = 6.2$

$\theta = 36.9^\circ$

APPENDIX 3

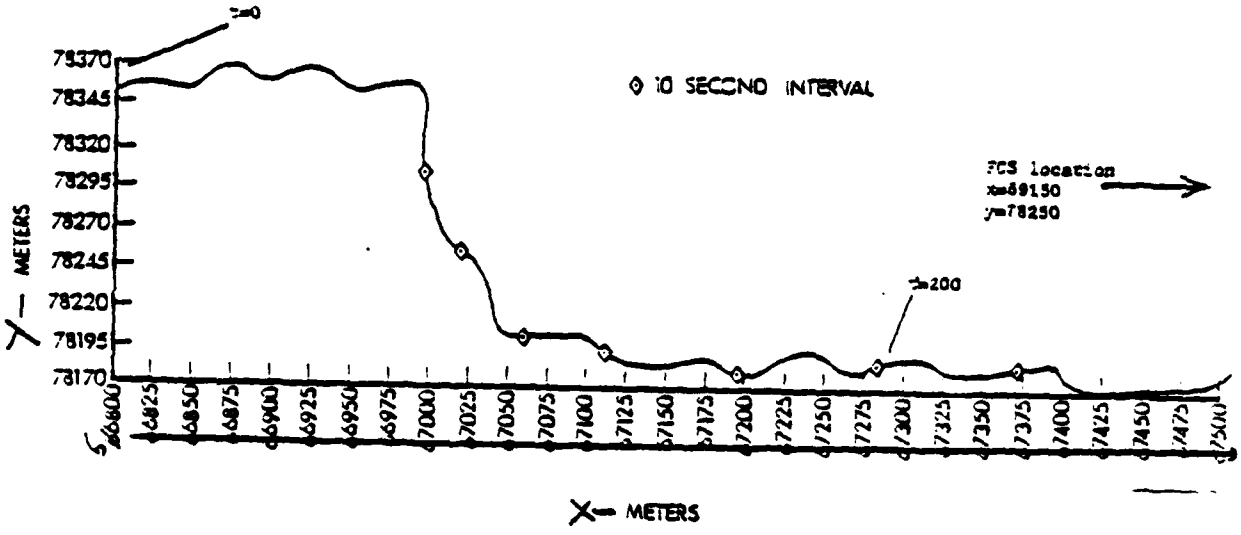

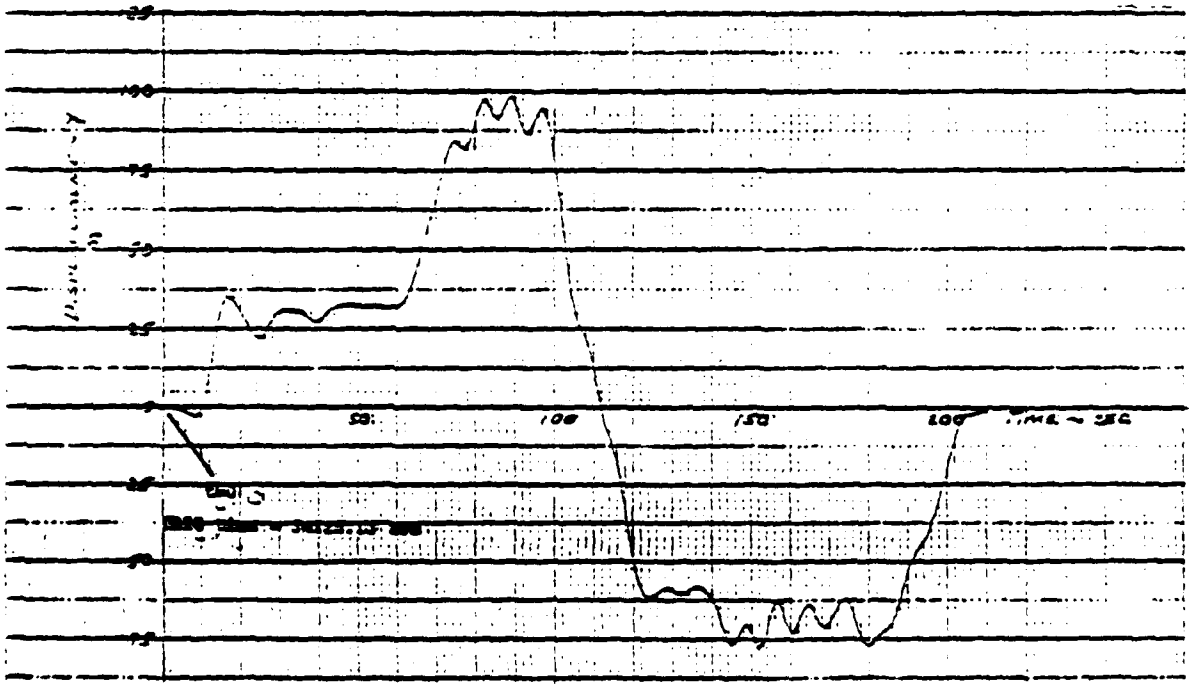

ATMT Path 315, Twister Vehicle

Inclosure 1b

ATMT 315

T_F = 1.5 sec

(1)
Firing Occurs At
7.8s
1.5tof
9.3s

	Miss Distance	
	2nd Order (M)	1st Order (M)
8.9		
9.0	-2.241	- 2.98
9.1	-1.996	- 2.88
9.2	-1.821	- 2.86
9.3	-1.022	- 2.55
9.4	- .374	- 2.51
9.5	- .247	- 2.26
9.6	- .382	- 2.42
9.7	- .556	- 2.58

V_X = 4.8

V_Y = 2.9

θ = 31.1°

(2)
Firing Occurs at

15.6s
1.5tof
17.1s

16.8		
16.9	-1.99	.793
17.0	-2.67	.258
17.1	-2.52	.220
17.2	-1.72	.613
17.3	-1.48	.683
17.4	-1.29	.714
17.5	- .601	.969
17.6	+ .449	1.43
17.7	+1.692	2.021

V_X = 8.2

V_Y = 1.4

θ = 9.7°

ATMT PATH 315

	Miss Distance	
	2nd Order (M)	1st Order (M)
(3) Firing Occurs At		
24.3s		
1.5tof		
25.8		
	25.3	
	25.4	
	25.5 -2.259	+3.46
	25.6 -1.520	-3.09
	25.7 -1.210	+3.01
	25.8 -1.042	+2.96
	25.9 -1.099	+3.00
	26.0 - .812	+2.86
	26.1 - .866	+2.892
	26.2 -1.47	-3.17

$V_X = 7.2$

$V_Y = 3.2$

$\theta = 24.0^\circ$

(4) Firing Occurs At		
29.4s	30.4	
1.5tof	30.5 + .969	1.165
30.9	30.6 + .884	1.092
	30.7 .557	.892
	30.8 + .208	.721
	30.9 - .611	.284
	31.0 -1.65	- .322
	31.1 -2.218	- .707
	31.2 -2.22	- .799
	31.3	
	31.4	
	31.5	

$V_X = 9.6$

$V_Y = .2$

$\theta = 1.2^\circ$

(5) Firing Occurs At		
38.9s	40.0 -1.226	-1.92
1.5tof	40.1 -1.077	-1.86
40.4s	40.2 -1.452	-2.06
	40.3 - .945	-1.79
	40.4 - .313	-1.39
	40.5 + .143	-1.12
	40.6 + .675	- .791
	40.7 +1.360	.257
	40.8 +2.75	- .527

$V_X = 7.2$

$V_Y = 1.3$

$\theta = 10.2^\circ$

ATMT PATH 315

(6)
Firing Occurs At
44.2s
1.5tof
45.7s

$V_X = 1.5$

$V_Y = .25$

$\theta = 9.5^{\circ}$

	Miss Distance 2nd Order (M)	1st Order (M)
45.3	1.28	.977
45.4	1.17	.965
45.5	.647	.698
45.6	- .235	.239
45.7	- .966	- .142
45.8	-1.4	- .455
45.9	-1.53	- .620
46.0	-1.77	

(7)
Firing Occurs At
59.1s
1.5tof
60.6

$V_X = 4.7$

$V_Y = 1.9$

$\theta = 22.0^{\circ}$

60.2	-2.3	2.365
60.3	-2.7	2.369
60.4	-2.5	2.254
60.5	-2.1	1.94
60.6	-1.3	1.46
60.7	- .411	1.12
60.8	+2.12	.908
60.9	+ .472	.655

(8)
Firing Occurs At
74.0s
1.5tof
75.5s

$V_X = 8.0$

$V_Y = 1.7$

$\theta = 12.0^{\circ}$

75.0	.514	1.86
75.1	.324	1.74
75.2	1.16	2.21
75.3	1.51	2.47
75.4	1.24	2.44
75.5	.974	2.37
75.6	- .089	1.73
75.7	- .786	1.31
75.8	-1.25	1.05
75.9	-1.92	.55

ATMT PATH 315

(9)
Firing Occurs At
76.6s
1.5tof
78.1s

$V_X = 6.2$

$V_Y = 4.4$

$\theta = 35.4^\circ$

	Miss Distance	
	2nd Order (M)	1st Order (M)
77.6	-6.35	6.30
77.7	-5.23	6.00
77.8	-4.15	5.77
77.9	-2.29	4.92
78.0	- .740	4.11
78.1	- .025	3.71
78.2	- .244	3.86
78.3	- .656	3.96
78.4	- .665	3.90
78.5	+ .020	3.61

(10)
Firing Occurs At
81.1s
1.5tof
82.6s

$V_X = 6.0$

$V_Y = 6.0$
$\theta = 45.0^\circ$

82.0	3.42	6.57
82.1	3.36	6.32
82.2	2.41	6.71
82.3	1.48	6.21
82.4	- .410	5.33
82.5	-1.30	4.68
82.6	-1.58	3.89
82.7	-1.13	4.04
82.8	- .814	4.08
82.9		
83.0		

(11)
Firing Occurs At
84.3s
1.5tof
85.8s

$V_X = 8.6$

$V_Y = 5.0$
$\theta = 30.2^\circ$

85.4	-3.84	-7.302
85.5	-2.011	-6,251
85.6	- .673	-5.40
85.7	+1.711	-4.01
85.8	+3.46	-2.87
85.9	+4.71	-1.90
86.0	+5.049	-1.23
86.1	4.93	- .957
86.2		

ATMT PATH 315

(12)
Firing Occurs At

87.5s
1.5tof
89.0

	Miss Distance 2nd Order (M)	1st Order (M)
88.6	3.628	5.938
88.7	2.963	5.695
88.8	1.981	5.331
88.9	.850	4.722
89.0	- .678	3.768
89.1	-1.49	3.197
89.2	-1.88	2.817
89.3	-2.13	2.542
89.4	-3.47	1.630
89.5		

V_X = 6.6

V_Y = 4.0

θ = 31.2°

(13)
Firing Occurs At

91.9s
1.5tof
93.4s

93.0	-2.75	-5.86
93.1	-1.68	-5.237
93.2	-1.29	-5.033
93.3	- .743	-4.603
93.4	-1.72	-3.088
93.5	3.03	-2.127
93.6	4.79	- .816
93.7		- .024
93.8		+ .789

V_X = 8.4

V_Y = 4.3

θ = 27.1°

(14)
Firing Occurs At

96.1s
1.5tof
97.6s

97.1	5.2	4.98
97.2	5.6	5.46
97.3	5.4	5.49
97.4	4.6	5.28
97.5	3.8	5.02
97.6	2.3	4.23
97.7	.934	3.43
97.8	.323	3.28
97.9	- .678	2.82
98.0	-1.67	2.26
98.1		

V_X = 1.6

V_Y = 5.0

θ = 72.3°

HYBRID COMPUTER SIMULATION OF COMBAT TANK DRIVEN RETICLE FIRE CONTROL

By John N. Groff
US Army Materiel Systems Analysis Activity

1. INTRODUCTION

The US Army Materiel Systems Analysis Activity (AMSAA) and the Ballistic Research Laboratory (BRL) have jointly developed a man-in-the-loop hybrid computer simulation of a combat tank's turret/weapon stabilization drives and those portions of the fire control that are necessary for lead angle generation. The model that has been implemented on the BRL EAI 690 Hybrid Computer is linear although it does possess the following non-linear features:

- Hand Control Dead Zones
- Response Rates versus Handle Control Deflection

Currently, the simulation is still undergoing development of the gunner's oscilloscope display, scaling of the input/output variables, and programming of the time series software necessary to reduce the data. However, qualitative rather than quantitative information concerning gunner tracking performance is being provided by the simulation.

2. BACKGROUND

In 1978 AMSAA and BRL jointly undertook the responsibility of investigating whether proposed modification to a driven reticle continuous lead insertion system had a significant effect in reducing weapon pointing errors. The basic problem was a response mismatch between the reticle projection unit (RPU) of the gunner's sight and the turret/weapon stabilization drive which resulted in the weapon lagging the RPU. The resulting offset appeared in the sight as apparent tracking error which the gunner attempted to null out. The problem tended to be further aggravated if evasive or sinusoidal target motion was introduced. This tended to produce an oscillatory instability or "rubberband" tracking error effect. The investigation took the form of a paper analysis using available system description documentation. The results of this paper analysis are presented in Section 3 and served as the basis for development of the AMSAA/BRL Hybrid Simulation. Further motivation for the hybrid work was provided by AMSAA's delivery accuracy efforts.

AMSAA has the responsibility of determining quasi-combat hitting probabilities for armored vehicles, and the use of engineering simulation techniques have proved to be useful in performing this work. Currently, engineering simulations for the M60A1, M60A3, and XM1 tanks are being developed in which all major components of these tanks' fire controls, weapon stabilization drive loops, suspension

system as well as terrain profile and human characteristics will be modeled and integrated into a single simulation.

Previous AMSAA man-in-the-loop studies have indicated that the gunner model used in these simulations may not be entirely satisfactory for delivery accuracy work. Part of the problem stems from the fact that the McRurer/Krendel gunner model which will be used does not possess adaptable features, i.e., the ability of the gunner model to make internal adjustments in gain, bandwidth, and neuromuscular reaction time in response to target motion and characteristics of the tracking system in which the gunner is operating. Another inadequacy of the present model is that it is a purely deterministic model lacking any residual randomness.

3. RESULTS OF THE PAPER ANALYSIS

Figure 1 depicts the block diagram of the driven reticle system that is being used in this study.

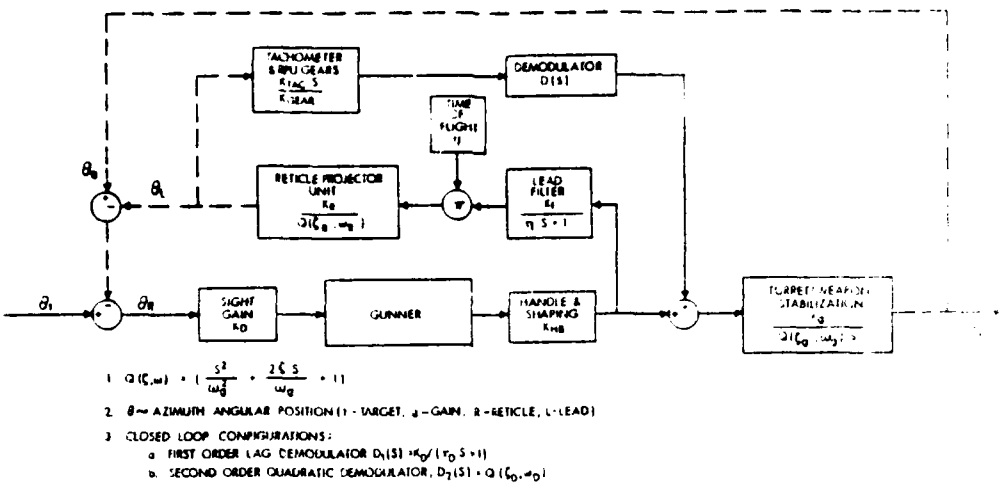

FIGURE 1. DRIVEN RETICLE/CLOSED LOOP CONFIGURATION

A McRurer/Krendal man-model was interfaced with this system and used in the analysis.

The general human transfer function used is of the form:

$$G(s) = \frac{K_g\,(S + \omega_2)\; e^{-\tau S}}{(s + \omega_1)\,(s + \omega_3)} \qquad (3.1)$$

Where, τ is a neurological time delay; K, ω_1, ω_2 are values that the human adjusts for the task at hand. Typically, he adjusts these to achieve a loop crossover frequency of 3 rad/sec with a phase margin of 35 to 45 degrees. ω_3 is associated with the human bandwidth.

For this investigation, the following nominal values were used; ω_1 = 0.0 rad/sec, ω_2 = 0.667 rad/sec, ω_3 = 6.667 rad/sec, and τ = 0.1 sec. The human gain, K, was established on the basis of subsequent analysis.

Specifically, open loop/root locus techniques were applied to the overall system for the purpose of determining relative stability of this system with the gunner model included. On the basis of these

analyses, the open loop gain was adjusted to provide a gain margin of 3DB at the crossover frequency. Figure 2 depicts a further simplification of the overall system shown in Figure 1. Essentially, the TACH feed-ahead loop shown in Figure 1 has been eliminated and replaced with two parallel branches; an RPU loop, and a Turret drive/stabilization loop. In addition, the common gain in both these loops has been combined with the human gain, optical sight gain, and the handle-bar gain to yield a total system gain, K_S. The open loop transfer function for the system depicted in Figure 2 is defined by Equation 3.2.

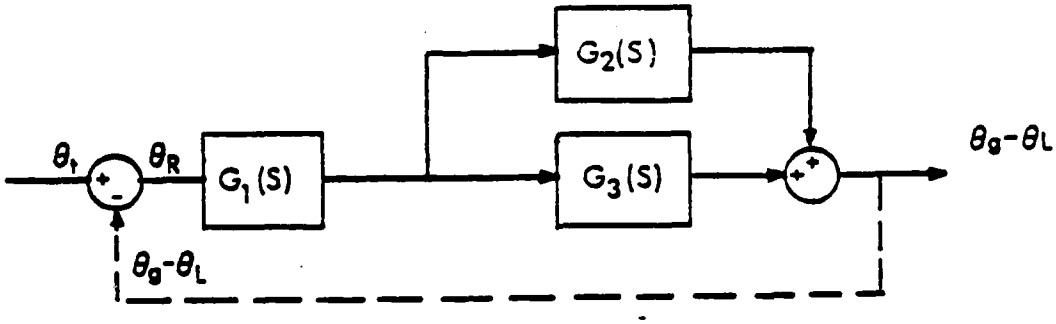

Figure 2. SIMPLIFIED AZIMUTH BLOCK DIAGRAM

Where,

$$G_1(s) = K_S (s + 0.667)\ EXP(-\tau s)/\ s(s + 6.667)$$

$$G_2(s) = (t_f/(1 + 0.39s)\ Q(.3, 21.9))\ ((1/\ D(s)\ Q(.45, 18.0)-1)$$

$$D(s) = \begin{cases} 1/(1 + 0.23s) & \text{First Order Demod} \\ 1/Q(.7, 100) & \text{Second Order Demod} \end{cases}$$

$$G_{ol}(s) = G_1(s)\ (G_2(s) + G_3(s)) \qquad 3.2$$

The subscript, ol, denotes open loop. The open loop gain, K_S, has been computed for the cases where D(S) was either a first order or second order demod filter, i.e.,

D (S)	Open Loop Gain
First Order Filter	6.3
Second Order Filter	12.5

With these gains, the respective closed loop frequency responses were generated for the systems having either a first order or second order demod filter. Figure 3 depicts the bode frequency response for these systems. It is apparent that substantial improvement would be realized from a system using a second order demod filter in place of the first order filter.

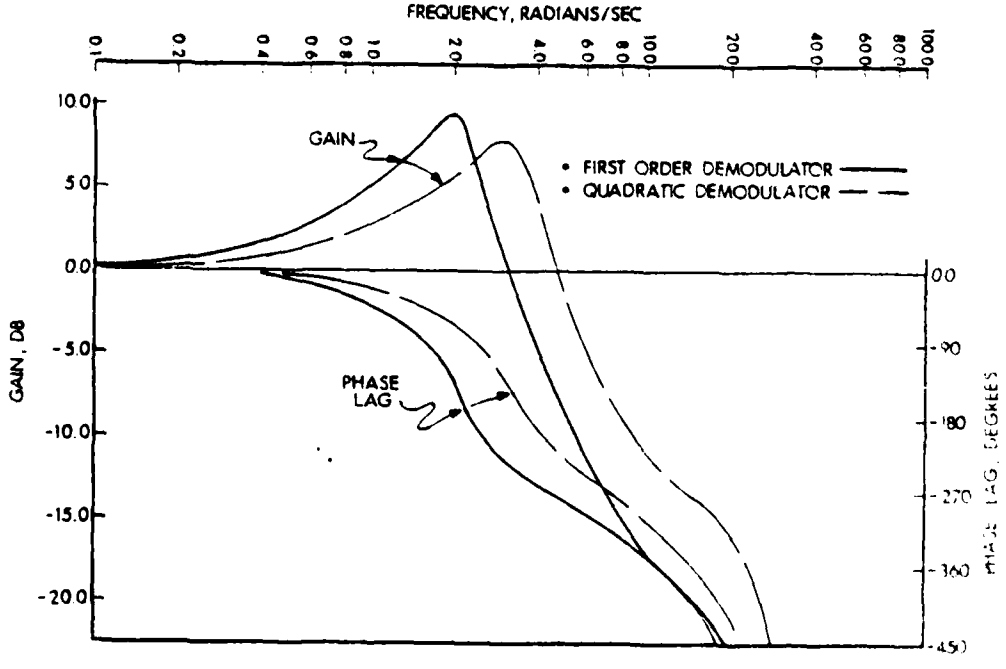

Figure 3 Driven Reticle/Closed Loop Frequency Response

In order to quantify this improvement, the following statistical techniques employing power spectral density of target motion were used. Equation 3.3 represents a one sided power spectral density model of target lateral linear acceleration, $\ddot{X}$.

$$\Gamma_{\ddot{X}}(\omega) = \frac{2\sigma^2\alpha\,(\omega^2 + (\alpha^2 + \omega_c^2)}{\omega^4 + 2(\alpha^2 - \omega_c^2)\omega^2 + (\alpha^2 + \omega_c^2)^2} \qquad 3.3$$

Where,

α and ω_c are positive constants

$1 - \sigma = 1,2,3$ meters/sec^2

ω = Angular frequency

The basic technique is to play the target PSD through an error transmissability relationship, i.e.,

$$\frac{\theta_g - \theta_L}{\theta_t} = \frac{G_{ol}(s)}{1 + G_{ol}(s)} = G_{cl}(s) \qquad 3.4$$

where $G_{cl}(s)$ = Closed Loop Transfer Function

$G_{ol}(s)$ = Open Loop Transfer Function

Now,

$$\varepsilon = \theta_t - (\theta_g - \theta_L) = \theta_t - G_{cl}(s)\theta_t \qquad 3.5$$

$$= (1 - G_{cl}(s))\theta_t \qquad 3.6$$

$$= \left[1 - \frac{G_{ol}(s)}{1 + G_{ol}(s)}\right]\theta_t \qquad 3.7$$

$$= \frac{1}{1 + G_{ol}(s)}\theta_t \qquad 3.8$$

Equation 3.8 may be rewritten in the following form:

$$\varepsilon = \frac{1}{s^2}\,\frac{1}{1 + G_{ol}(s)}\,\ddot{\theta}_t \qquad 3.9$$

For sufficiently small θ_t,

$$\ddot{\theta}_t = \frac{\ddot{X}}{R} .$$

Equation 3.9 now becomes

$$\varepsilon = \frac{1}{s^2}\,\frac{1}{1 + G_{ol}(s)}\,\frac{\ddot{X}}{R} \qquad 3.10$$

In terms of PSD relationships, Equation 3.10 becomes,

$$\Gamma_{\varepsilon}(\omega) = \Gamma_{X}(\omega) / (1 + G_{OL}(i\omega)\,\overline{G_{OL}}(i\omega))\,\omega^4 R^2 \qquad 3.11$$

Integration of $\Gamma_{\varepsilon}(\omega)$ over the frequency domain yields the variance of the error, i.e.,

$$\sigma_{\varepsilon\varepsilon}^2 = \frac{1}{2\pi} \int \Gamma_{\varepsilon}(\omega) d\omega. \qquad 3.12$$

Table 3.1 presents the error one-sigma values for the two different systems as a function of lateral acceleration. A 1500 meter range was used.

TABLE 3.1 CLOSED LOOP ERROR, $\sigma_{\varepsilon\varepsilon}$ (R = 1500 METERS)

Lateral Acceleration meters/sec.^{2} σ_X	First Order Demod Filter, σ_ε	Second Order Demod Filter, σ_ε
1.0	0.280	0.135
2.0	0.559	0.270
3.0	0.839	0.406

4. DESCRIPTION OF HYBRID SIMULATION

4.1 Oscilloscope Display.

The AMSAA/BRL simulation presents a fixed base display to the gunner whereas the actual system has the ability to slew the turret. In terms of task description, the actual systems might be viewed as a pursuit tracking task while the simulation is compensatory. Figure 4 shows the oscilloscope display presented to the gunner which consists of a point target and a cross hair reticle. Both the point target and reticle possess the ability to be offset from the center of the scope display. This is accomplished by commands received from the EAI680 analog consoles. These commands may be generated in a variety of different ways depending on how the various angular offsets depicted in Figure 1 are formed into different display commands.

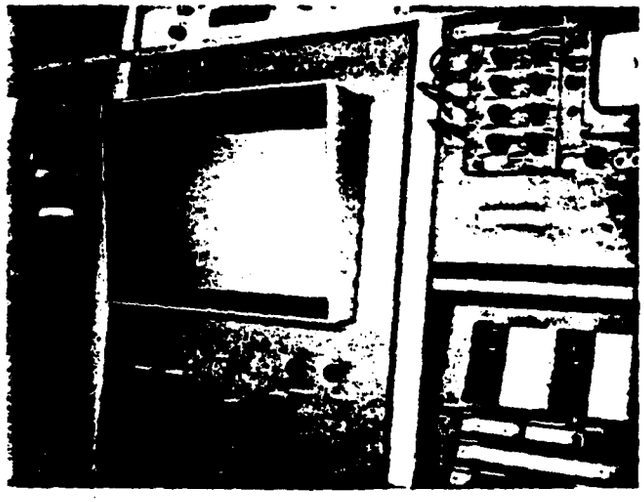

FIGURE 4. DRIVEN RETICLE DISPLAY

Consider the residual error Θ_R which is presented to the gunner,

$$\Theta_R = \Theta_t + \Theta_L - \Theta_g \qquad 4.1$$

In terms of the control handle output, $\dot{\Theta}_{g_c}$, Equation 4.1 takes the form;

$$\Theta_R = \Theta_t + G_{L_{t_f}}(s)\, G_{RPU}(s)\, \dot{\Theta}_{g_c} - G_g(s)\, G_{TAC}(s)\, D(s)\, G_{RPU}(s)\, \dot{\Theta}_{g_c} - G_g(s)\, \dot{\Theta}_{g_c} \qquad 4.2$$

Where,

Θ_R = Angular Offset between Point Target and Reticle,

Θ_t = Angular Offset of Target, Motion

$\dot{\Theta}_{g_c}$ = Commanded Gun Rate

$G_{L_{t_f}}(s) = \dfrac{T_f K_f}{T_1 S+1}$, where t_f is time of flight,

$G_{TAC}(s) = \dfrac{K_{tac}\, s}{K_{Gear}}$,

$D(S)$ = Demodulator Transfer Function,

$G_{RPU}(s) = K_R/Q\ (\zeta_R, \omega_R)$, and

$$G_g(s) = \frac{1}{s} \quad \frac{K_g}{Q\ (\zeta, \omega_g)} \quad .$$

Equation 4.2 may be rewritten in terms of the commanded inputs, i.e.,

$$\Theta_R = C_1 + C_2 - C_3 - C_4 \qquad 4.3$$

Where,

$$C_1 = \Theta_t,$$

$$C_2 = \Theta_L = G_{L_{t_f}}(s)\ G_{RPU}(s)\ \Theta_{gc},$$

$$C_3 = G_g(s)\ G_{TAC}(s)\ G_{L_{t_f}}(s)\ D(S)\ \dot{\Theta}_{gc}$$

$$C_4 = G_g(s)\ \dot{\Theta}_{gc}.$$

Let C_s represent the spot command and C_{ch} the cross hair command. Various ways exist of summing the various commands (C_1,C_2,C_3,C_4) into the spot command. C_s and cross hair command C_{ch}. Three ways of summing the commands are presented in this paper.

Method 1.

$$C_s = C_1 + C_2 - C_3 - C_4$$

$$C_{ch} = 0.0, \text{ and}$$

Method 2.

$$C_s = C_1$$

$$C_{ch} = C_2 - C_3 - C_4.$$

Method 3.

$$C_s = C_1 - C_4$$

$$C_{ch} = C_2 - C_3$$

The first method results in a purely compensatory type of tracking task presented to the gunner. This proved unsatisfactory, since none of the "rubberband" phenomenon was exhibited. The gunner simply nulled out the residual error.

The second mechanization presents a pursuit tracking task to the gunner in which he must chase the point target over the display

screen: whereas, in the actual tank the pursuit track task results in the turret rotating and the reticle staying close to the center of the sight display.

Method two has not yet been mechanized and checked out and may prove unfeasible for certain types of target motion.

Method three is currently mechanized and will be demonstrated. This mechanization, while compensatory, does simulate the "rubberband" phenomenon and can accommodate all types of target motion.

4.2 Overview of Hybrid Computer Simulation.

Figure 5 provides the reader with an overview of the AMSAA/ BRL Hybrid Computer Simulation.

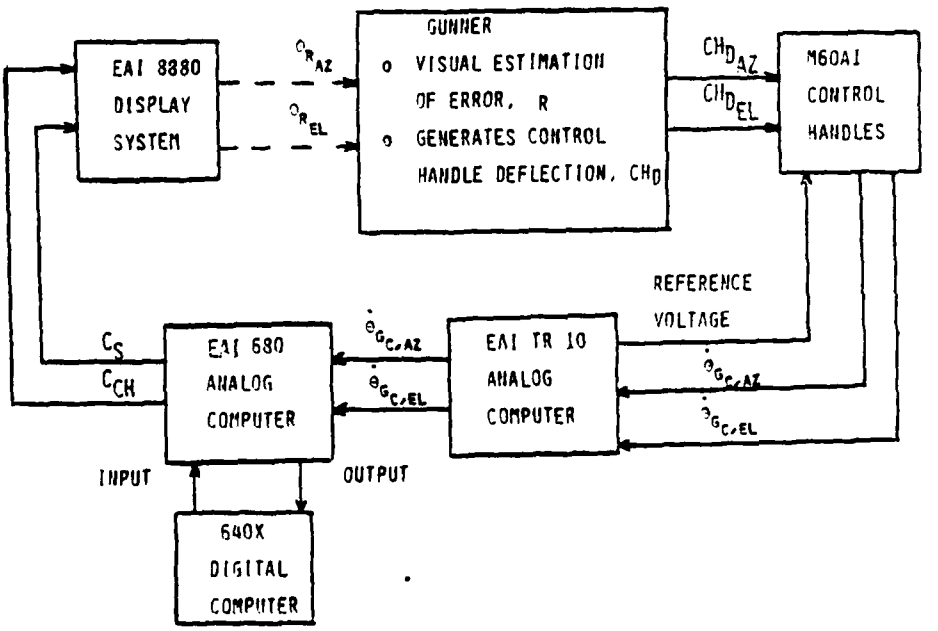

FIGURE 5 OVERVIEW OF HYBRID SIMULATION

All of the major computing components have been identified and for the most part their functions are self-evident. However, some classification concerning the model that has been programmed and the planned use of the output data is needed. It is:

a. The turret drive and fire control model shown in Figure 1 of this paper has been programmed on the EAI 680 analog computer. An elevation drive model has also been implemented. For the time being a very simple target path generator has also been programmed on the 680. The following equation defines the evasive part of the target path generator.

$$\dot{\Theta}_t(s) = G(s)\, W_n(s) \qquad 4.4$$

Where

$$G(s) = K/(\tau s + 1)$$

W_n = White Noise

$\dot{\Theta}_t$ = Target Angular Velocity

The constants K and τ have been chosen so as to provide zero to peak amplitude of 12 mils/sec with a bandwidth of 0 to .2 Hz. The simulation also can be exercised against a constant velocity target.

b. The analytical objectives of this effort are:

(1) Confirm the results obtained from the paper study of Section 3.0.

(2) Create a data base suitable to refine the gunner model currently being used in digital engineering simulation.

Initially, it is planned to develop a residual error model which describes the random portion of the human. Box Jenkins and Parameter Identification techniques appear suitable for this purpose. Ultimately, a simplified version of the Kleinman (Kalman Filter/Predictor) model would be the desired goal of this work.

Next page is blank

ROBUST AUTOREGRESSIVE MODELS FOR PREDICTING AIRCRAFT MOTION FROM NOISY DATA

Stephen F. Huling and Max Mintz
Dept. of Systems Engineering
University of Pennsylvania
Philadelphia, Pa. 19104

Walter Dziwak and Stanley Goodman
US Army Armament Research and
Development Command
Dover, New Jersey 07801

INTRODUCTION:

Traditionally fire control prediction algorithms have been based upon third-order system models in each coordinate (1). In a previous paper by the authors (2), the concept of using higher order autoregressive(AR) models was introduced. It was found that in a noiseless environment these models provided robust predictors which could significantly improve the capabilities of an anti-aircraft (AA) artillery weapon system against a large class of aircraft maneuvers at extended times of flight. This follow-up study examines the case where the observations made by the weapon system are corrupted by noise. The achieved results show that robust higher order AR models still yield considerable improvement, especially in the filtering of the sensor signals. In addition, an artificial flight path was constructed by finding those autoregressive coefficients which maximize the variance of the estimated aircraft velocity. It was found that AR predictors modeled after real aircraft data work well against this "worse case" flight path.

TEST DATA AND SIMULATION PROGRAM:

The system models discussed here and in Reference 2 were determined using time series analysis from test data. This data was collected by the US Navy from flight paths flown by an A-7E high performance aircraft simulating bombing a defended ground target. The recorded data was manipulated and smoothed to yield consistent position, velocity, acceleration and acceleration-dot(the first derivative of acceleration) data at 0.1 second intervals in the XYZ coordinate system. The following descriptions should make it clear that leaving the fourth and higher derivatives of position all undefined does not cause any of the complexities of the maneuvers to be lost. Although the complete data set consists of eleven different flight paths, results for only three representative ones will be presented here. These will be the same passes that were used in Reference 2 and the reader is encouraged to refer to this paper for a schematic figuration of these passes.

Flight path #1 is representative of a general class of maneuvers known as a "dive toss". That is,the payload is released while the aircraft is rolling and pitching which gives the effect of the bomb being tossed. Hence, the weapon release point can be some distance from the target; in this case, the aircraft is 1400m downrange. The tracking data for this pass is initiated

at a range of 5180m--4020m downrange and 3270m in elevation. In the middle of the pass there is a sharp 3.4g diving turn followed by ten seconds of rolling back and forth and then a 5.5g maneuver away from the target. Less than 25 seconds elapse between the initial point and the instant of minimum altitude (560m), which occurs just after the aircraft passes the target.

Flight path #2 bears some similarity to pass #1. The significant differences are that the rolling back and forth in the middle of the pass is not as pronounced and the weapon release point is closer to the target since this pass is representative of the common "dive" maneuver.

Flight path #3 is called a "pop-up" maneuver. Here, the pass is initiated with the aircraft 5800m downrange, at an altitude of 260m and pulling almost 6g's as it starts a climb. As the aircraft climbs over the next 10 seconds to an altitude of 1440m, it rolls over so that at the peak of its climb it is on its back. It continues to roll as it begins to dive at the target. It performs a 3g turn one way followed quickly by a 4g turn the other before it steadies to deliver its payload. Then it executes a 6g bank away from the target. All this maneuvering occurs within 30 sec.

To compare the effectiveness of the various prediction algorithms, the simulation program discussed in Reference 2 is used. This program generates a two-dimensional histogram (prediction times vs miss distance), which will be the means of comparison. The ballistics (i.e. range as a function of time) of the AA rounds are assumed to be

$$R = V_m t/(1+0.129t) \qquad (1)$$

where V_m (assumed to be 1175m/sec) is the muzzle velocity. The results presented in Reference 2 used constant velocity ballistics).

PREDICTION WITH NOISELESS OBSERVATIONS:

Heretofore, models in fire control predictors have been rather simple. The current field peice utilizes a linear or position-plus-rate-times-time algorithm. Previous studies have suggested the use of a quadratic algorithm which is the above plus an extra term comprised of acceleration multiplied by one-half of the prediction time squared. A variation of this approach to prediction is based on a first-order Markov model of acceleration in continuous time, i.e.,

$$\dot{a}(t) = -\omega a(t) + u(t) \qquad (2)$$

Solving this general equation gives the following discrete predictors

$$\dot{x}_{n+k} = x_{n-1} + T\dot{x}_{n-1} + 1/\omega^2 \, (\exp(-\omega T) + \omega T - 1)\, \dot{x}_{n-1}$$

$$\hat{y}_{n+k} = y_{n-1} + T\dot{y}_{n-1} + 1/\omega^2(\exp(-\omega T) + \omega T - 1)\ddot{y}_{n-1}$$

$$\hat{z}_{n+k} = z_{n-1} + T\dot{z}_{n-1} + 1/\omega^2(\exp(-\omega T) + \omega T - 1)\ddot{z}_{n-1}$$

where $T = (k+1)\Delta = (k+1)\cdot 0.1$ second (3)

This prediction algorithm will be used as the benchmark for comparison since it demonstrated a prediction capability better than the other predictors mentioned above. The results obtained using this predictor in the simulation program assuming no noise in the observations are presented in Table 1. Notice that for prediction times of less than one second all the rounds for all three passes score "hits" (defined as a miss distance less than 5m). For prediction times of one to two seconds, the fractions of hits ranges from one-third (passes #1 and #2) to one-fifth (pass #3). The number of rounds within fifteen meters is important too, for close rounds can have an effect on the pilot's resolve to carry out his mission. However, Table I does not show any hits, or even a consistent number of close rounds, for prediction times much greater than two seconds. The similarity of the effectiveness of this algorithm across the different flight paths should be noted.

The authors in Reference 2 proposed that acceleration-dot can be modeled as a fifth-order autoregressive process (see difference 3 and 4), i.e.,

$$\dot{a}_n = \beta_1\dot{a}_{n-1} + \beta_2\dot{a}_{n-2} + \beta_3\dot{a}_{n-3} + \beta_4\dot{a}_{n-4} + \beta_5\dot{a}_{n-5} + u_n \quad (4)$$

where the residuals (u_n) are uncorrelated and zero-mean. This AR model can be combined with the standard expansions, (for X-direction),

$$\begin{aligned} x_n &= x_{n-1} + \Delta v_{n-1} + (\Delta^2/2)a_{n-1} + (\Delta^3/6)\dot{a}_{n-1}, \\ v_n &= v_{n-1} + \Delta a_{n-1} + (\Delta^2/2)\dot{a}_{n-1}, \\ a_n &= a_{n-1} + \Delta\dot{a}_{n-1}, \end{aligned} \quad (5)$$

(where Δ =0.1 second), to yield a matrix one-step predictor

$$\hat{\underline{s}}_n = \begin{bmatrix} \underline{A} & \underline{B} \\ \underline{0} & \underline{\Phi} \end{bmatrix} \underline{s}_{n-1}, \quad (6)$$

where $\underline{s}_n = (x_n, v_n, a_n, \dot{a}_n, \dot{a}_{n-1}, \dot{a}_{n-2}, \dot{a}_{n-3}, \dot{a}_{n-4})'$

$$\underline{A} = \begin{bmatrix} 1 & \Delta & \Delta^2/2 \\ 0 & 1 & \Delta \\ 0 & 0 & 1 \end{bmatrix}$$

$$\underline{B} = \begin{bmatrix} \Delta^3/6 & 0 & 0 & 0 & 0 \\ \Delta^2/2 & 0 & 0 & 0 & 0 \\ \Delta & 0 & 0 & 0 & 0 \end{bmatrix}$$

$$\underline{\Phi} \quad \begin{bmatrix} \beta_1 & \beta_2 & \beta_3 & \beta_4 & \beta_5 \\ 1 & 0 & 0 & 0 & 0 \\ 0 & 1 & 0 & 0 & 0 \\ 0 & 0 & 1 & 0 & 0 \\ 0 & 0 & 0 & 1 & 0 \end{bmatrix}$$

and $\underline{0}$ is the zero matrix. Although Akaike's AIC statistic (5) indicates that the optimal model order is larger than five, it was found that models with lower orders provide a significantly poorer fit to the data while models with higher orders do not give substantial improvements. Therefore, a fifth-order AR model is used. Predictions for longer times of flight can be made by raising the partitioned matrix in Equation 6 to the appropriate power. For position prediction there are similar matrices for the Y and Z directions.

Implementation of this prediction algorithm leads to the results in Table II. The robustness of this type of predictor that was reported in Reference 2 can be seen in these results since a single set of coefficients

$$\beta_1 = 4.029471$$

$$\beta_2 = -6.536585$$

$$\beta_3 = 5.313477$$

$$\beta_4 = -2.148406$$

$$\beta_5 = 0.340802$$

was used for all three directions and for all three flight paths . This single set was derived via a least-squares criterion from the X-direction acceleration-dot of flight path #2. Notice that now almost all the rounds score hits for prediction times up to two seconds, twice as long as for the benchmark predictor. Also, there is a reasonable amount of success for prediction times of two or three seconds -- about one-fifth score hits for passes #2 and #3 while one-third doe for pass #1, plus more than half the rounds are within 15m for all three passes. For longer prediction times the results differ from pass to pass. Pass #1 still has a good number of close rounds while pass #3 has almost nothing. But again, for prediction times up to three seconds at least, the results for this algorithm over very different flight profiles demonstrate a consistent performance which is a great improvement over the benchmark algorithm.

PREDICTION WITH NOISE-CORRUPTED OBSERVATIONS

When the observations are corrupted by noise, the problems become two-fold; first the observations must be filtered to give estimates of the various quantities at the appropriate time instants, and second, these estimates must be manipulated to yield reasonable position predictions. Since the theory says that a Kalman filter is optimal for a linear system (6) and since the assumption that acceleration-dot is an AR process allows a linear definition of the aircraft motion, a Kalman filter will be used to provide the state estimates in each direction.

Given a model of the aircraft's kinematic motion in one coordinate

$$\underline{s}_n = \underline{\underline{F}}\underline{s}_{n-1} + \underline{u}_n \quad , \tag{7}$$

where the model residual vectors ($\underline{u}_n$) are zero-mean and uncorrelated with covariance matrix $\underline{\underline{Q}}$. The position and velocity observations are given by

$$\underline{z}_n = \underline{\underline{H}}\underline{s}_n + \underline{v}_n, \text{ where } \underline{v}_n \sim N[\underline{0}\ \underline{\underline{R}}_n] \tag{8}$$

Then the Kalman filter can be written as follows:

$$\hat{\underline{s}}_n = \underline{\underline{F}}\hat{\underline{s}}_{n-1} + \underline{K}_n\left[\underline{z}_n - \underline{\underline{H}}\underline{\underline{F}}\hat{\underline{s}}_{n-1}\right] \tag{9}$$

where the Kalman filter gain matrix is

$$\underline{K}_n = \underline{P}_n \underline{\underline{H}}' (\underline{\underline{H}}\underline{P}_n\underline{\underline{H}}' + \underline{R}_n)^{-1} \tag{10}$$

and the error covariance matrix is

$$\underline{P}_m = E\ (\underline{\underline{I}} - \underline{K}_{n-1}\underline{\underline{H}})\underline{P}_{n-1}\underline{\underline{F}}' + \underline{\underline{Q}} \tag{11}$$

The quantity in the square brackets in Equation 9 forms the innovations process which should be a white noise process if the filter is properly tuned. The filtering algorithm to be part of the fire control simulation program will include three such Kalman filters -- one for each direction.

The sensors employed by AA weapons systems measure range R, the elevation angle E, the azimuth angle A, range-rate $\dot{R}$ and the angle rates $\dot{E}$ and $\dot{A}$. Each of these measurements will have some independent noise in it. The results to be presented were produced assuming gaussian noises with the following one-sigma values: range-2m, elevation and azimuth angles - 0.5 milrad, range rate - 2m/sec and angle rates - 1% of the actual rate. The observations $\underline{z}$ which include position and velocity in the X, Y and Z direction of a particular Kalman filter are simply

transformations of the noisy (R, E, A, $\dot{R}$, $\dot{E}$, $\dot{A}$),

Since the work in this study was performed in the XYZ coordinate system while the noise occurs in REA, the 2x2 $\underline{R}_n$ matrices that enter into the three XYZ Kalman filters must be derived from the ocvariance matrix $\underline{\Sigma}_n$ for (R, E, A, $\dot{R}$, $\dot{E}$, $\dot{A}$). Since the noise added to the different quantities is assumed to be uncorrelated, this matrix will be zeros everywhere except on the diagonal which will be made up of the appropriate variances. Notice that since the angle rate variances are a function of the data, $\underline{\Sigma}_n$ (and hence the $\underline{R}_n$'s) will change with time. Now, the full 6x6 covariance matrix in XYZ is given by

$$\underline{R}_n = \underline{\Lambda}_n \underline{\Sigma}_n \underline{\Lambda}_n' \tag{12}$$

where $\underline{\Lambda}_n$ is the Jacobian matrix of the transformation at time t_n. In order to simplify the calculations, a decoupling of the XYZ direction filters is forced on $\underline{R}_n$. For example, the $\underline{R}_n$ matrix for X has the variance of the X-position noise and the variance of the X-velocity noise on the diagonal and the covariance between the two on the off-diagonals. The covariances between directions are lost. Preliminary work indicates that filtering in REA which would eliminate the need for this decoupling will provide better estimates. However, it still seems that prediction is best done in XYZ.

This study will present results obtained using two different filters. The first is based on the type of model used in the benchmark predictor. In fact, a first-order AR model of acceleration with the coefficient $\alpha = 0.995$ will be used. Tests show that the performance of this filter is rather insensitive to the exact value of this coefficient. The vectors and matrices in the Kalman filter formulation defined above are the following for the X-direction case:

$$\underline{s}_n = (x_n, v_n, a_n)',$$

$$\underline{F} = \begin{bmatrix} 1 & \Delta & \Delta^2/2 \\ 0 & 1 & \Delta \\ 0 & 0 & \alpha \end{bmatrix}$$

$$\underline{Q} = \begin{bmatrix} 0 & 0 & 0 \\ 0 & 0 & 0 \\ 0 & 0 & q_x \end{bmatrix} \tag{13}$$

$$\underline{H} = \begin{bmatrix} 1 & 0 & 0 \\ 0 & 1 & 0 \end{bmatrix}$$

$$\underline{u}_n = (0, 0, u_n)'$$

where $E[u_n^2] = q_x$. Only position, velocity and acceleration are being estimated so only predictors that require these variables can be used with this filter.

The results in Table III were produced by the benchmark predictor, which is based on a first-order Markov model of acceleration, operating on the estimates produced by three third-order Kalman filters. The results in these histograms form the benchmark in this scenario of noisy measurements.

The second filter is based on the fifth-order AR model of acceleration-dot. This means that the state transition matrix $\underline{F}$ (now an 8x8 matrix) is the same as the predictor matrix of Equation 6. The results presented here were generated by three Kalman filters -- a different set of coefficients for each direction (produced from pass #2). However, the same filters were used on all three flightpaths. Equation 6 also defines the state vector $\underline{s}$. The 8x8 residual covariance matrix $\underline{Q}$ will be all zeros except for the element q(4,4) which is equal to the variance of the residuals of the X, Y or Z AR model in pass #2. Again the observations are of position and velocity so the $\underline{H}$ matrix is now 2x8. Since this filter produces estimates of position through acceleration-dot, the benchmark and higher order predictors can both be used.

Figure 1 contains the spectral density estimates of the velocity innovations processes for the X-direction of pass #2 for this and the third-order Kalman filters. As was previously stated, if a filter is properly tuned, these processes should be white. It is clear from the figure that the higher order filter has a flatter spectrum which indicates that it is more closely tuned to the data and hence that it will provide better estimates.

Table IV contains the results obtained using this eigth-order Kalman filter with the benchmark predictor. A large increase in accuracy for short prediction times (less than one second) is evident in all three flight paths. Also, except for pass #2, there is a significant over-all improvement in effectiveness for prediction times between one and three seconds. It seems clear that given reasonable noise levels little can be expected for prediction times greater than three seconds.

A single third-order AR model of acceleration-dot with coefficients

$$\beta_1 = 1.451057$$

$$\beta_2 = -0.725526$$

$$\beta_3 = 0.125000$$

provides the basis for a position predictor that was used against all directions and flight paths. This predictor together with the three-eigth order Kalman filters used above gives the results in Table V. Note there is a further increase

in the accuracy for short prediction times. But here, for the longer prediction times, only pass #3 shows any significant improvement over the results in Table IV. The results for the other flight paths are only minimally better.

PREDICTION AGAINST A "WORSE CASE FLIGHT PATH"

One can associate with a p_{th} order autoregression process a characteristic equation whose roots lie inside the unit circle of the complex plane if the process is stable. Thus, for (4), the corresponding characteristic equation is

$$\sum_{i=0}^{5} \beta_i z^{5-i} = 0 \qquad (14)$$

When the roots associated with (14) for each of the flight passes are plotted in the complex plane, it is seen that they congregate in clusters. One can identify five clusters per coordinate. Furthermore, the groupings of the clusters is remarkably similar in each coordinate. This is suggestive of a robust property of the models which resulted in the single set of coefficients for each coordinate exhibited above.

One can partition each cluster and design a fifth order A-R process which has "worse case" properties from the point of view of the A-A artillery weapon. The resulting class of "worse case flight paths" formed by determining the β coefficients from the root locations can then be used to test the effectiveness of the fifth order predictors based on real flight data. One can also use the WCFP predictor to see how well it performs against the real aircraft data.

The WCFP was designed in the following way: One root per cluster was chosen to produce a set of β coefficients such that the steady state variance of the velocity estimate is maximized. The condition of maximum variance is achieved by roots located on the boundary of each cluster. A magnified view of two clusters and the WCFP root locations is shown in Figure 2. A computer search over each boundary determined the desired roots. The ground track of a WCFP is exhibited in Figure 3.

Table VI shows the performance of three predictors against the WCFP. Observe that the a-dot predictor with the WCFP coefficients achieves the highest

average hit probability, with the fifth order in a-dot with x coefficients from flight pass 10 a close second. The benchmark predictor is a distant third.

It was found that the WCFP predictor also performs well against the real attack flight paths.

CONCLUSIONS:

Higher order AR Models of acceleration-dot provide robust models of high performance aircraft maneuvers which are much improved over the models based on a first-order model of acceleration. The filtering capabilities of a fire control system could be greatly enhanced by the incorporation of the higher order models. Further enhancement can be achieved by the use of the higher order model in the predictor as well.

These improvements are noise level dependent, of course. Higher noise levels mean a bigger payoff by changing to the higher order filter with less of a return for the higher order predictors. Lower noise levels mean the reverse with the payoff for the higher order predictors approaching the noiseless case. However, in the case of lower noise levels, the higher order filter is still expected to yield significantly better estimates than the lower order filter. In addition, it is needed to provide the higher order predictor with the estimated quantities that it requires.

REFERENCES:

1. Singer, Robert, Behnke, Kenneth, "Real-time Tracking Filter Evaluation and Selection for Tactical Applications," IEEE Transactions on Aerospace and Electronic Systems. Vol. AES-7, No. 1, January 1971, pp. 100-110.

2. Huling, Stephen, Mintz, Max, Goodman, Stanley, Dziwak, Walter, "Robust AR Models for Prediction of Aircraft Flight Paths," Proceedings of the Nineth Annual Pittsburgh Conference on Modeling and Simulation. 1978, pp. 1045-51

3. Fuller, W.A., Introduction to Statistical Time Series. John Wiley and Sons, Inc., New York, New York 1976.

4. Anderson, T.W., The Statistical Analysis of Time Series. John Wiley and Sons, Inc., New York, New York, 1971

5. Parzen, Emmanuel, "Some Recent Advances in Time Series Modeling," IEEE Transactions on Automatic Control. Vol. AC-19, No. 6, December 1974, pp. 723-730

6. Gelb, Arthur, Applied Optimal Estimation. The M.I.T. Press, Cambridge, Mass., 1974

FIGURE 1. SPECTRAL DENSITY ESTIMATES OF X-DIRECTION VELOCITY INNOVATIONS PROCESSES FOR PASS 32

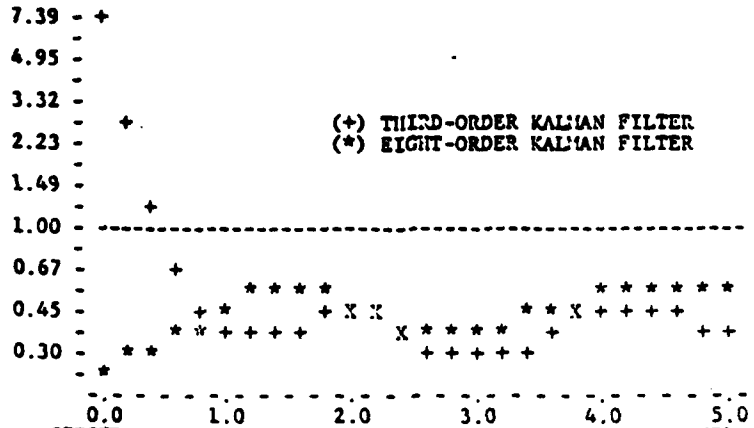

TABLE I. BENCHMARK PREDICTOR (NOISELESS)

FLIGHT PATH 1

Pred. time between	Number of rounds w/ miss between 0-5	-10	-15	-20	T	Mean Miss
0 - 1	46	0	0	0	= 46	1.24
1 - 2	15	11	16	0	= 42	7.66
2 - 3	0	5	6	3	= 37	29.77
3 - 4	0	0	3	2	= 39	48.82
4 - 5	0	0	0	0	= 30	94.86
					Total=194	32.11

FLIGHT PATH 2

Pred. time between	Number of rounds w/ miss between 0-5	-10	-15	-20	T	Mean Miss
0 - 1	49	0	0	0	= 49	1.61
1 - 2	16	17	5	3	= 41	6.61
2 - 3	0	4	2	4	= 37	49.69
3 - 4	0	0	0	0	= 33	77.48
4 - 5	0	0	0	0	= 34	141.31
					Total=194	49.23

FLIGHT PATH 3

Pred. time between	Number of rounds w/ miss between 0-5	-10	-15	-20	T	Mean Miss
0 - 1	44	0	0	0	= 44	1.23
1 - 2	9	29	7	0	= 45	7.52
2 - 3	1	1	2	2	= 38	47.00
3 - 4	0	0	0	0	= 38	117.06
4 - 5	0	0	0	0	= 34	200.84
					Total=199	67.63

TABLE II. AR A-DOT PREDICTOR (NOISELESS)

FLIGHT PATH 1

Pred. time between	Number of rounds w/ miss between 0-5	-10	-15	-20	T	Mean Miss
0 - 1	46	0	0	0	= 46	0.07
1 - 2	42	0	0	0	= 42	1.67
2 - 3	12	16	3	2	= 37	11.97
3 - 4	0	1	3	5	= 37	33.35
4 - 5	2	5	3	4	= 33	52.21
					Total=195	26.46

FLIGHT PATH 2

Pred. time between	Number of rounds w/ miss between 0-5	-10	-15	-20	T	Mean Miss
0 - 1	49	0	0	0	= 49	0.20
1 - 2	37	4	0	0	= 41	2.74
2 - 3	7	15	8	1	= 37	13.71
3 - 4	0	1	4	3	= 35	44.19
4 - 5	0	0	0	2	= 31	109.50
					Total=193	48.14

FLIGHT PATH 3

Pred. time between	Number of rounds w/ miss between 0-5	-10	-15	-20	T	Mean Miss
0 - 1	44	0	0	0	= 44	0.07
1 - 2	44	1	0	0	= 45	1.86
2 - 3	6	10	6	12	= 39	12.71
3 - 4	0	0	1	1	= 36	61.54
4 - 5	0	0	0	0	= 33	102.17
					Total=197	49.82

TABLE III. THIRD-ORDER FILTER WITH BENCHMARK PREDICTOR

FLIGHT PATH 1

Pred. time between	Number of rounds w/ miss between 0-5	-10	-15	-20	T	Mean Miss
0 - 1	34	12	0	0	= 46	3.37
1 - 2	4	9	7	13	= 42	14.43
2 - 3	1	4	3	9	= 36	36.78
3 - 4	0	1	2	0	= 39	60.63
4 - 5	0	0	0	0	= 29	112.99
					Total=192	40.24

FLIGHT PATH 2

Pred. time between	Number of rounds w/ miss between 0-5	-10	-15	-20	T	Mean Miss
0 - 1	20	21	8	0	= 49	5.96
1 - 2	9	15	10	2	= 41	10.18
2 - 3	0	4	2	2	= 37	63.34
3 - 4	0	0	0	0	= 31	105.92
4 - 5	0	0	0	0	= 35	146.63
					Total=193	60.38

FLIGHT PATH 3

Pred. time between	Number of rounds w/ miss between 0-5	-10	-15	-20	T	Mean Miss
0 - 1	27	17	0	0	= 44	4.38
1 - 2	3	10	28	4	= 45	11.07
2 - 3	0	0	0	1	= 36	57.72
3 - 4	0	0	0	0	= 39	130.05
4 - 5	0	0	0	0	= 37	212.25
					Total=201	78.08

TABLE IV. EIGHTH-ORDER FILTER WITH BENCHMARK PREDICTOR

FLIGHT PATH 1

Pred. time between	Number of rounds w/ miss between 0-5	-10	-15	-20	T	Mean Miss
0 - 1	40	6	0	0	= 46	2.43
1 - 2	11	6	10	15	= 42	11.21
2 - 3	2	5	3	7	= 36	31.63
3 - 4	0	1	3	1	= 39	53.45
4 - 5	0	0	0	0	= 33	107.54
					Total=196	37.52

FLIGHT PATH 2

Pred. time between	Number of rounds w/ miss between 0-5	-10	-15	-20	T	Mean Miss
0 - 1	35	14	0	0	= 49	3.34
1 - 2	9	16	12	0	= 41	9.45
2 - 3	0	2	5	3	= 37	58.16
3 - 4	0	0	0	0	= 32	86.83
4 - 5	0	0	0	0	= 34	150.54
					Total=193	54.92

FLIGHT PATH 3

Pred. time between	Number of rounds w/ miss between 0-5	-10	-15	-20	T	Mean Miss
0 - 1	38	6	0	0	= 44	2.72
1 - 2	7	21	17	0	= 45	8.57
2 - 3	0	0	3	2	= 37	50.16
3 - 4	0	0	0	0	= 38	122.41
4 - 5	0	0	0	0	= 36	209.39
					Total=200	72.76

TABLE V. EIGHTH-ORDER FILTER WITH THIRD-ORDER A-DOT PREDICTOR

FLIGHT PATH 1

Pred. time between	Number of rounds w/ miss between 0-5	-10	-15	-20	T	Mean Miss
0 - 1	45	1	0	0	= 46	2.37
1 - 2	11	8	14	9	= 42	10.20
2 - 3	1	4	3	8	= 36	29.10
3 - 4	0	0	1	1	= 40	62.15
4 - 5	0	0	1	1	= 33	87.04
					Total=197	35.24

FLIGHT PATH 2

Pred. time between	Number of rounds w/ miss between 0-5	-10	-15	-20	T	Mean Miss
0 - 1	40	9	0	0	= 49	2.89
1 - 2	10	16	11	2	= 41	8.89
2 - 3	2	2	4	4	= 37	56.46
3 - 4	0	0	1	0	= 32	76.88
4 - 5	0	0	0	0	= 36	153.82
					Total=195	54.32

FLIGHT PATH 3

Pred. time between	Number of rounds w/ miss between 0-5	-10	-15	-20	T	Mean Miss
0 - 1	39	5	0	0	= 44	2.71
1 - 2	14	13	13	0	= 45	7.02
2 - 3	1	1	3	3	= 38	43.84
3 - 4	0	0	0	0	= 38	116.09
4 - 5	0	0	0	0	= 37	232.89
					Total=202	74.90

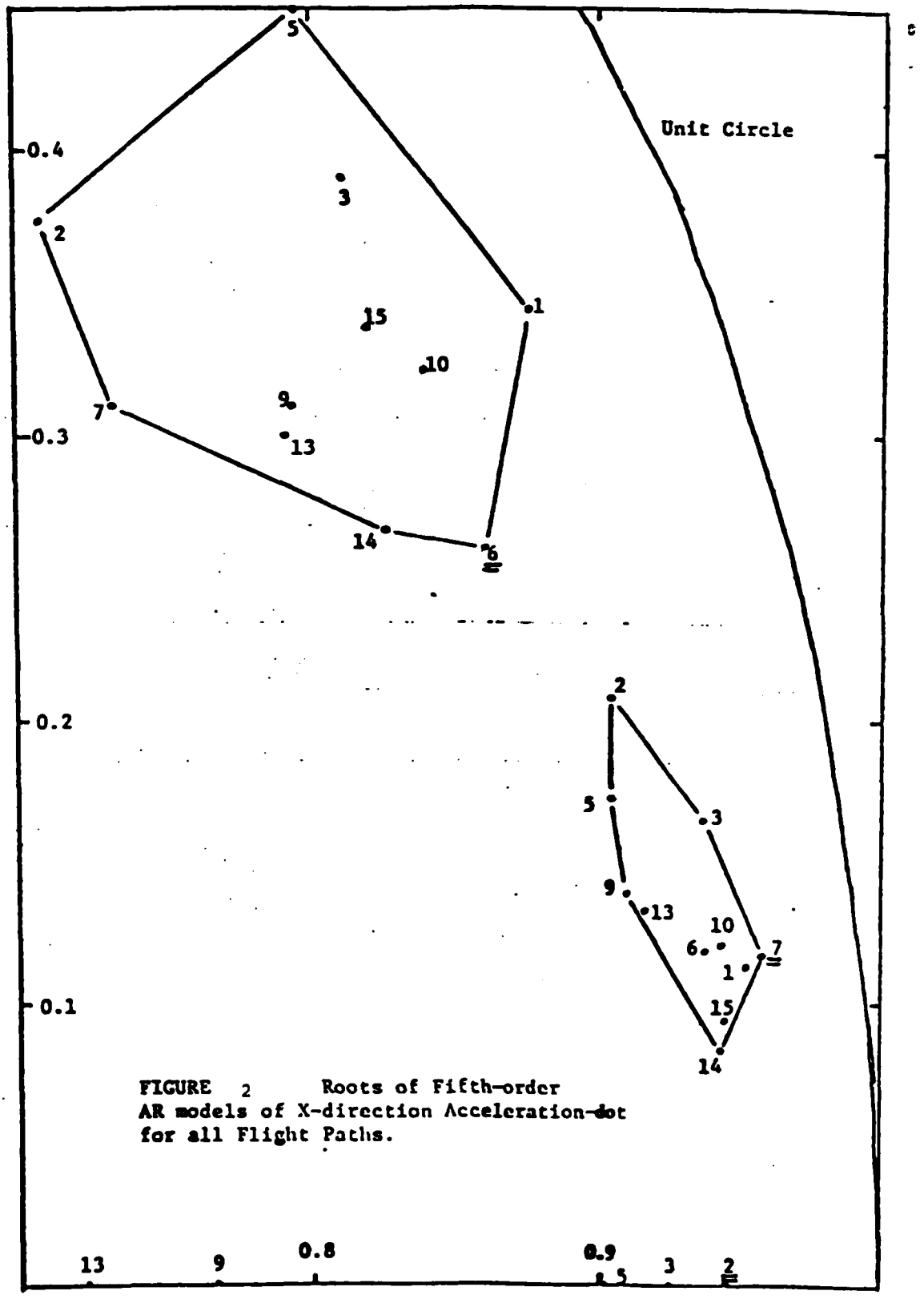

FIGURE 2 Roots of Fifth-order AR models of X-direction Acceleration-dot for all Flight Paths.

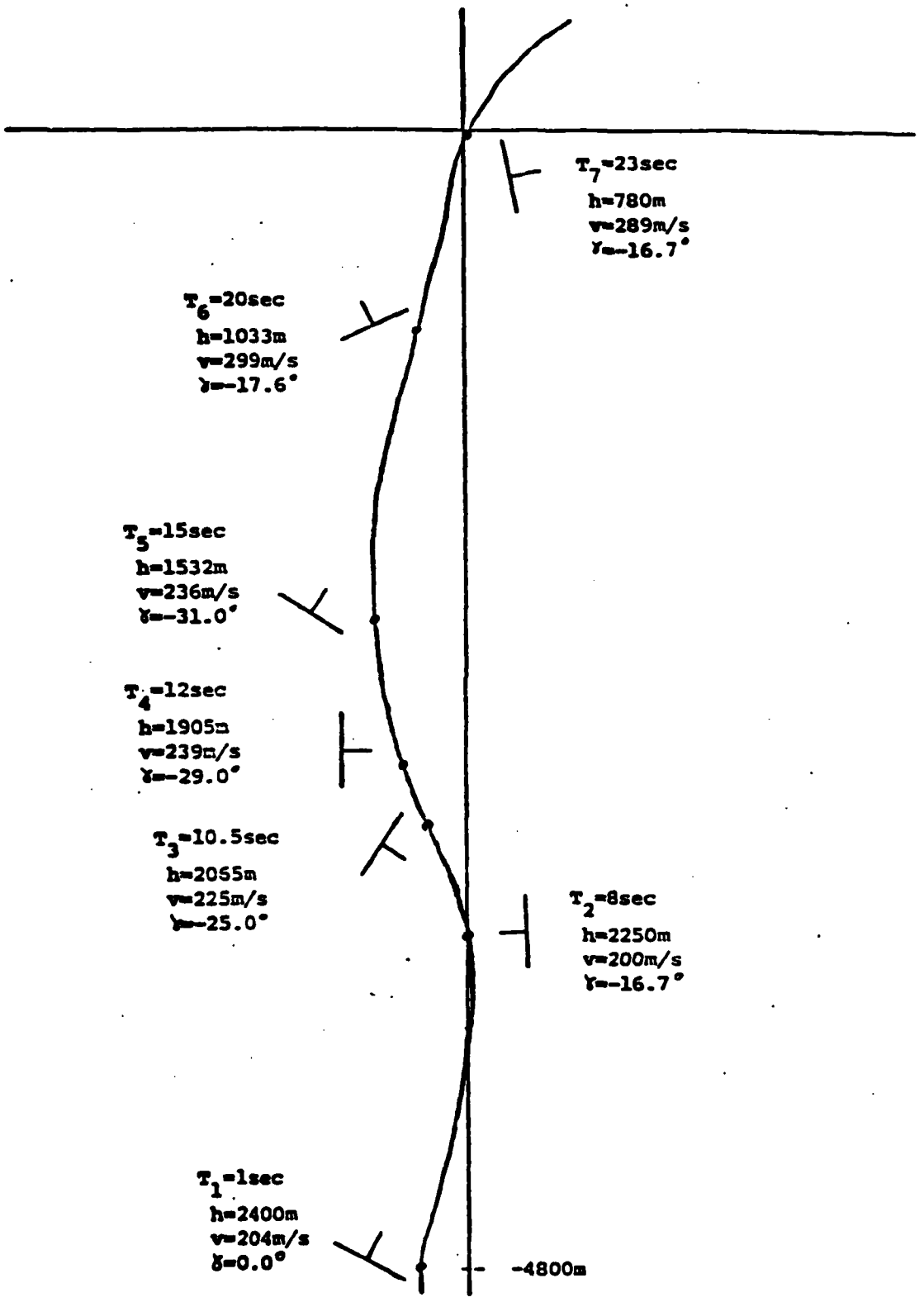

FIGURE 3 Ground Trace of WCFP

TABLE IV WORST CASE FLIGHT PATH (NOISELESS)

FIFTH-ORDER AR IN A-DOT PREDICTOR (WCFP COEFFICIENTS)

Prediction Time between	Number of Rounds with Closest Approach Miss (in meters) between: 0-5	5-10	10-15	15-20	20-25	>25	Total	Miss RMS Error
0.0 - 1.0	31	0	0	0	0	0	= 31	0.01
1.0 - 2.0	43	0	0	0	0	0	= 43	0.48
2.0 - 3.0	30	8	1	0	0	0	= 39	4.88
3.0 - 4.0	2	12	8	4	5	4	= 35	16.40
4.0 - 5.0	1	0	0	1	3	24	= 29	64.27
(seconds)	---	----	-----	-----	-----	---	-----	------
						Total Rounds	= 177	

Average Hit Probability = 0.61578; Total RMS Error = 27.116

FIRST-ORDER IN A PREDICTOR (BENCHMARK)

Prediction Time between	Number of Rounds with Closest Approach Miss (in meters) between: 0-5	5-10	10-15	15-20	20-25	>25	Total	Miss RMS Error
0.0 - 1.0	31	0	0	0	0	0	= 31	2.69
1.0 - 2.0	16	21	6	0	0	0	= 43	6.74
2.0 - 3.0	1	2	8	4	6	19	= 40	24.68
3.0 - 4.0	4	2	1	1	1	20	= 29	93.31
4.0 - 5.0	0	0	0	0	0	35	= 35	111.84
(seconds)	---	----	-----	-----	-----	---	-----	------
						Total Rounds	= 178	

Average Hit Probability = 0.30626; Total RMS Error = 63.458

FIFTH-ORDER AR IN A-DOT PREDICTOR (PASS#10 X COEFFICIENTS)

Prediction Time between	Number of Rounds with Closest Approach Miss (in meters) between: 0-5	5-10	10-15	15-20	20-25	>25	Total	Miss RMS Error
0.0 - 1.0	31	0	0	0	0	0	= 31	0.04
1.0 - 2.0	44	0	0	0	0	0	= 44	0.65
2.0 - 3.0	19	8	11	0	0	0	= 38	7.80
3.0 - 4.0	0	15	6	1	1	11	= 34	30.49
4.0 - 5.0	0	0	0	2	3	27	= 32	71.85
(seconds)	---	----	-----	-----	-----	---	-----	------
						Total Rounds	= 179	

Average Hit Probability = 0.55486; Total RMS Error = 33.352

Next page is blank

A DESIGN METHODOLOGY FOR ESTIMATORS AND PREDICTORS IN FIRE CONTROL SYSTEMS

BY

JAMES F. LEATHRUM
CONSULTANT TO AMSAA

ABSTRACT

The state-of-the-art in the design of Kalman filters for fire control systems leaves the designer with several parameters to be used to overcome the effects of modelling errors. The fixing of these parameters usually requires extensive simulation and trial-and-error searching for satisfactory operating conditions. In the process, the effects of the various modelling errors are easily confounded and the intuitive understanding of target behavior often lost.

The purpose of the analysis reported here is to establish a design methodology which begins with the allowable variances in miss distance and leads directly to filter parameters for an optimal filter. Structural mismatching between the filter and the actual target are left to analysis by simulation. The advantage of this methodology is that the performance of the fire control system in terms of miss distance enters the design process at the outset rather than as a "take what we get" outcome. Mathematically, the process involves explicit solution of the steady state matrix Riccati equation.

Conventional Design Methodology

The conventional approach to the design of estimators and predictors for fire control systems is best illustrated by the following development of models and parameters. One would start by formulating target and observer models of the form.

(a) Target Model

$$X_{k+1} = \Phi_k X_k + B_k U_k$$

(2) Observer Model

$$Y_k = H_k X_k + V_k$$

These models immediately involve a linearization approximation. The target model captures the well defined motion in the state transition matrix, Φ_k, and leaves the less defined part of the motion to a noise term, $B_k U_k$. The observer is usually a statement that not all the state components are visible, and that the observations are corrupted by an error, V_k. (The index, k, is a discrete time index).

If one can further approximate U_k and V_k by white gaussian, zero mean processes, an estimator of X_k can be formulated as:

$$\tilde{X}_{k+1} = \Phi_k \hat{X}_k$$

$$\hat{X}_k = \tilde{X}_k + K_k (Y_k - H_k \tilde{X}_k)$$

Which is the Kalman Filter wherein

$$K_k = P_k H'_k (R_k + H_k P H'_k)^{-1}$$

$$\tilde{P} = \Phi_k \tilde{P}_k \Phi_k + B_k Q_k B_k$$

$$\hat{P}_k = \tilde{P}_k - K_k H_k \tilde{P}_k$$

$$R_k \equiv E(U_k U_k')$$

$$Q_k \equiv E(V_k V_k')$$

In the most sophisticated fire control systems, the target noise is represented in a target oriented coordinate system. Thus, the given Q_k will rotate as the target moves which in turn leads to a nonsteady K_k. The Kalman gains tend to change throughout the estimation process. In addition, R_k may be range dependent which leads to further variability in K_k.

In designing such a filter, the implementor is left with choices of the magnitude of Q_k and R_k (i.e., $\|Q_k\|$ and $\|R_k\|$). A conventional design process would require assessing $\|R_k\|$ from the accuracy of the instrumentation used by the observer. Since $\|Q_k\|$ represents unmodelled behavior, it is usually adjusted to achieve some other objective, such as white innovation, or minimum ensemble miss distances. Whatever the objective, the last phase is unguided by the theory and thus usually requires extensive simulation. The design process for a filter-predictor in tandom is illustrated by

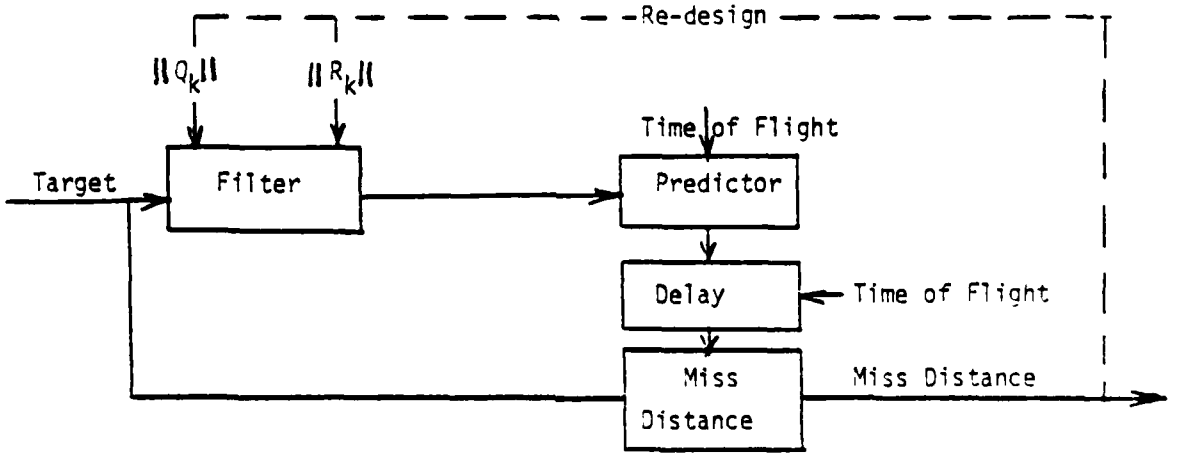

A Direct Design Methodology

A methodology which could utilize maximum allowable miss distances to assess the design parameters directly would have some obvious advantages over the conventional process. Such a methodology is proposed here with the following features.

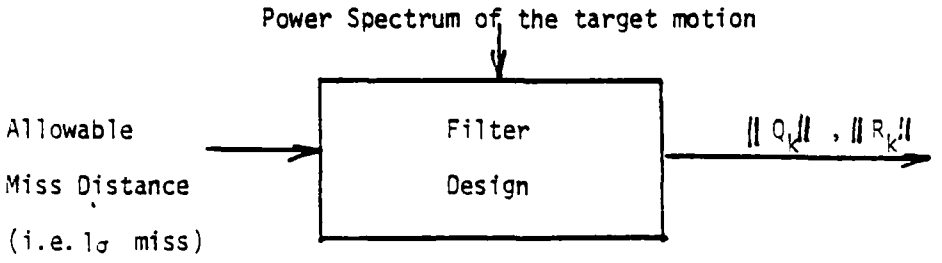

Predictor Algorithm

The principles of the design will be illustrated by restricting the discussion to a single dimension and further restricing models to

ϕ : Upper Triangular

Q_k: Scalar constant, q

R_k: Scalar constant, r

These restrictions do not limit variability of the gains in the final design, but only allow one to focus attention on the magnitudes of the parameters in each direction. The design process requires solution of the steady state filter operations which become

$$\tilde{P} = \phi\tilde{P}\phi' + B_q B' - \phi\tilde{P}H'(R + H\tilde{P}H')^{-1}H\tilde{P}\phi$$

The solution for $\tilde{P}$ in terms of r and q requires iteration. However a closed form solution for P/q and r/q in terms of band width of the target motion is possible. It requires the observation from the analogous

continuous models that

$$P_{33}/q = (\omega_v^2/\omega_a^3)\,\Delta t$$

Where ω_v is the bandwidth for velocity.

ω_a is the bandwidth for acceleration

$\Delta t \equiv t_{k+1} - t_k$; the time increment between observations

The required bandwidths can be assessed from the power spectrum observed in field tests of generic targets. The ratios (P/q and r/q) completely specify the one dimensional, steady state design, but they do not product the parameters needed for $\| Q_k \|$ and $\| R_k \|$ in a multidimensional design. The required magnitudes are obtained from the variance of miss distance

$$\frac{\sigma miss}{\sqrt{rq}} = \sqrt{\hat{P}_{11/q}} + \sqrt{\hat{P}_{22/q}} \cdot t_f + \sqrt{P_{33/q}} \cdot t_f^2/2$$

Where in an optimal design, the P is interpreted as the variance of the estimator error. The above equation represents the variance propagation through a second order predictor (t_f is the time of flight.) Other predictor algorithms could be used at this point. Since the ratio $P/_q$, is computed, by asserting a 1σ miss, one can directly determine q. Further, knowledge of r/q leads directly to r.

The logical outcome of this process is the question of whether an observer with an accuracy on the order of $\sqrt{r}$ is achievable. The power spectrum of the target motion, and the limits of miss distance in conjunction may force the enhancement of instrumentation technology.

A Typical Design

The purpose of this section is to illustrate the design process by starting with

1) A Second order predictor.

2) Bandwidths of the target motion

ω_v = 0.128hz

ω_k = 0.160hz

3) 1 σmiss distance = 1 meter.

4) Time offlight = 2.0 sec.

In the order which they would be computed, the variance ratios are

i, j	$P_{i,j/q}$
3.3	.0737
2,3	.02716
1,2	.00367
1,3	.00534
2,2	.0146
1,1	.00126

and then $r/q = 1.59X10^{-3}$

In this computation, the model coefficents are

$$\Phi = \begin{bmatrix} 1. & 1. & .05 \\ & 1. & .1 \\ & & 1. \end{bmatrix}; \qquad B = \begin{bmatrix} 10^{-3}/6 \\ .005 \\ 0.1 \end{bmatrix}$$

$$H = \begin{bmatrix} 1. & 0 & 0 \end{bmatrix};$$

where the Φ and B parts of the model are determined by the data rate of Δt = 0.1 sec. From the 1σ miss distance, the q is fixed at

q = 1.88

thence = 2.99×10^{-3}

Given the parameters of this example, the technological conclusion is that an observer with a 1σ accuracy of r = 0.0547 meters is needed to achieve a 1 σ miss distance of 1 meter.

The observer accuracy vs. miss distance is summarized in the following table.

1σ Miss Distance, meters	q	$\sqrt{r}$, meters
1.0	1.88	0.0547
1.5	4.23	0.0820
2.0	7.52	0.1094
2.5	11.75	0.1367
3.0	16.92	0.1641

Conclusions

The design process is completely characterized by assessing the proportionality constant in

$$r = C \cdot \sigma_{miss}$$

where C is determined by the bandwidths of the target motion and by the predictor algorithm. The computation of C may be tedious, but it is straight forward and free of iteration.

Although the impact of this methodology is clear from the models used here, its full generalization is yet to be worked out. More general forms of ϕ, B, and H need to be considered in the interest of establishing the theoretical limits of the design process.

AN ADAPTIVE LEAD PREDICTION ALGORITHM FOR MANEUVERING TARGET ENGAGEMENT

Pak T. Yip & Norman P. Coleman
USA ARRADCOM
Dover, NJ 07801

ABSTRACT. An algorithm concept which processes target bearing and range input data and provides "optimal" estimates of target position, velocity and acceleration a time-of-flight in the future is discussed. Since the algorithm concept involves certain important statistical assumptions about target acceleration dynamic models, these assumptions will be discussed in detail along with several important methods used in the model identification process. Secondly, the filter algorithm itself will be discussed. This algorithm involves the parallel processing of target range and bearing data by several extended Kalman Filters corresponding to distinct maneuver characteristics of anticipated target vehicles. At time of fire the filter with the largest computed likelihood function is selected for lead prediction. Finally, results of simulation studies in which actual target path data is used to generate filter input data for hit probability evaluation is discussed. Comparisons are made between the adaptive algorithm and non-adaptive first order algorithms.

I. INTRODUCTION. This paper describes a multiple model adaptive Kalman Filter approach to the problem of estimating and predicting the position, velocity and acceleration states of tank targets of varying maneuverability. The estimation and prediction problem presupposes that the range and angle DATA (measurements corrupted by Gaussian white noise) is available. The target dynamics is described by a system equation. Our solution to this problem is an adaptive algorithm implementable in real time with a microprocessor to compute target position a projectile time of flight in the future. This study begins with the selection of the Antitank Missile Test (ATMT) Phase II data, to identify the filter acceleration models. It consists of three dimensional (x,y,z) position data recorded at approximately 10 samples per second. Maximum likelihood identification method is applied to this data to identify a finite set of Markov Acceleration Models which are representative of a broad spectrum of vehicle maneuvers considered likely to occur in actual engagements. These models provide the required state variable description of the target dynamics used in the formulation of the multiple model extended Kalman Filter Algorithm for lead prediction. The extended Kalman Filter is required in this application as a result of nonlinearities induced by target coordinate transformations and nonlinear measurement equation.

The adaptive lead prediction concept is based on the simultaneous (parallel) processing of the discrete extended Kalman Filters corresponding to the distinct target models identified from the ATMT data. The likelihood function associated with each filter is computed up to the time of fire of the weapon, and the filter having the greatest likelihood is automatically selected for lead prediction.

In the present study, only the azimuth and range information of the target is processed in the filter with the target elevation considered constant. The performance of this design is examined with a Monte Carlo simulation and the sensitivity of the lead estimates to measurement noise, level of target maneuver, range sampling rate, and time of flight of projectile are analyzed to determine the feasibility of using this algorithm for fire control lead prediction against various maneuvering targets.

II. DATA ANALYSIS. The ATMT data consists of six tracks produced by a M60A1 tank, a Scout Vehicle and a Twister Vehicle undergoing evasive maneuvers. The M60A1 tank is capable of speeds of 10 to 16 miles per hour and with a maximum acceleration of approximately .3g. The Scout is an armored reconnassiance vehicle capable of moving at a speed of 15 to 25 miles per hour and a maximum acceleration of approximately .5g. Since our only interest is in modeling the acceleration, the position data is sampled at a frequency of 2 cps and twice differentiated to obtain the acceleration estimates which are then resolved into along-track and cross-track components. The power spectral density of this data is computed by the maximum entropy method[3] which assumes the data is generated by an autoregressive process. The power spectral desity S(f) is given by

$$S(f) = \frac{2\,\sigma_q^2}{\left| 1 - \sum_{i=1}^{M} \alpha_i \exp(-j2\pi f i) \right|}$$

where σ_q is the standard deviation of a Gaussian noise process; α_i is the i-th coefficient of the autoregressive process; M is the number of coefficients, and the coefficients α_i' are estimated recursively[3].

The number of the autoregressive coefficients is usually larger than 3 which is not desirable for Kalman Filtering. However, the power density spectrum affords enough information for estimating essential poles and zeros of a simplier model structure. Later the maximum likelihood identification program is used to fine tune the pole and zero estimates.

The simplified model determined from the spectral analysis has the following form:

$$A(s) = \frac{S + \gamma}{S^2 + \beta_1 S + \beta_2}\; q(s)$$

where q(s) is the Gaussian noise process; A(c) is the system acceleration; γ, β_1 and β_2 are parameters to be identified for the chosen tracks and each of the along-track and cross-track formulations.

III. DISCRETE EXTENDED KALMAN FILTER. The system and the measurement equations are readily defined as follows:

$$\underline{X}_k = \underline{\Phi}(\underline{X}_{k-1}, dt) + \underline{q}_k$$

$$\underline{Z}_k = \underline{h}(\underline{X}_k) + \underline{Y}_k$$

where $\underline{X}_k$ is the system state vector at the discrete time kdt in the cartesian coordinate system, $\underline{\Phi}$ the system function containing all information about the system dynamics, $\underline{q}_k$ the plant noise vector, $\underline{Z}_k$ the measurement vector, $\underline{h}(\underline{X}_k)$ a vector containing the true range and azimuth angle of the target position at time kdt, $\underline{r}_k$ the measurement noise vector, and dt the time between two samples.

The necessary statistics and conditions are:

$$\begin{aligned}
&\mathrm{cov}(\underline{q}_i, \underline{q}_j) = Q_i \, \delta_{ij} \\
&\mathrm{cov}(\underline{r}_i, \underline{r}_j) = R_i \, \delta_{ij} \\
&\mathrm{cov}(\underline{q}_i, \underline{r}_j) = 0. \qquad\qquad \forall i, j \\
&E(\underline{X}_0) = \hat{X}_0 \\
&\mathrm{cov}(\hat{X}_0) = P_0
\end{aligned}$$

where δ_{ij} is the Kronecker Delta.

Given the above, the discrete Extended Kalman Filter equations can be written as follows: The predicted state estimate vector is given by

$$\hat{X}_{k+1|k} = \underline{\Phi}(\hat{X}_k, dt)$$

and the state error a priori covariance matrix by

$$P_{k+1|k} = \Phi \, P_k \, \Phi^T + Q_k$$

where

$$\Phi = \left. \frac{\partial \underline{\Phi}(\underline{X}, dt)}{\partial \underline{X}} \right|_{\underline{X} = \hat{X}_k}$$

$$\underline{\Phi} = \hat{X}_k + \hat{\dot{X}}_k \, dt + \hat{\ddot{X}} \, (dt)^2/2$$

$$\hat{\dot{X}}_k = \frac{d}{dt} \hat{X}_k$$

$$\hat{\ddot{X}}_k = \hat{\dot{X}}_k \frac{\partial \hat{\dot{X}}_k}{\partial \hat{X}_k}$$

The updated state estimate vector can be written as follows:

$$\hat{X}_{k+1} = \hat{X}_{k+1|k} + K \, \tilde{\underline{Z}}_{k+1}$$

where

$$\tilde{\underline{Z}}_{k+1} = \underline{Z}_{k+1} - \underline{h}(\hat{X}_{k+1|k})$$

$$K = P_{k+1|k} \, H^T (H \, P_{k+1|k} \, H^T + R_{k+1})^{-1}$$

$$H = \left. \frac{\partial \underline{h}(\underline{X})}{\partial \underline{X}} \right|_{\underline{X} = \hat{X}_{k+1|k}}$$

$$\underline{h}(\hat{X}_{k+1|k}) = \left\{ \left[(X_1)^2 + (X_2)^2 \right]^{1/2}, \tan^{-1}(X_1/X_2) \right\}$$

x_1, x_2 represents x,y position state estimates respectively in fixed cartesian coordinates. The state error a posteriori covariance matrix is given by

$$P_{k+1} = P_{k+1|k} - K H P_{k+1|k}$$

and

$$Q_k = \int_{t_{k-1}}^{t_k} \Phi(t_k - \tau) Q_s \Phi^T(t_k - \tau)\, d\tau$$

where the continuous case plant noise covariance matrix, Q_s, is known.

The continuous time system dynamic equations used in deriving the discrete time equations are given by

$$\dot{X}_1 = X_3 \quad , \qquad \dot{X}_2 = X_4$$

$$\dot{X}_3 = (X_3 A_a + X_4 A_c)/V$$

$$\dot{X}_4 = (X_4 A_a - X_3 A_c)/V$$

$$\dot{X}_5 = -\beta_{a1} X_5 - \beta_{a2} X_6 \quad , \qquad \dot{X}_6 = X_5$$

$$\dot{X}_7 = -\beta_{c1} X_7 - \beta_{c2} X_8 \quad , \qquad \dot{X}_8 = X_7$$

$$A_a = \frac{S + \gamma_a}{S^2 + \beta_{a1} S + \beta_{a2}}\, q_a$$

$$A_c = \frac{S + \gamma_c}{S^2 + \beta_{c1} S + \beta_{c2}}\, q_c$$

$$V = (X_3^2 + X_4^2)^{1/2}$$

where X_3 and X_4 are the corresponding X and Y components of the velocity vector; A_a is the target acceleration along the velocity vector; A_c is the target acceleration perpendicular to the velocity vector.

With this filter, target range and angle measurements may be processed to generate target state estimate recursively. Before defining an adaptive filter procedure, the parameters of the Markov model need to be identified.

IV. LIKELIHOOD FUNCTION & MAXIMUM LIKELIHOOD IDENTIFICATION OF PARAMETERS[2]. Given a parameter vector $\underline{\alpha}$, the probability of occurence of the measurement vector sequence $\underline{Z}_k$ can be represented by a multivariate gaussian distribution.

$$p(\underline{Z}^k ; \underline{\alpha}) = p(\underline{Z}_k | \underline{Z}^{k-1}; \underline{\alpha}) \cdots p(\underline{Z}_2 | \underline{Z}^1 ; \underline{\alpha})\, p(\underline{Z}_1 ; \underline{\alpha})$$

$$p(\underline{Z}_k | \underline{Z}^{k-1}; \underline{\alpha}) = \frac{\exp\left(-\frac{1}{2} \tilde{\underline{Z}}_k \underline{S}_k^{-1} \tilde{\underline{Z}}_k\right)}{(2\pi)^{n/2} (\det \underline{S}_k)^{1/2}}$$

$$\underline{S}_k = H P_{k|k-1} H^T + R_k$$

where

$P(\underline{Z}^k;\underline{\alpha})$ = the likelihood function
n = number of elements in the measurement vector $\underline{Z}_k$.

In order to identify the best parameter vector $\underline{\alpha}$ to give a maximum $p(\underline{Z}^k;\underline{\alpha})$, we can equivalently minimize the negative log likelihood function:

$$M(\underline{Z}^k;\underline{\alpha}) = \sum_{i=1}^{k} \left\{ \frac{1}{2} \tilde{Z}_i^T \underline{S}_i^{-1} \tilde{Z}_i + \frac{1}{2} \ell n \left(\det \underline{S}_i \right) \right\}$$

Since the term $(2\pi)^{n/2}$ in the likelihood function does not contribute any interesting information it has been eliminated in forming $M(\underline{Z}^k;\underline{\alpha})$. The Gauss-Newton method is used in the minimization procedure.

$$\underline{\alpha}_{j+1} = \underline{\alpha}_j - \rho\, D^{-1} \frac{\partial M(\underline{Z}^k;\underline{\alpha}_j)}{\partial \underline{\alpha}_j}$$

where $\rho = 1$ for this method, and D, the expected Hessian

$$D = E\left\{ \frac{\partial^2 M(\underline{Z}^k;\underline{\alpha}_j)}{\partial \underline{\alpha}_j^2} \right\}$$

The test for convergence is given by

$$\left(\underline{\alpha}_{j+1} - \underline{\alpha}_j\right)^T D \left(\underline{\alpha}_{j+1} - \underline{\alpha}_j\right) < 10^{-3}$$

V. PARALLEL FILTERS & ADAPTIVE ESTIMATION. Target state prediction for maneuvering ground targets have never been a simple task to undertake. The major uncertainty comes from the target driver's (stochastic) decision to maneuver. However, it appears there exists a maximum level of maneuver that the ground vehicles studied can attain. This maximum level provides a non-trivial range of dynamic motion that can be quantized to a finite number of maneuver levels. In this study, five filters are incorporated into the multiple model filter. Model M1 (Filter 1) is a simple 4 states constant velocity filter. The remaining 4 filters are identified with various maneuver levels.

The adaptive estimation is a straight forward decision making process. Measurement in range and azimuth angle are processed through the parallel filters. The filter having the largest likelihood function is automatically chosen to provide the best estimate for lead prediction and gun orders. Two concepts of adaptive prediction are examined. In concept A the likelihood functions account for the entire measurement history up to the time of fire. Thus this adaptive prediction concept is good against targets with constant maneuver level. In concept B, only the last ten samples prior to the firing time are used to compute the likelihood functions. This adaptive filter concept tends to be more sensitive to changes in target maneuver levels.

VI. SIMULATION. A Monte Carlo simulation of 100 runs was set up to process a number of 10 second segments from the ATMT data representing various maneuver levels for the M60, Twister and Scout Vehicles. These segments of data are different from those used for the parameter identification tasks discussed earlier.

For evaluating the system performance, the perpendicular miss distance of the predicted line of sight from the real target position is defined as the prediction error E_p in meters. The firing time points are fixed for each segment under process. The performance indicator ph at each firing time point is defined as the ratio of the number of times that the prediction error E_p is less than 1.15 meters to the total number of runs. Actually, they are hit probabilities considering the prediction errors alone.

Assuming engagement range of approximately 2000 meters, 45° cross range (across the range vector), 1 σ range measurement error of 2 meters, 1 σ azimuth tracking error of 0.3 mils, a projectile speed of 1500 meters per second and using the adaptive prediction concept A, the hit probability results are illustrated in Figure 1 and summarized in the following table:

Target Type	Number of Cases, 7 Firing Points per Case	Mean ph Const. Velocity Prediction	Mean ph Adaptive Prediction
M60A1	13	.41	.49
Scout	10	.27	.38
Twister	8	.20	.26

For an engagement range of approximately 1158, 60° cross range, 1 σ range measurement error of 3 meters, 1 σ azimuth tracking error of 0.3 mils, a projectile speed of 1158 meters per second and using the adaptive prediction concept B, the hit probability results are summarized in the following table:

Target Type	Number of Cases, 7 Firing Points per Case	Mean ph Const. Velocity Prediction	Mean ph Adaptive Prediction
M60A1	6	.51	.56
Twister	6	.31	.37

With the latter conditions, the sensitivities of the system are observed for a particular maneuvering segment as shown in Figure 2. Figure 3 illustrates the system range (hence the time of flight of projectile) sensitivity. Figure 4 illustrates the system sensitivity to angular measurement noise. Figure 5 illustrates the system sensitivity to range measurement noise. Figure 6 illustrates the system sensitivity to range sampling rate.

VII. DISCUSSION & FUTURE PLAN. This study has demonstrated that maneuvering target acceleration may be adequately modeled as a discrete set of stationary Markov processes whose parameters can be identified off line. Parallel discrete extended Kalman filters have been used to successfully process range and angle measurements. The adaptive selection of the most appropriate filter at each time step, based on its largest likelihood function, has been accomplished on line. Representatives maneuver patterns and levels used in this study were taken from the ATMT data base. The results from the Monte Carlo simulations indicate that the performance of the multiple model adaptive filter design is generally comparable to a filter which is tuned to the target dynamics of that particular tracking interval. In particular, the results show that the adaptive prediction consistently performed better than the constant velocity prediction with an improvement in prediction ranging from 10 to 40 percent.

Since the range data is currently not a uniformly accessable measurement, the range sampling rate has been examined as an area of uncertainty

together with range, angular measurement noise, and range measurement noise. The results indicate that the system performance for the azimuth channel is heavily dependent of angular measurement noise and projectile time of flight in terms of range, and is not very sensitive to range measurement noise and range sampling rate. The results also indicate that higher probability of hit can be obtained in the cross range geometry than in the down range (coming down along the range vector) geometry.

Implementation of this filter algorithm in real time with a state of the art microprocessor is in the planning stage. We have noticed that Bierman's UD factorization for the state error covariance propagation is a desirable feature considering computation accuracy and stability. Several variations of the existing filter algorithm are also under consideration. Finally, a complete real time simulation of the fire control system with the auto-tracker or human operator in the loop and filter modifications to improve maneuver detection will be subjects of our future work.

References

1. "Antitank Missile Test, Experiment FC019," Phase II, Project Analysis, ACN22273, USADEC, Fort Ord, CA, 30 June 1975.

2. N. K. Gupta, R. K. Mehra, "Computational Aspects of Maximum Likelihood Estimation & Reduction in Sensitivity Function Calculations," IEEE Trans. on AC, December 1974, pp 774-783.

3. Tad J. Ulrych, Thomas N. Bishop, "Maximum Entropy Spectral Analysis & Autoregressive Decomposition," Reviews of Geophysics & Space Physics, Volume 13, No. 1, February 1975, pp 183-200.

4. G. J. Bierman, "Factorization Methods for Discrete Sequential Estimation," Academic Press, New York, 1977.

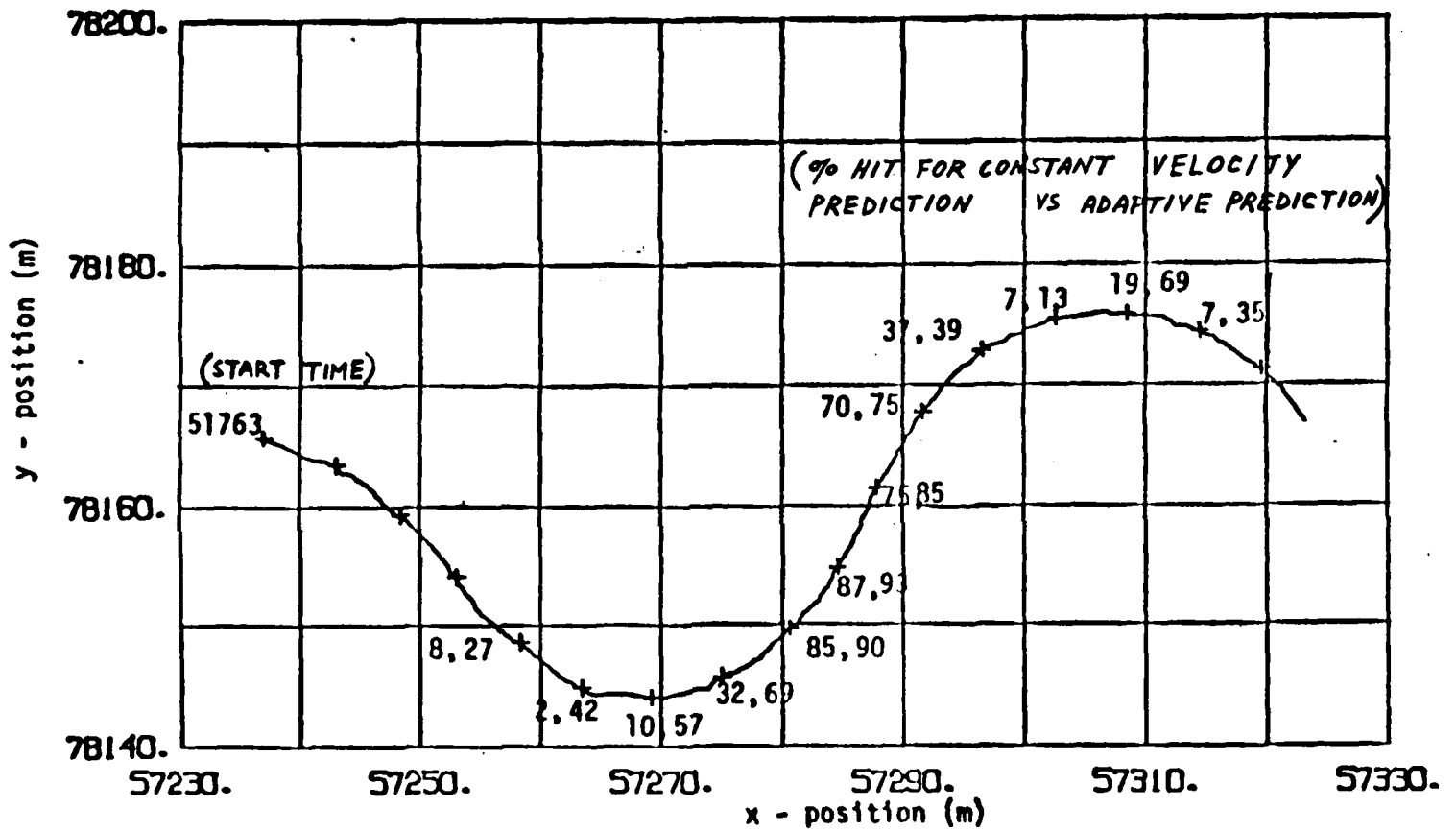

FIGURE 1. HIT PROBABILITY AT FIXED FIRING POINTS ALONG A SEGMENT OF PATH 431, M60A1 TANK DATA

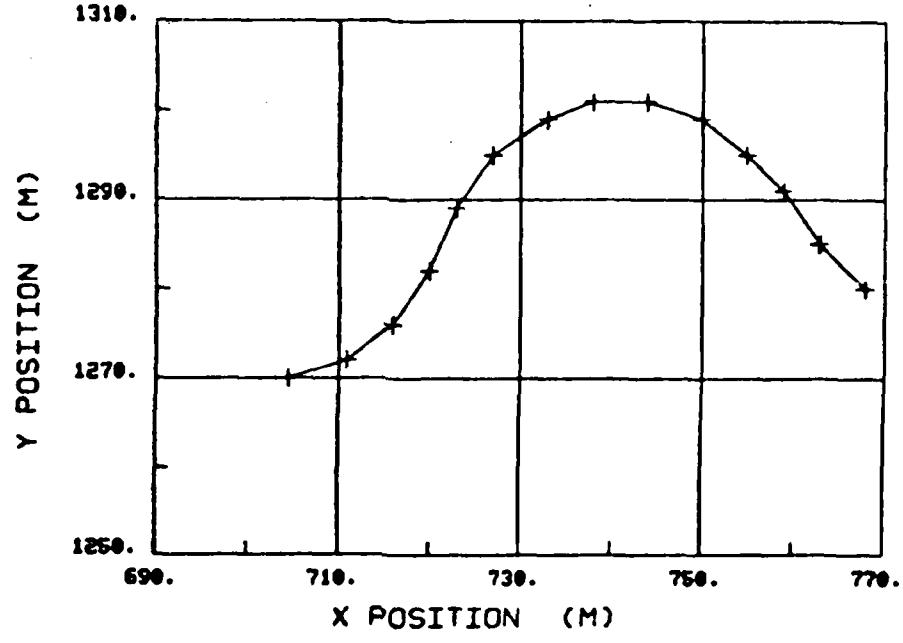

FIGURE 2. ATMT DATA SEGMENT 36

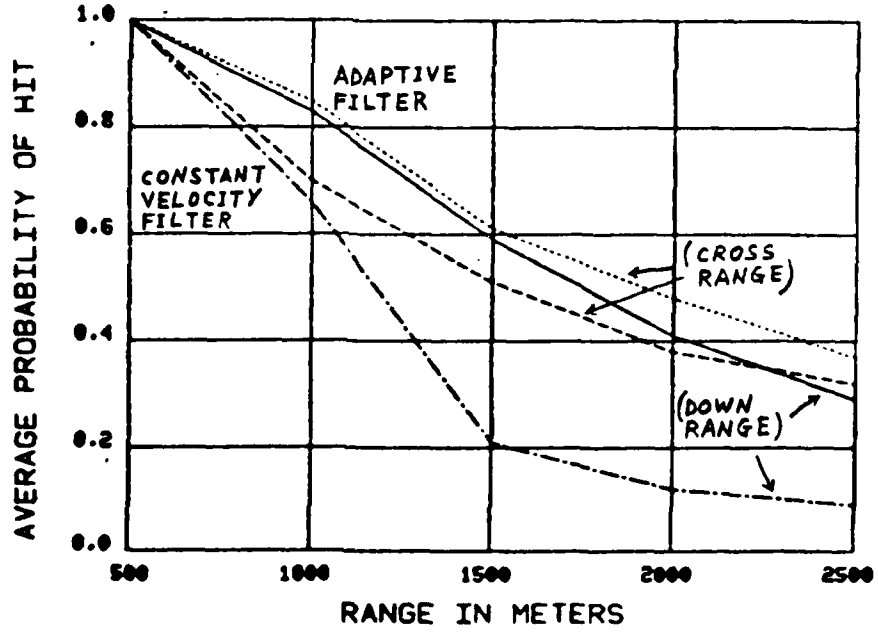

FIGURE 3. SYSTEM RANGE SENSITIVITY

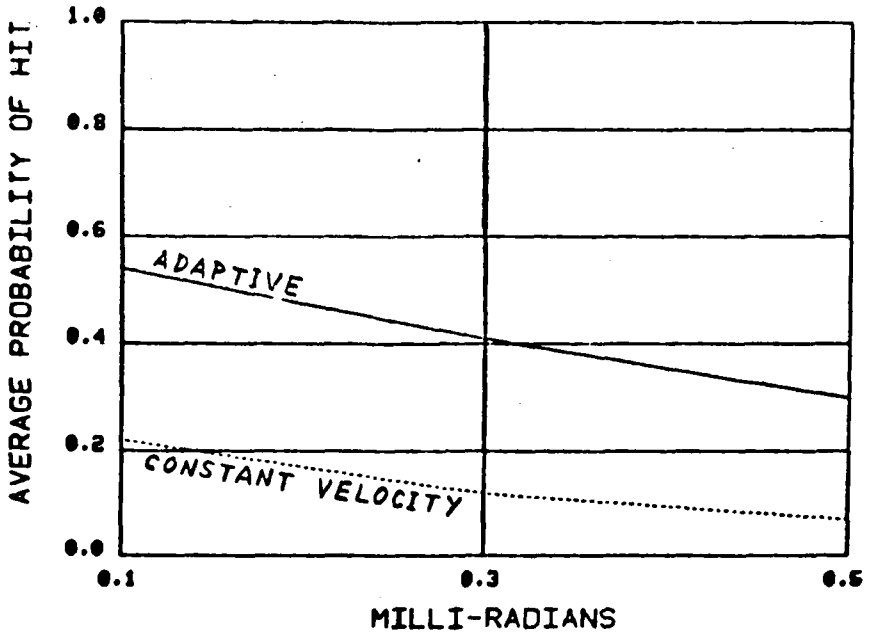

FIGURE 4. FILTER SENSITIVITY TO ANGULAR MEASUREMENT NOISE

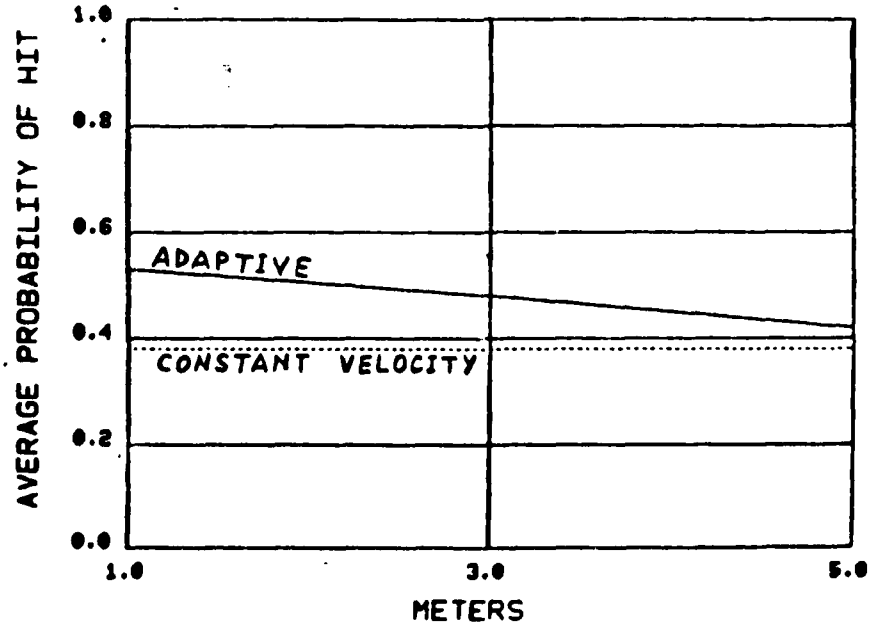

FIGURE 5. FILTER SENSITIVITY TO RANGE MEASUREMENT NOISE

AD-A089 314 ARMY MATERIEL SYSTEMS ANALYSIS ACTIVITY ABERDEEN PROV--ETC F/G 12/1
PROCEEDINGS OF THE MEETING OF THE SPECIAL INTEREST GROUP ON CON--ETC(U)
MAY 80 H E COHEN

UNCLASSIFIED NL

2 OF 2
AD A089 314

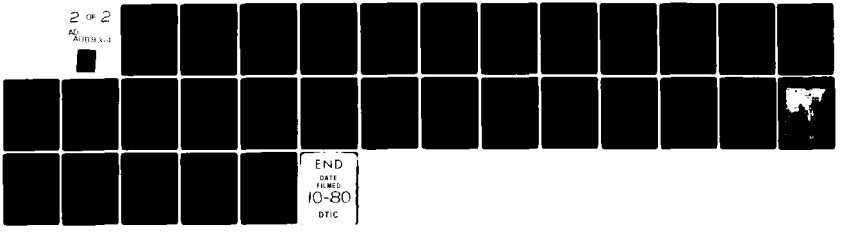

END
DATE FILMED
10-80
DTIC

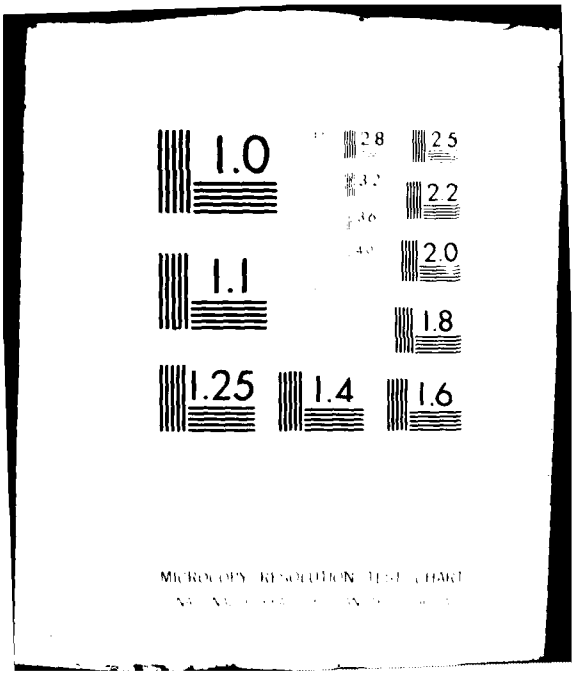
1.0
1.1
1.25
1.4
1.6
2.0
1.8
2.2
2.5
MICROCOPY RESOLUTION TEST CHART

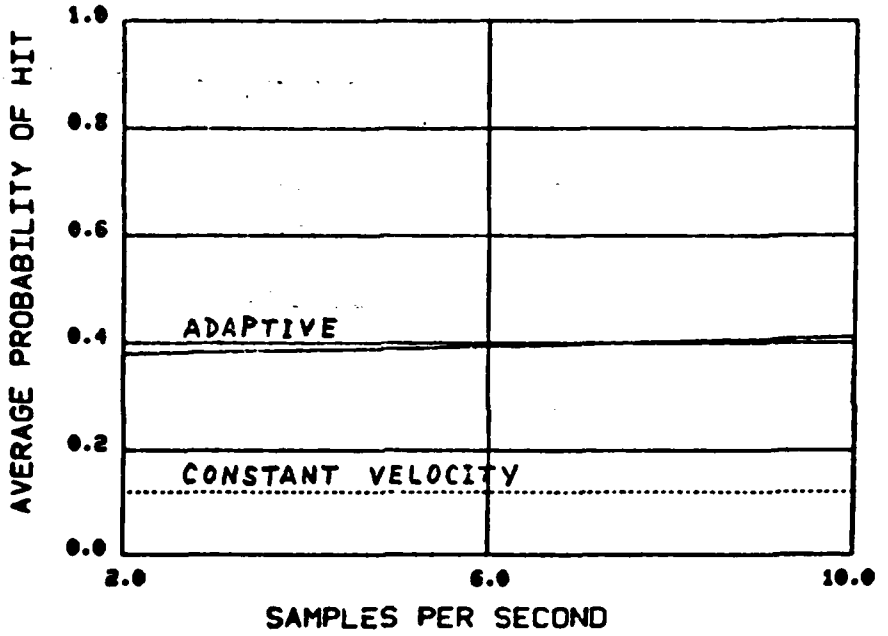

FIGURE 6. FILTER SENSITIVITY TO RANGE SAMPLING RATE

APPLICATIONS OF DELAY FEEDBACK IN CONTROL SYSTEMS DESIGN

N. P. Coleman, E. Carroll, D. Lee and K. Lee
US ARRADCOM
Dover, NJ 07801

ABSTRACT: Necessary and sufficient conditions for exact state reconstruction using delays are discussed together with an example in which the technique is implemented in real time using an 8080/8085 microprocessor. Also, a frequency domain technique for synthesizing certain feedback control laws with delays is developed and several examples discussed.

I. INTRODUCTION: In designing a control system using optimal control theory or classical frequency domain techniques, one often encounters situations in which certain required signals or states of the system are unavailable by direct measurement. In modern control design this problem is usually handled by implementing some form of reduced order or full order observer which provides an asymtotic estimate of the unmeasured state. In this paper a technique is developed for exact state reconstruction of unmeasured system states using values of the measured variables, their delayed values and the control variables on the maximum delay interval. Several examples are discussed which demonstrate the application of this technique on a laboratory servo system using an 8080 microprocessor.

A second application of delay feedback for frequency domain compensation is also discussed. A frequency domain technique is developed for selecting appropriate gain and delay parameters for synthesizing a feedback controller using delays in the output and several applications as discussed.

II. REAL TIME STATE RECONSTRUCTION USING DELAYS: In this section a technique is presented for exact state reconstruction using delay feedback of measured states of a control system and the values of the control input over the delay interval. A real time application of this technique in a servo control system using an 8080 microprocessor is also discussed. For simplicity, consider the linear time invariant system:

$$\dot{x}(t) = Ax(t) + Bu(t) \tag{1}$$

where x is an nxl state vector, u is an rxl control vector, A is an nxn constant matrix, and B is an nxr constant matrix. Let the observation vector y(t) be given by:

$$y(t) = Hx(t)$$

where y is a mxl vector, and H is an mxn constant matrix. Let $o \le h_1 < h_2 < \cdots < h_\lambda < a$ be time delays.

The problem is to reconstruct the state x(t) from the measurements y(t), y(t-h), $\cdots$, $y(t-h_\lambda)$ and the measureable control vector u(s), $t-h_1 \le s \le t$.

The following argument due to D. H. Chyung, Reference (1) provides the basis for a real time state reconstruction algorithm discussed in the examples. This argument makes use of the well known variation of parameter expression

for the time response x(t) of the system (1) given by:

$$x(t) = e^{A(t-h_i)}x(t-h_i) + \int_{t-h_i}^{t} e^{A(t-s)}Bu(s)ds \qquad (2)$$

$$= e^{Ah_i}x(t-h_i) + \int_{-h_i}^{o} e^{-As}Bu(t+s)ds \qquad i = 1,2,\cdots\ell$$

Multiplying both sides of equation (2) by He^{-Ah_i} results in the equation:

$$He^{-Ah_i}x(t) = Hx(t-h_i) + He^{-Ah_i}\int_{-h_i}^{o} e^{-As}Bu(t+s)ds$$

$$= y(t-h_i) + He^{-Ah_i}\int_{-h_i}^{o} e^{-As}Bu(t+s)ds \qquad (3)$$

$$i = 1,2,\cdots\ell$$

in which the right hand side is completely known. Letting C denote the matrix given by:

$$C \triangleq \begin{bmatrix} He^{-Ah_1} \\ He^{-Ah_2} \\ \vdots \\ He^{-Ah_\ell} \end{bmatrix} \qquad (4)$$

we can now write equation (3) in the form

$$Cx(t) = Z(t) \qquad (4)^*$$

where;

$$z(t) = \begin{bmatrix} y(t-h_1) + He^{-Ah_1}\int_{-h_1}^{o} e^{-As}Bu(t+s)ds \\ y(t-h_2) + He^{-Ah_2}\int_{-h_2}^{o} e^{-As}Bu(t+s)ds \\ \vdots \\ y(t-h_\ell) + He^{-Ah_\ell}\int_{-h_\ell}^{o} e^{-As}Bu(t+s)ds \end{bmatrix}$$

is a known $m\ell x1$ vector and C is an $m\ell xn$ constant matrix depending on the parameters $h_1, h_2, \cdots h_\ell$. If the matrix C has rank n, then equation (4) can be written as:

$$x(t) = \left[C^TC\right]^{-1}C^Tz(t) \qquad (5)$$

where C^T denotes matrix transpose.

Equation (5) has several important implications; First, if the matrix $[C^TC]^{-1}$ exists, then the state x(t) can be exactly reconstructed from the measurement y(t), its delayed values and the input signal u(t), $o \leq t \leq h_\lambda$; secondly, the C matrix depends only on the delays $h_1, \cdots h_\lambda$ so the right hand matrix calculation can be performed completely off line. This leaves only the relatively straight forward calculation of x(t) and a matrix multiplication for on-line microprocessor computation. This latter comment is of particular importance in real time control applications in which relatively low speed microprocessors are utilized for control law implementation. The following result establishes the condition under which the matrix C has rank n.

Result: There exists a set of n delays $o \leq h_1 < h_2 \cdots < h_n \leq a$, for any $a > o$ such that the matrix C has rank n, if and only if rank (Q) = n, where

$$Q = \begin{bmatrix} H \\ HA \\ \vdots \\ HA^{n-1} \end{bmatrix}$$

Proof: Let $a > o$ and assume rank (Q) = n. Then the row vectors of the matrices He^{-Ah} $h \in [o,a]$ contains n independent vectors since, if not, there exists $b \in R^n$ such that $He^{-Ah}b=0$ for all $h \in [o,a]$. Repeated differentation with respect to h gives $He^{-Ah}b=HA^{-Ah}b=HA^{n-1}e^{-Ah}b=0$. This implies that the non zero vector $e^{-Ah}b$ is in the null space of the matrix Q and hence rank $(Q) < n$.

Conversely, assume rank C = n, then rank (Q) = n since, if not, there exists $b \neq o \in R^n$ such that $Hb = HAb = \cdots = HA^{n-1}b = o$. This implies $He^{-Ah}b = o$ for all h and hence rank $C < n$, a contradiction.

Example: Evaluation of the state reconstruction technique given by equation (5) was carried out on an 8080 microprocessor development system which was in turn interfaced with a laboratory servo system as shown in Figure 1. In this example the system state vector is given by $x = \begin{bmatrix} x_1 \\ x_2 \end{bmatrix}$ where x_1 is the motor shaft output position and x_2 is the motor shaft velocity. The measured signal is x_1 and x_2 is reconstructed using equation (5). Once the software was developed and debugged the program was down-loaded to a single board 8085 microprocessor shown in Figure 2, for faster execution.* The block diagram of the servo system without tack feedback is shown in Figure 3.

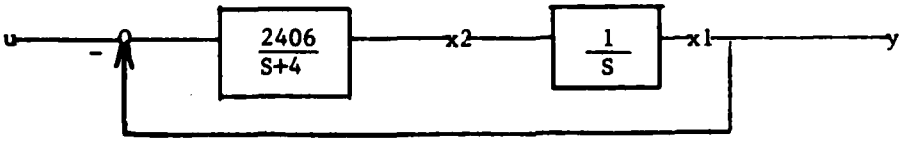

Figure 3

* The 8085 configuration shown in Figure 3 is currently being used to evaluate digital control concepts for the XM97 turret system shown in Figure 21.

The state space equation is given by:

$$\begin{bmatrix}\dot{x}_1\\ \dot{x}_2\end{bmatrix} = \begin{bmatrix}0 & 1\\ -2406 & -4\end{bmatrix}\begin{bmatrix}x_1\\ x_2\end{bmatrix} + \begin{bmatrix}0\\ 2406\end{bmatrix} u \qquad (6)$$

$$y = x_1 = \begin{bmatrix}1,0\end{bmatrix}\begin{bmatrix}x_1\\ x_2\end{bmatrix}$$

The state transition matrix for this system is readily computed to be

$$e^{At} = e^{-2t}\begin{bmatrix}\cos 49t + \frac{2}{49}\sin 49t & \frac{1}{49}\sin 49t\\ -49.1\sin 49t & \cos 49t - \frac{2}{49}\sin 49t\end{bmatrix} \qquad (7)$$

with the associated C matrix of equation (4) being given by:

$$C = \begin{bmatrix}H\\ He^{-Ah}\end{bmatrix} = \begin{bmatrix}1 & 0\\ e^{2h}(\cos 49h - \frac{2}{49}\sin 49h) & \frac{-e^{2h}}{49}\sin 49h\end{bmatrix} \qquad (8)$$

with $h_1 = 0$ and $h_2 = h$.

For values of $h \neq \frac{2n\pi}{49}$, the matrix C is non singular and we may compute $(C^TC)^{-1}C^T = C^{-1}$ directly as

$$C^{-1} = \begin{bmatrix}1 & 0\\ 49\cot(49h) - 2 & -49e^{-2h}\csc 49h\end{bmatrix} \qquad (9)$$

Using equation (5) one obtains the required state reconstruction equation for $x_2(t)$ in terms of the measurements $x_1(t)$, $x_1(t-h)$ and $u(s)$, $k-h \leq s \leq t$.

$$\begin{aligned} x_2(t) = {} & \left[49\cot(49h) - 2\right] x_1(t) - (49e^{-2h}\csc 49h)x_1(t-h)\\ & + 2406\left[e^{2h}\cos 49h - \frac{2e^{2h}\sin 49h}{49}\right]\int_{-h}^{0}\frac{-e^{2s}}{49}(\sin 49s)u(t+s)ds\\ & + 2406\left[\frac{-e^{2h}\sin 49h}{49}\right]\int_{-h}^{0}(e^{2s}\cos 49s + \frac{2e^{2s}}{49}\sin 49s)u(t+s)ds \end{aligned} \qquad (10)$$

The implementation of this state reconstruction algorithm was carried out on an 8080 microprocessor with a delay value $h = .01$ sec. The position output state was sampled at 2.2 milisecond intervals and the accuracy of the A/D and D/A converters was 12 binary bits.

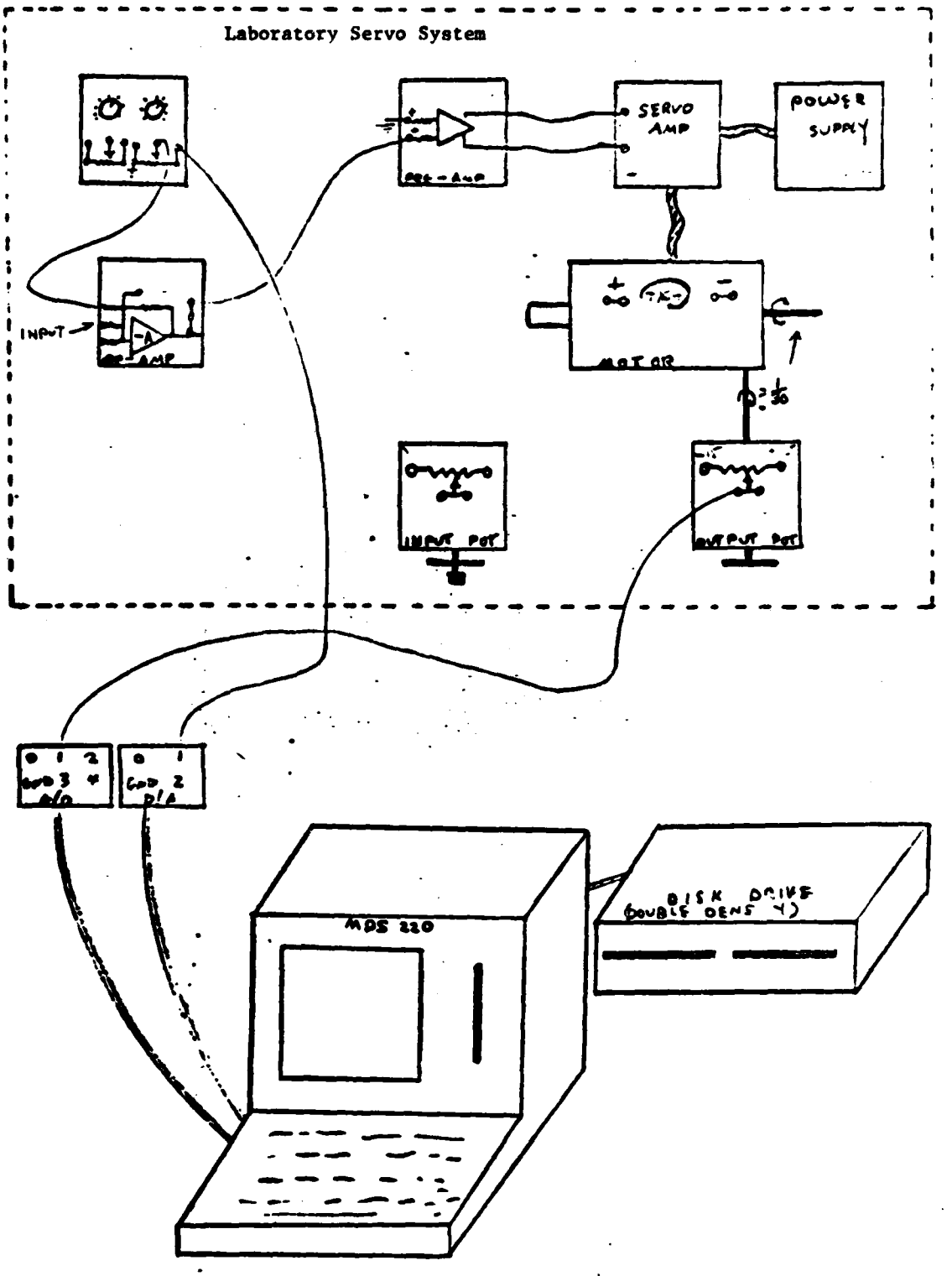
Laboratory Servo System
SERVO AMP
POWER SUPPLY
INPUT
MOTOR
INPUT POT
OUTPUT POT
MDS 220
DISK DRIVE (DOUBLE DENS 4)

Figure 1

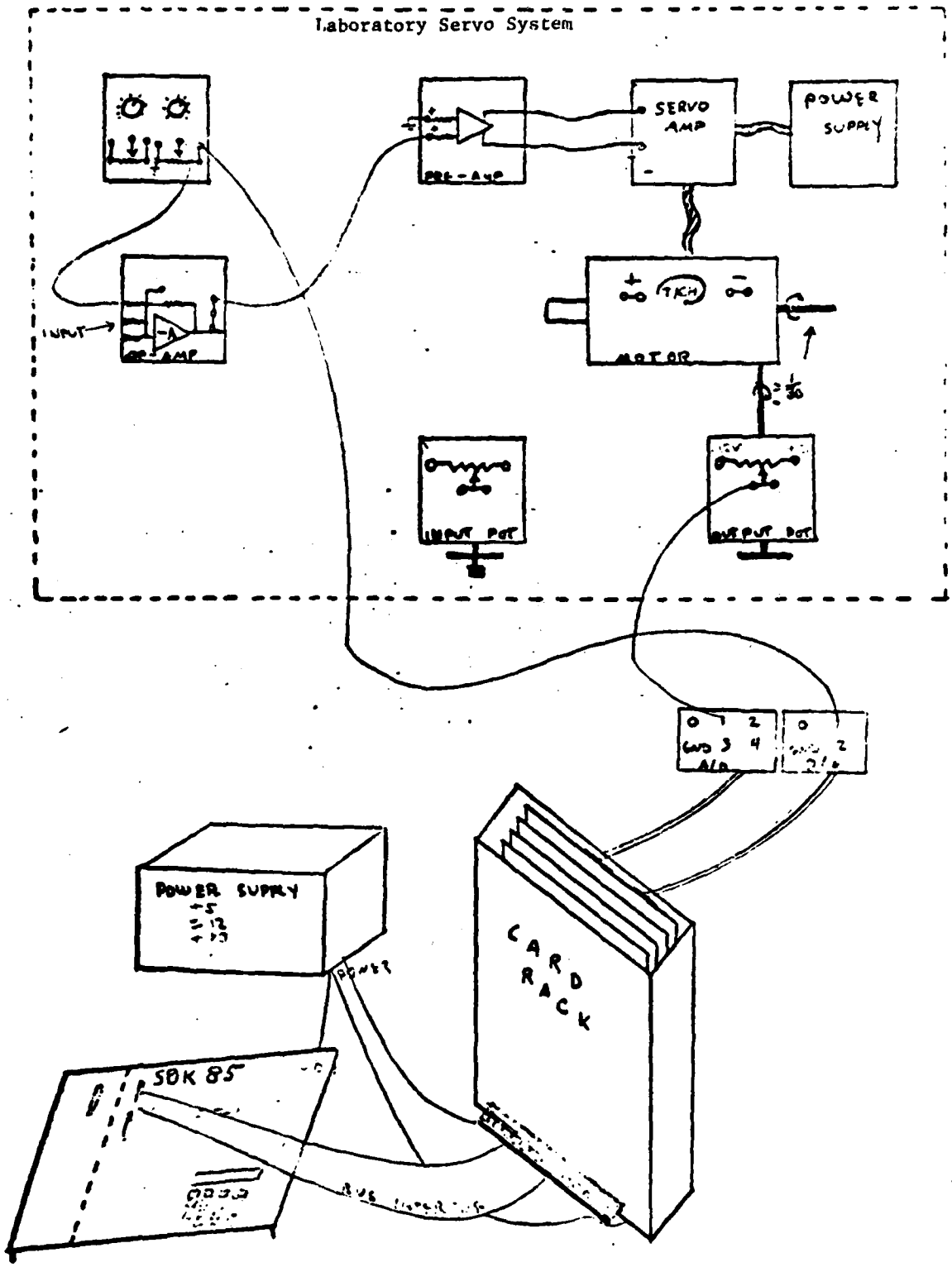
Laboratory Servo System
SERVO AMP
POWER SUPPLY
PRE-AMP
INPUT
MOTOR
INPUT POT
OUTPUT POT
POWER SUPPLY
CARD RACK
SBK 85

Figure 2

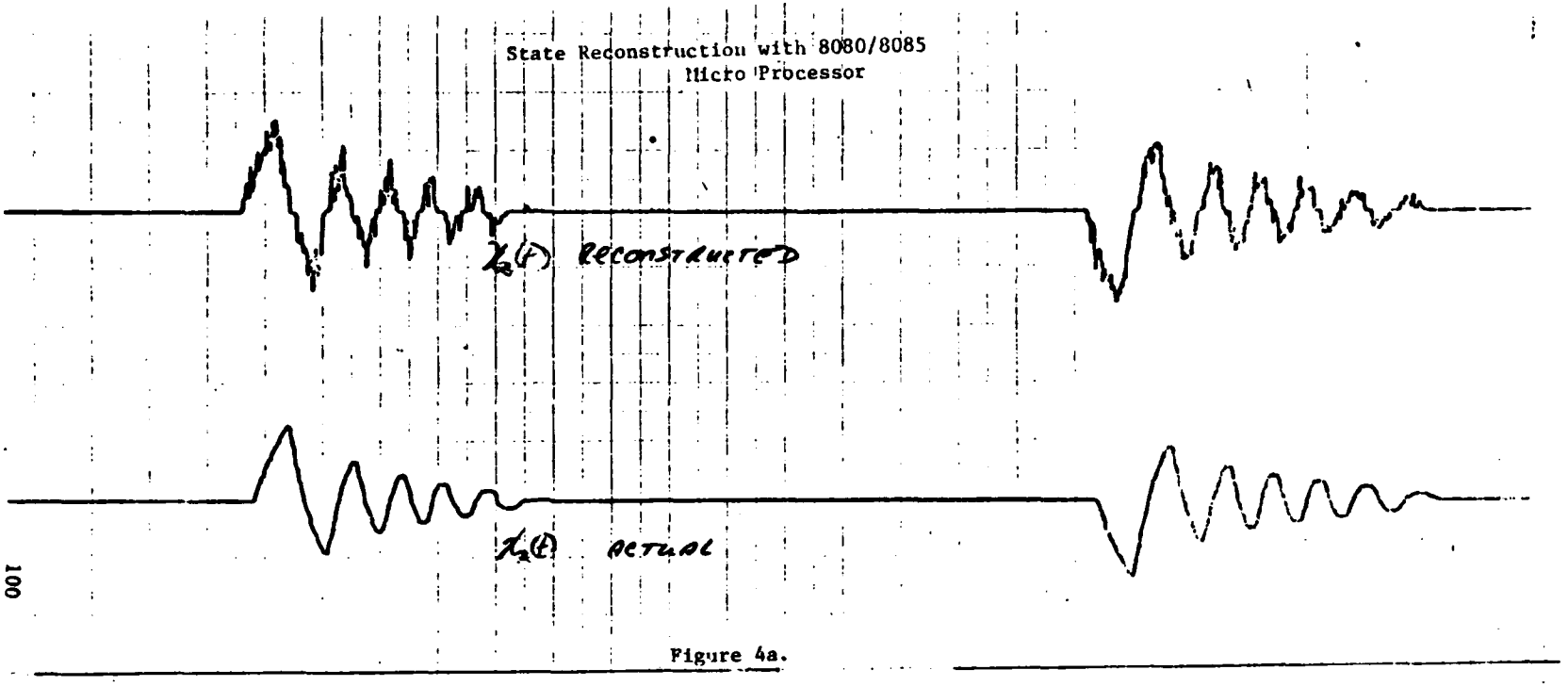

Figure 4a.

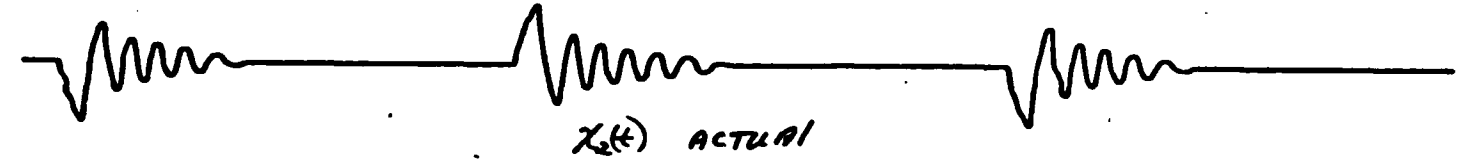

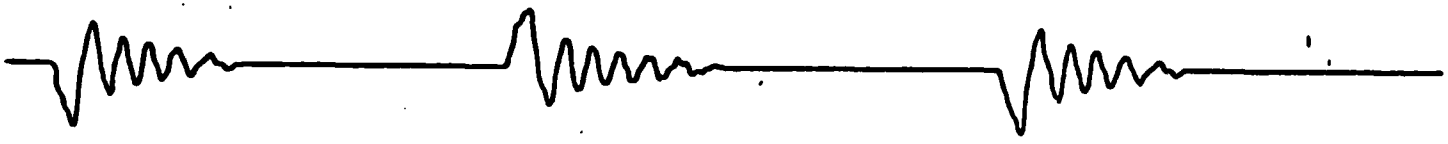

Figure 4b.

Figure 4a compares the actual tach output signal representing the $x_2(t)$ state with the microprocessor output signal which attempts to reconstruct $x_2(t)$ via equation (10) using only the first two terms of this expression. Note: In this case equal weighings must be used for $x_1(t)$ and $x_1(t-h)$. The effects of measurement noise are readily apparent in this figure. Figure 4b again compares measured tach output with the microprocessor output signal, however, in this case the full state reconstruction equation (10) is implemented. This implementation is seen to give a very accurate state reconstruction which is less sensitive to measurement noise.

III. FREQUENCY DOMAIN CONTROL SYNTHESIS USING DELAY FEEDBACK: Several papers, (see Reference (5) and (6)) have appeared in the recent literature which address the problem of feedback control using delays. Reference (6) develops several feedback control laws using delays in the state and derivative of the state which are shown to drive the full state of the system to zero and keep it there. The constructions, however, have limited utility in servo control applications since they assume first that the control space has the same dimenstion as the state and all states of the system are accessible for on-line measurement.

In this section we consider a restricted class of delay feedback controllers shown in Figure 5. This configuration has proved quite useful in turret and servo control applications in which G(s) represents the open loop transfer function between the command input and the position output. The two design parameters introduced by delayed feedback are seen to be K, the feedback gain, and T, the feedback time delay. The reason for chosing the two feedback gains in the form K and K-1 differing by unity in the general case, will be made clear below. The equivalent feedback transfer function, H(s), for the system in Figure is:

$$H(s) = K - (K-1)e^{-Ts} \tag{11}$$

We may represent the e^{-Ts} term by its equivalent Taylor series form as:

$$e^{-Ts} = 1 - Ts + \frac{T^2s^2}{2} - \frac{T^3s^3}{6} + \ldots$$

The frequency band of primary interest from a stability and transient response point of view in $[s: |G(s)H(s)| \geq 1]$ or $[s: s \leq w_c]$ where w_c denotes the gain crossover frequency of the compensated open loop system. Setting $s = jw$ and assumming $|wT| << 1$, we may approximate e^{-Ts} by the first two terms of its Taylor series expansion or;

$$e^{-Ts} = 1 - Ts = 1 - jwT \tag{12}$$

Substituting (12) into equation (11) yeilds;

$$H(s) = K - (K-1)(1-jwT) = 1 + j(K-1)Tw \tag{13}$$

Since $K>1$ will be required, this corresponds to a phase lead network (on a first order approximation basis) in the controller feedback path. If this phase lead term is properly positioned in frequency, it will produce a stabilizing effect upon the control systems unit step or impulse response characteristics. As will be seen in the examples, the time delay or feedback gain can be adjusted

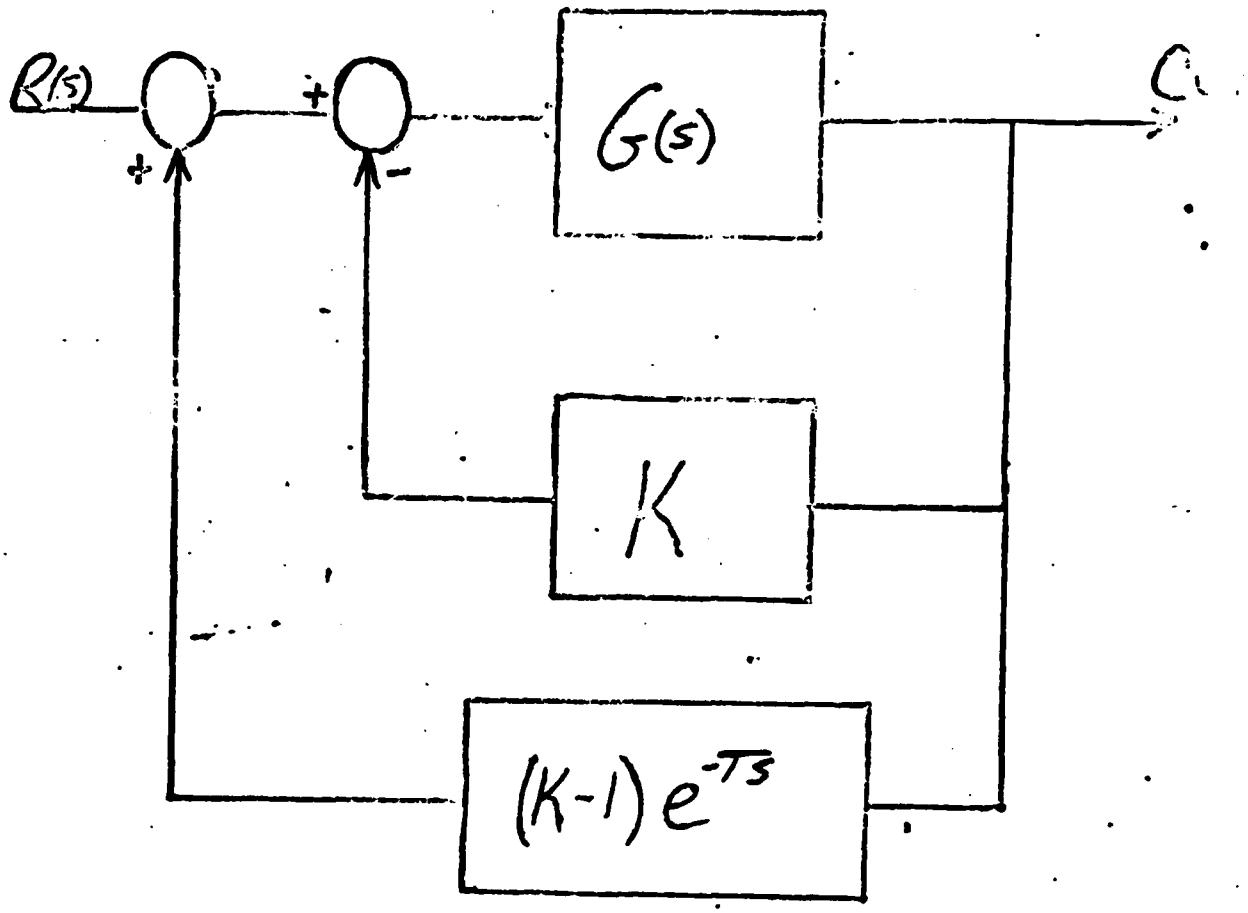

Feedback control with delay

Figure 5

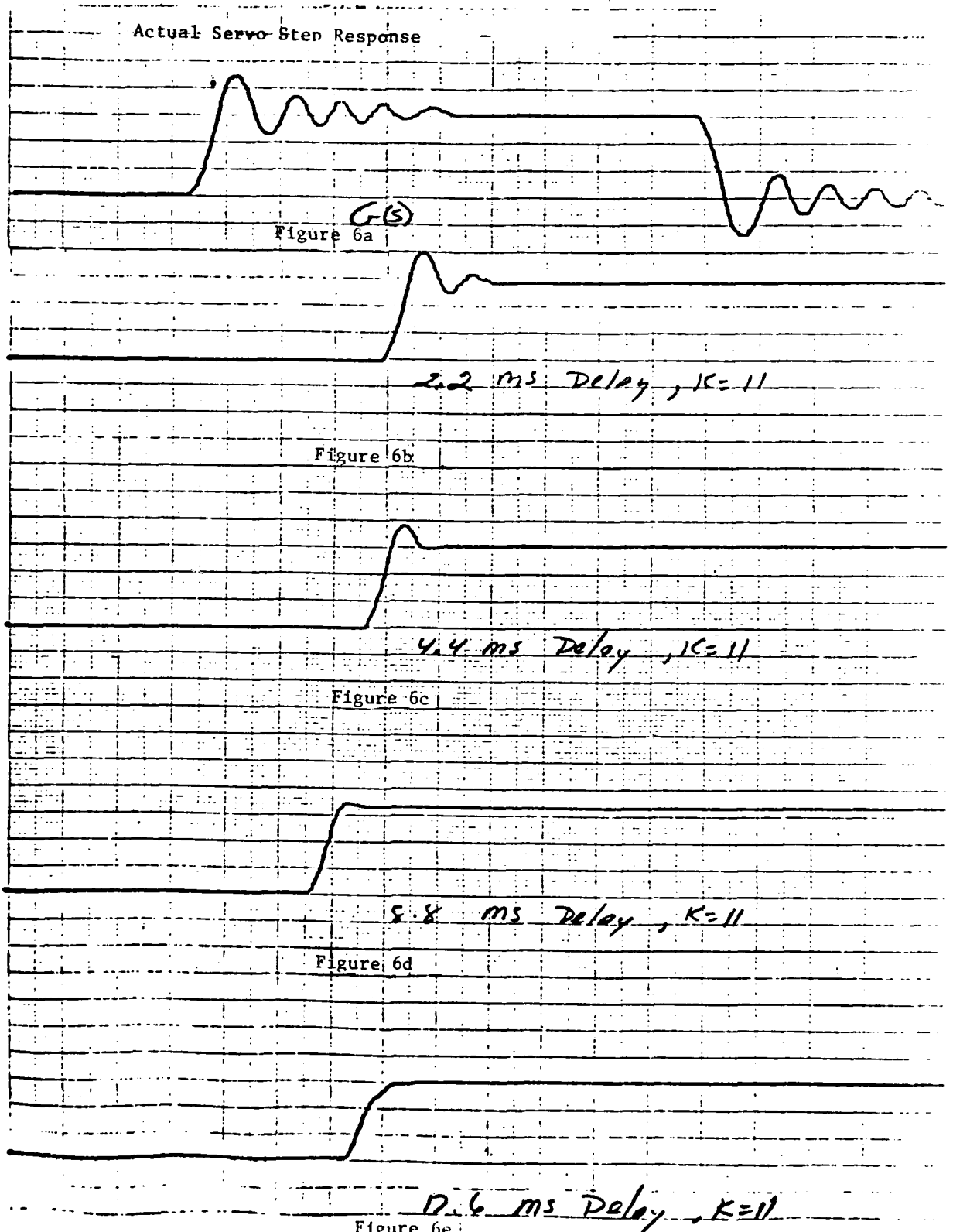

Figure 6a

Figure 6b

Figure 6c

Figure 6d

Figure 6e

to provide any desired damping in the system response. The procedure for introducing a lead network effect around $w = w_c$ using delayed feedback can now be developed.

First, choose w_c such that $\left|G(jw_c)\right| = \frac{1}{\sqrt{2}}$

Second, select the feedback time delay, T, such that $Tw_c << 1$. The choice of $Tw_c = .1$ is reasonable and is used in the examples. For this choice, the first term disregarded in the series expansion has magnitude .005 at w_c and rapidly becomes smaller for higher frequencies. Third, select the feedback gain parameter, K, such that the lead time constant becomes effective at or near $w = w_c$ i.e. $(K-1)T = \frac{1}{w_c}$. Note under this condition using step 1 and equation (8), that;

$$\left|G(w_c)H(w_c)\right| = \left|G(w_c)\right|\left|H(w_c)\right|$$

$$\frac{\sqrt{2}}{\sqrt{2}} = 1 \text{ and } K = 11$$

The delayed feedback design procedure thus is seen to be straight forward in concept. The effect of the particular delayed feedback configuration discussed here is to replace the more standard tach feedback stabilization loop. When the delay time and gain parameters are properly chosen, system response characteristics may be improved substantially.

Example:

We consider first a simple laboratory servo system whose open loop transfer function, G(s), is given by;

$$G(s) = \frac{600}{s(1+\frac{s}{4})} \tag{14}$$

The -3db crossover frequency, w_c, of the open loop transfer function G(s) is 56 rad/sec and the delay time, T, is computed from step 3 and satisfies $10T = \frac{1}{56}$ or T = .0017 sec. The gain K is fixed and satisfies the relation;

$$K - 1 = \frac{1}{Tw_c} = \frac{1}{.1} = 10$$

Due to limitations of the 8080 microprocessor, the above design using a delay of 1.7 ms could not be implemented. The smallest delay which could be implemented with the 8080 was 2.2 ms. The performance of this design for a step input command is shown in Figure 6b. Figure 6 illustrates that the effective damping introduced by the feedback delay can be further increased by increasing the delay parameter T. The desired damping can also be achieved by adjusting the gain parameter K.

To evaluate the effects of delay parameters which were too small for implementation on an 8080 microprocessor, simulations were run for values of T = .8 msec, 1.7 msec, 2.2 msec, 4.4 msec, 8.8 msec and 17.6 msec, using the servo transfer function (14). These results are shown in Figures 7 - 12. Deficiencies in the linear model of the servo system are readily apparent since the simulations indicate more damping than is evident in the test results of Figure 6 and Figure 12

indicates an instability with the 17.6 msec delay in constrant to the over damped response in the hardware test shown in Figure 6e.

Example:

In this example we illustrate the application of the delay feedback control synthesis technique to the design of a controller for an XM97 helicopter turret control system shown in Figure 13. The transfer function block diagram of this system is shown in Figure 14. The -3db crossover frequency for the open loop system (tach loop open) was computed to be 20 rad/sec resulting in a feedback time delay of .005 sec. The step response of the original XM97 design is shown in Figure 15 and that of the delay feedback design in Figure 16. The latter design exhibits a dramatic improvement with respect to overshoot and settling time. This improvement can be explained partially by the fact that the original system uses motor tachometer feedback for stabilization while the delay feedback design effectively uses actual turret position and rate for feedback stabilization. Figures 17 - 22 also show the effects of increasing and decreasing the delay feedback parameter. Saturation, columb friction and deadband non-linearities are included in the simulation.

IV. CONCLUSION: Applications of delay feedback for state construction and feedback control are presented together with simulation results and examples of actual implementations using Intel 8080 and 8085 microprocessors. These examples demonstrate the practicality of the ideas and suggest that these techniques may provide a useful adjunct to the more standard frequency domain and state variable techniques for estimation and control applications.

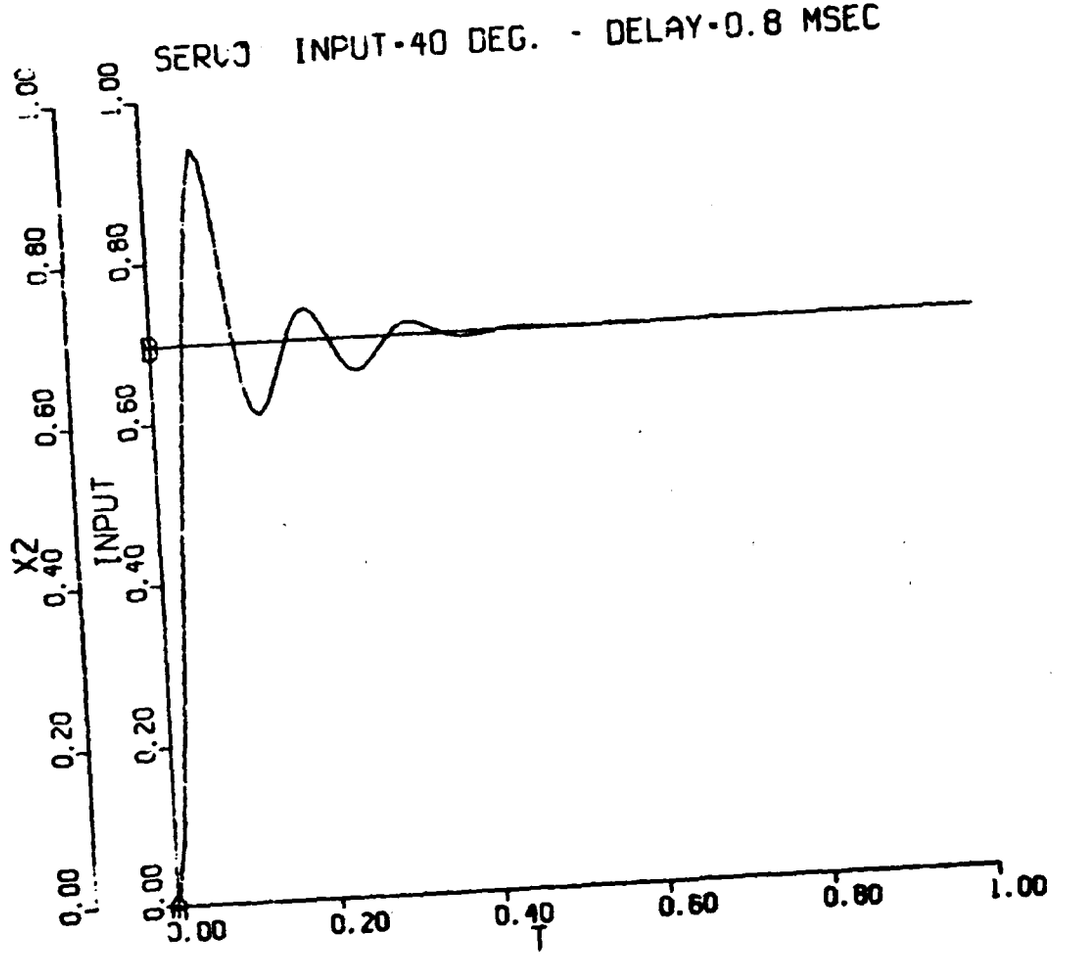
SERVO INPUT-40 DEG. - DELAY-0.8 MSEC
X2
INPUT
T
0.00
0.20
0.40
0.60
0.80
1.00

Figure 7

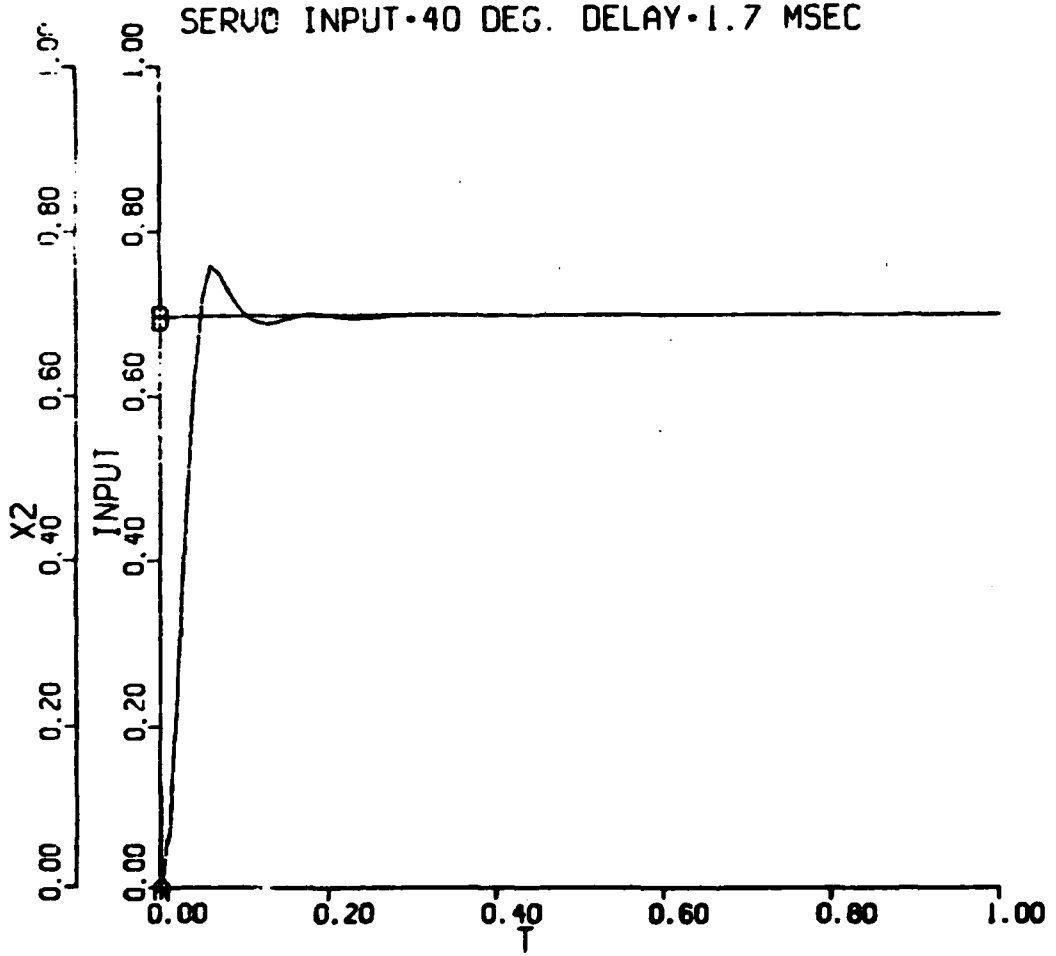
SERVO INPUT•40 DEG. DELAY•1.7 MSEC
X2
INPUT
0.00
0.20
0.40
0.60
0.80
1.00
T

Figure 8

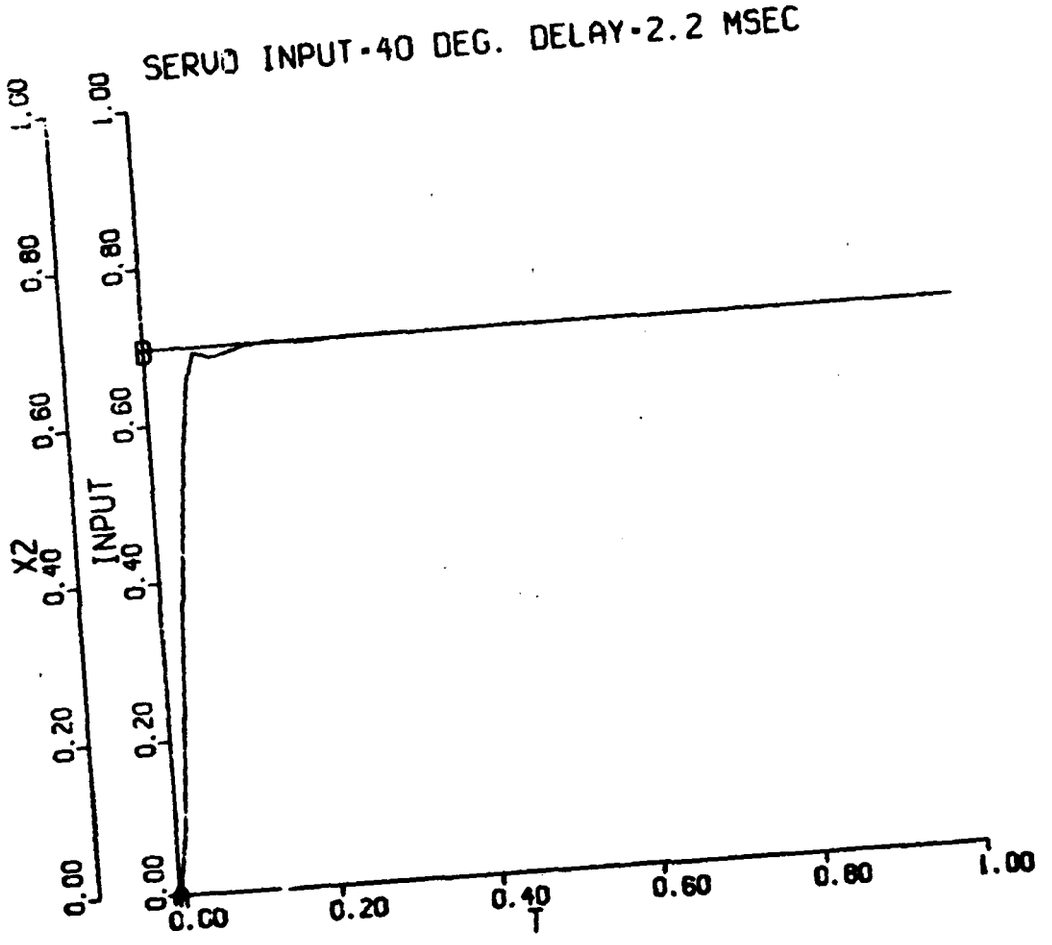
SERVO INPUT-40 DEG. DELAY-2.2 MSEC
X2
INPUT
T
0.00
0.20
0.40
0.60
0.80
1.00

Figure 9

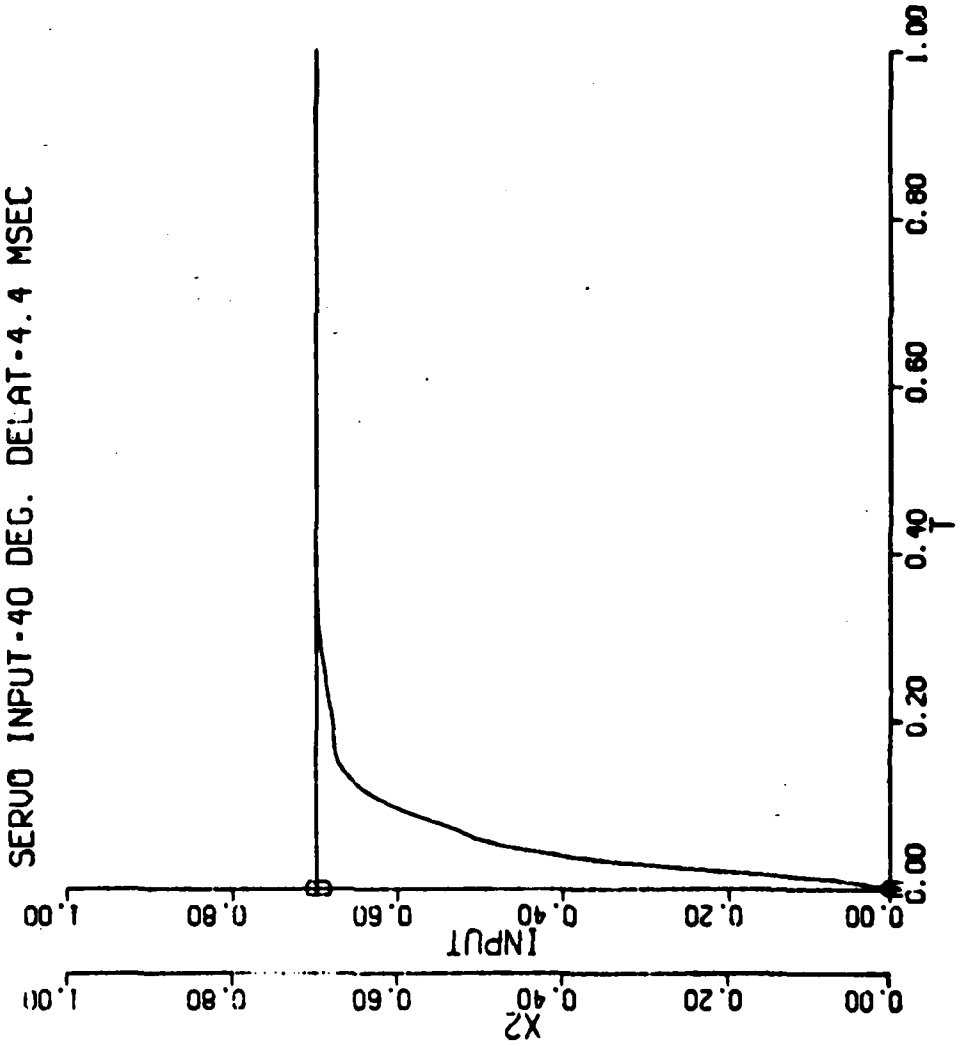
SERVO INPUT-40 DEG. DELAT-4.4 MSEC
INPUT
T
X2
0.00
0.20
0.40
0.60
0.80
1.00

Figure 10

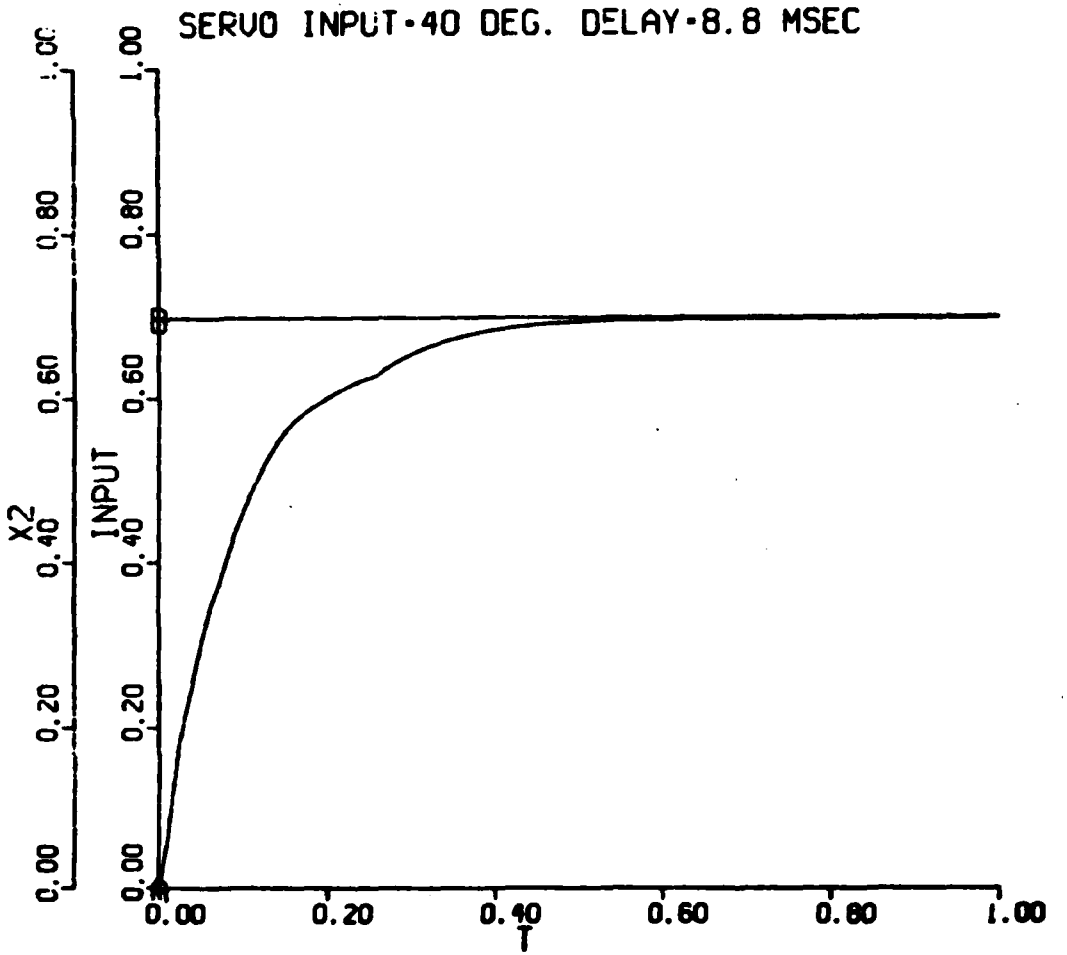
SERVO INPUT·40 DEG. DELAY·8.8 MSEC
X2
INPUT
0.00
0.20
0.40
0.60
0.80
1.00
T

Figure 11

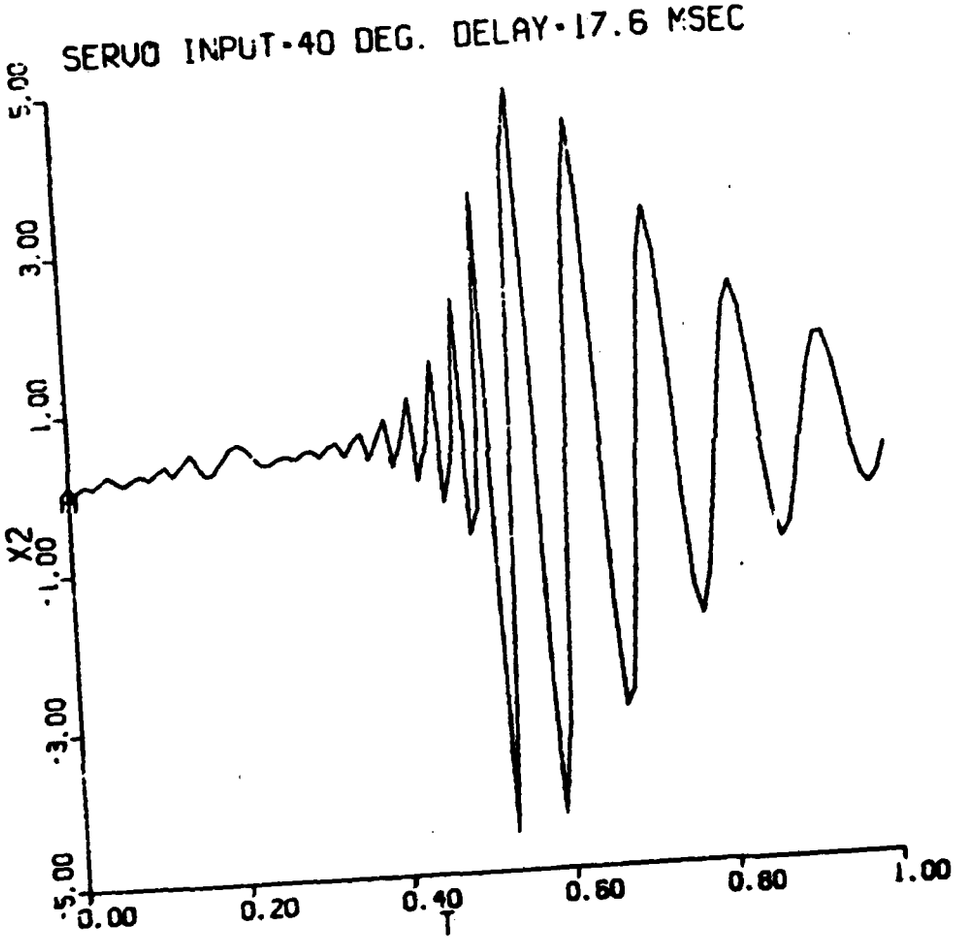
SERVO INPUT-40 DEG. DELAY-17.6 MSEC
5.00
3.00
1.00
-1.00
-3.00
-5.00
X2
0.00
0.20
0.40
0.60
0.80
1.00
T

Figure 12

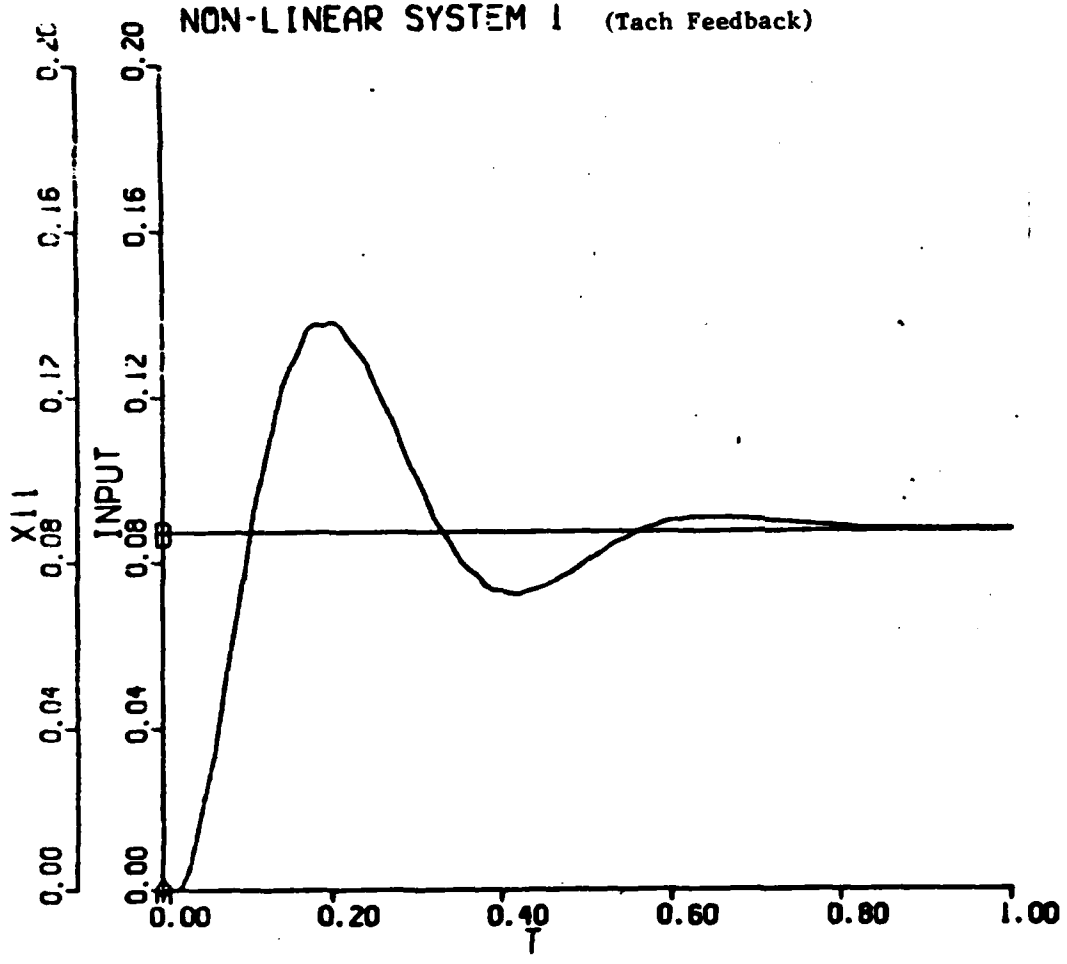
NON-LINEAR SYSTEM 1 (Tach Feedback)
X11
INPUT
0.00
0.04
0.08
0.12
0.16
0.20
0.00
0.20
0.40
0.60
0.80
1.00
T

Figure 15

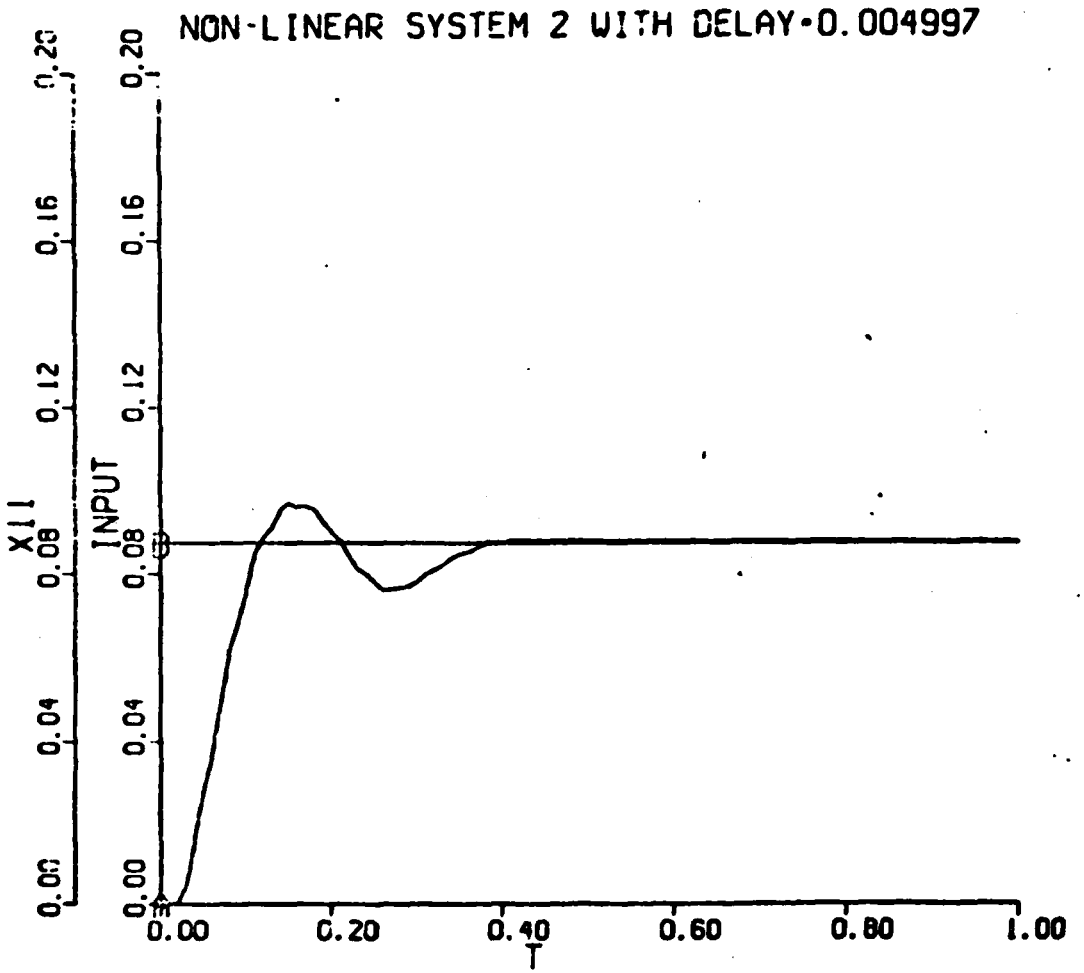
NON-LINEAR SYSTEM 2 WITH DELAY=0.004997
X11
INPUT
0.00
0.04
0.08
0.12
0.16
0.20
0.00
0.20
0.40
0.60
0.80
1.00
T

Figure 16

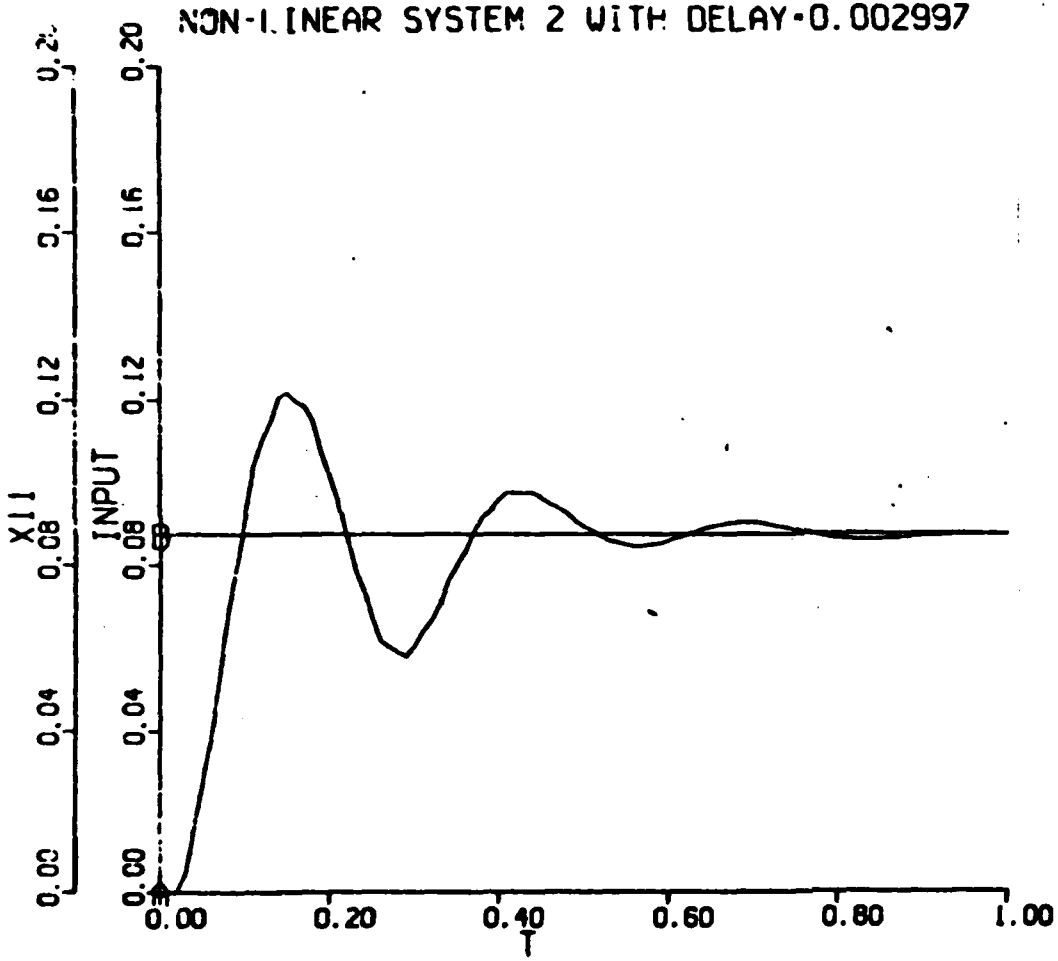
NON-LINEAR SYSTEM 2 WITH DELAY=0.002997
X11
INPUT
0.00
0.04
0.08
0.12
0.16
0.20
0.00
0.20
0.40
0.60
0.80
1.00
T

Figure 17

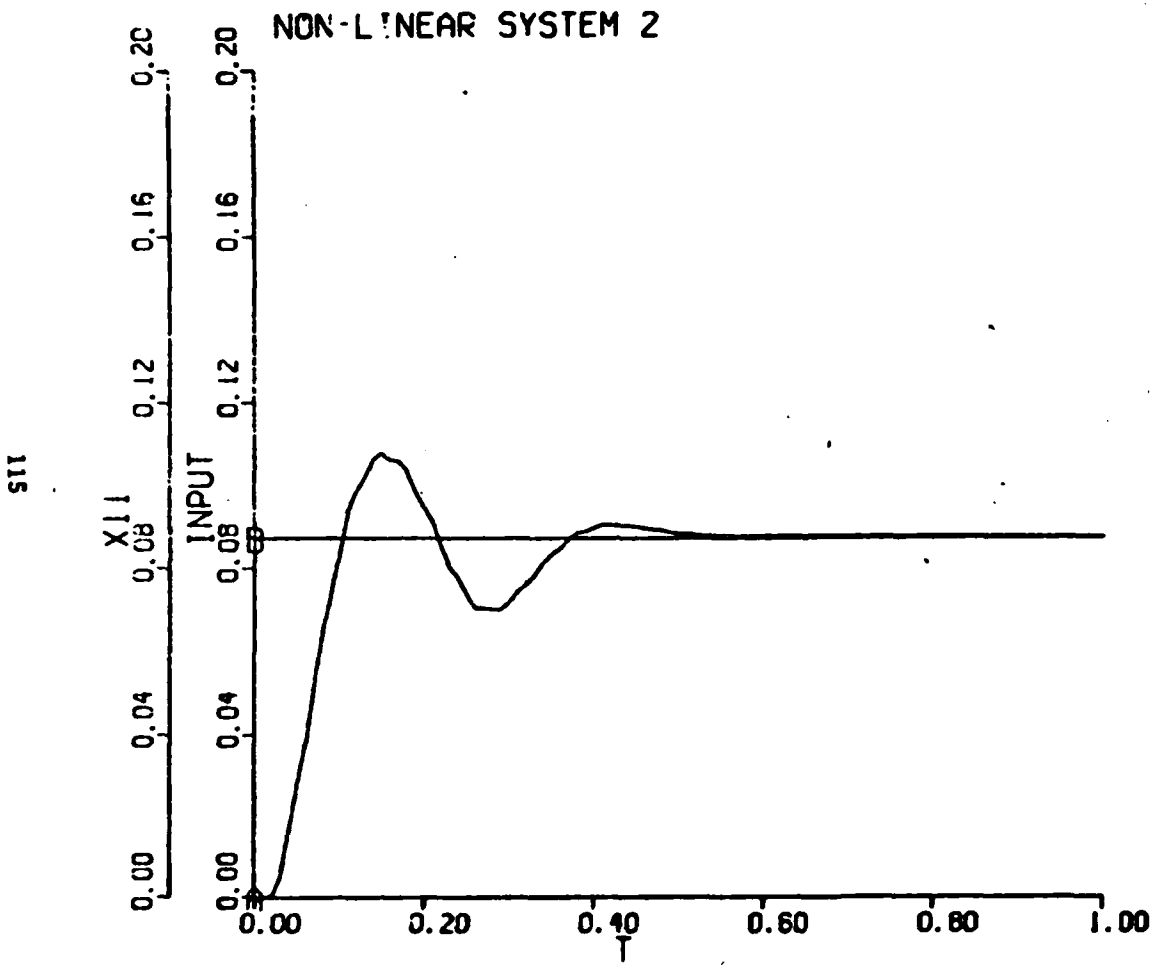
NON-LINEAR SYSTEM 2
X11
INPUT
T
0.00
0.04
0.08
0.12
0.16
0.20
0.00
0.20
0.40
0.60
0.80
1.00

Figure 18

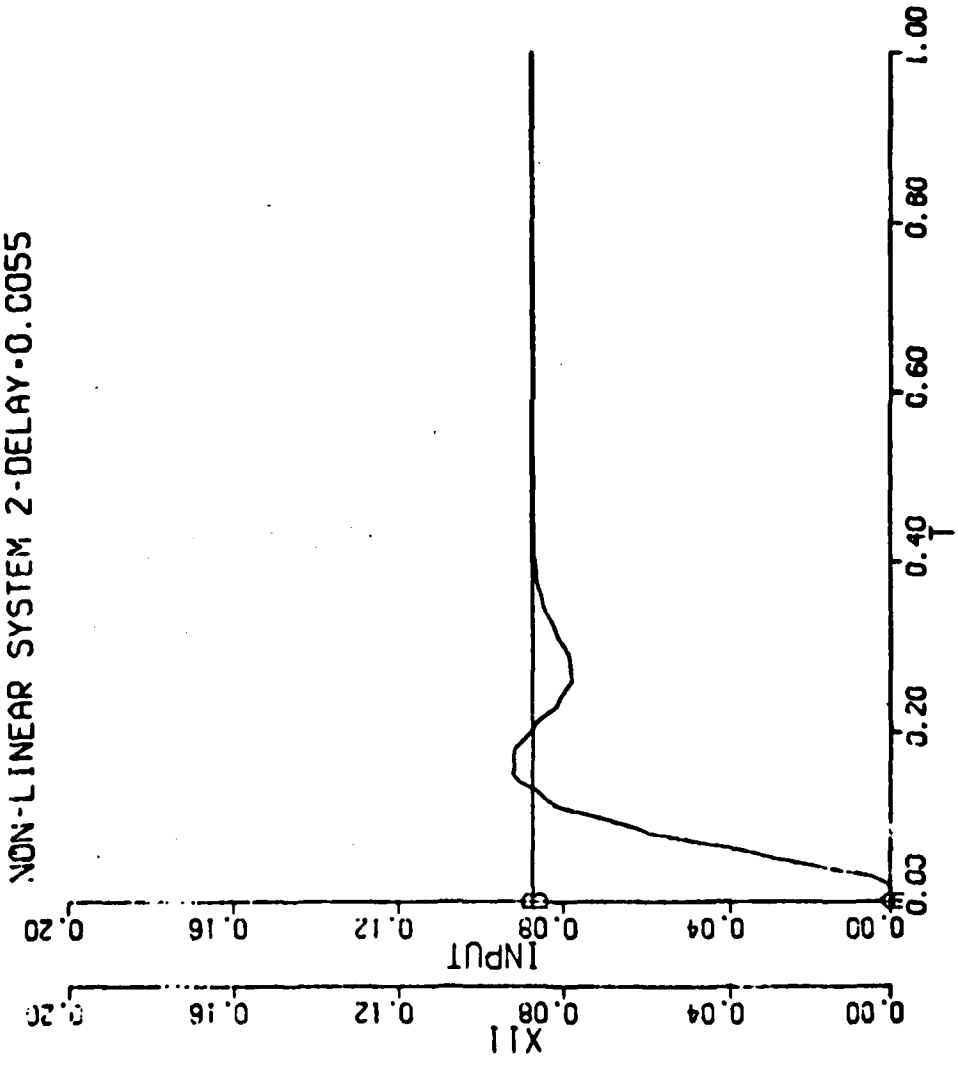
NON-LINEAR SYSTEM 2-DELAY-0.0055
INPUT
X11
T
0.00
0.04
0.08
0.12
0.16
0.20
0.00
0.20
0.40
0.60
0.80
1.00

Figure 19

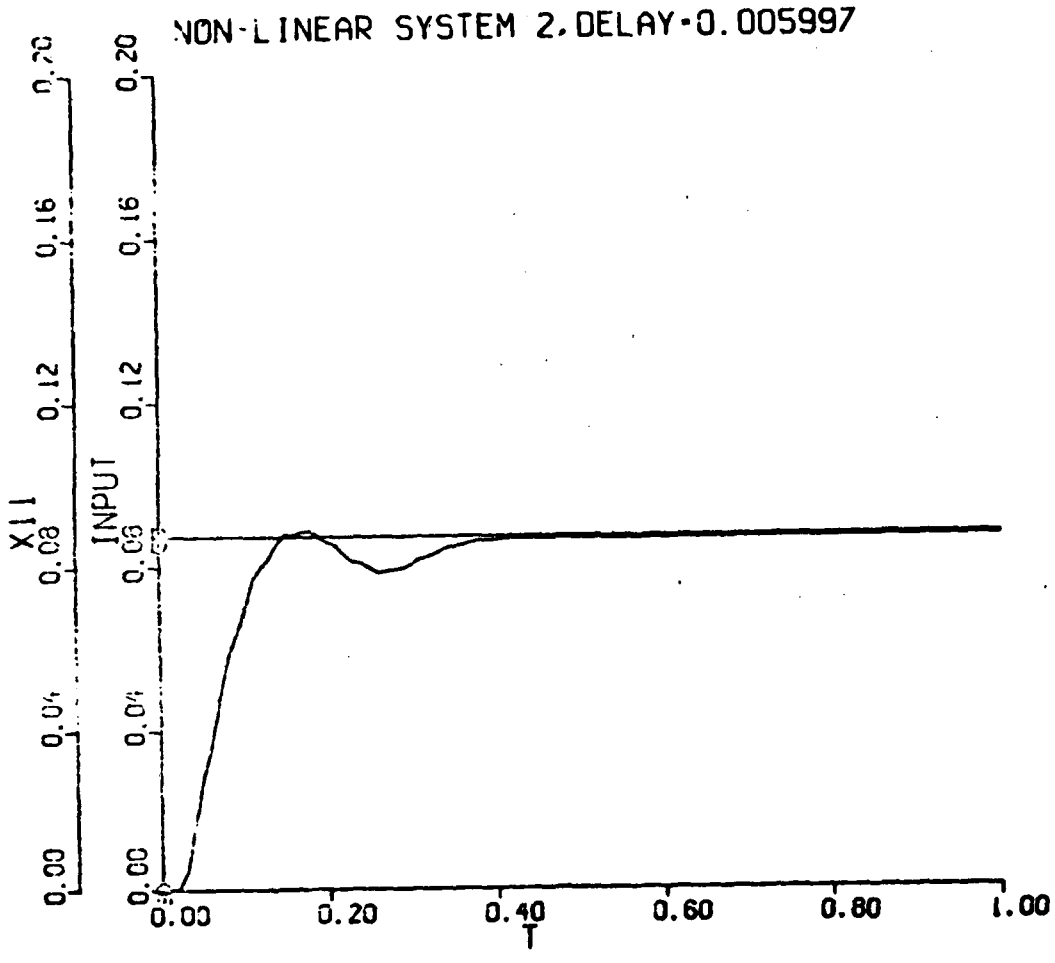
NON-LINEAR SYSTEM 2. DELAY=0.005997
X11
INPUT
0.00
0.04
0.08
0.12
0.16
0.20
0.00
0.20
0.40
0.60
0.80
1.00
T

Figure 20

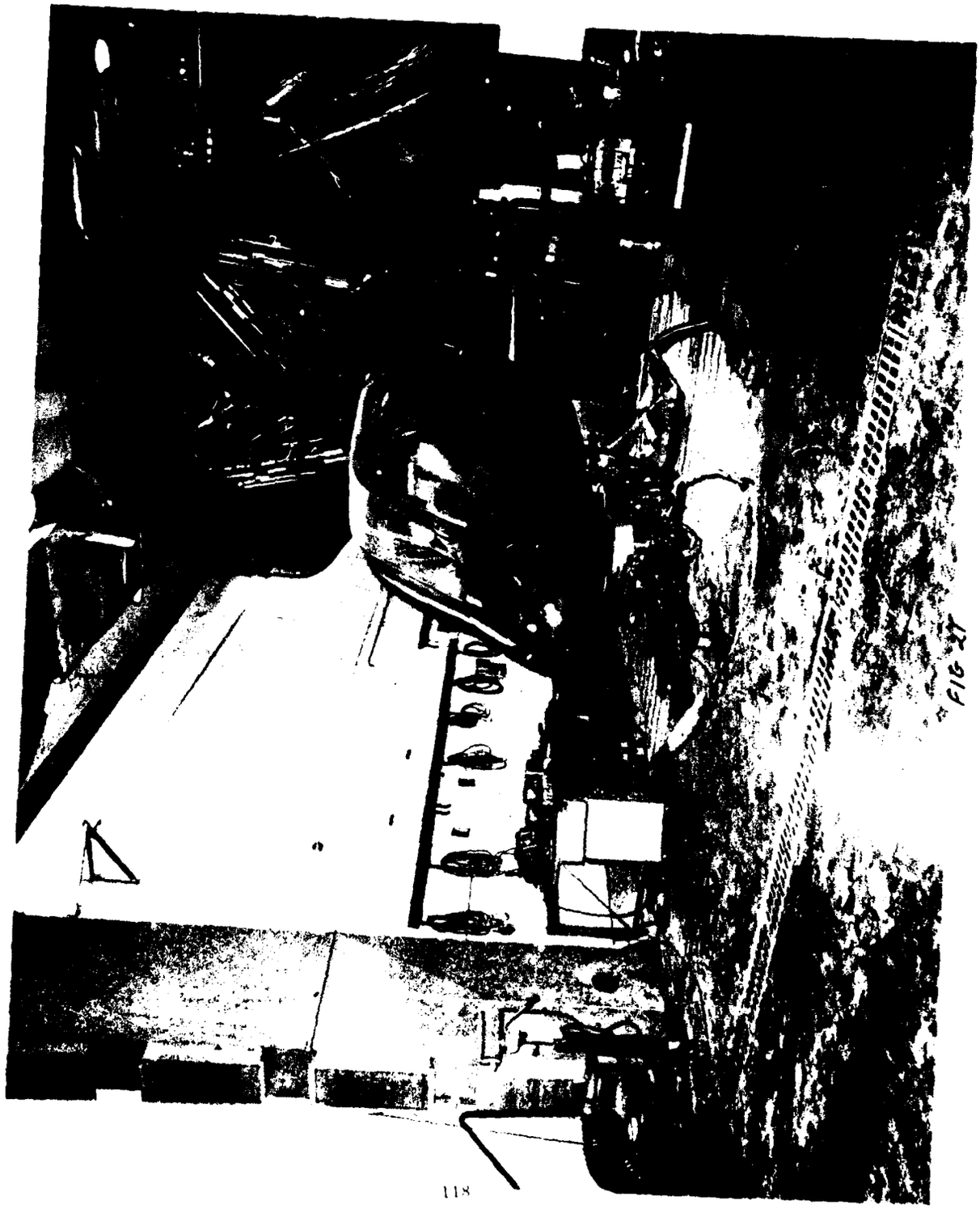

FIG 27

References

1. D. H. Chyung, "On A Method For Reconstructing Inaccessible State Variables Using Time Delays." Unpublished Paper.

2. N. K. Loh & D. H. Chyung, "State Reconstruction From Delayed Observations." Proceedings Of The Fifth Annual Pittsburg Conference On Modeling & Simulation, Volume 5, April 1974.

3. D. G. Luenberger, "An Introduction To Observers." IEEE Trans. Automat. Contr., Volume AC-16, No. 6, December 1971.

4. J. D. Gilchrist, "N-Observability For Linear Systems." IEEE Trans. Automat. Contr., Volume AC-11, No. 3, July 1966.

5. A. Thowsen, "On Pointwise Degeneracy, Controllability & Minimal Time Control Of Linear Dynamical Systems With Delays." Int. J. Control, Volume 25, No. 3, 1977.

6. B. Asner & A. Halanay, "Indirect Delay-Feedback Control Of Linear Systems." Proc. Of 14th Allerton Conference.

7. A. Thowsen, "Function Space Null Controllability By Augmented Delay Feedback Control." IEEE Trans. Automat. Contr., April 1976.

8. V. M. Popov, "Delay-Feedback, Time-Optimal, Linear Time-Invariant Control Systems." Ordinary Differential Equations, L. Weiss, Ed. New York; Academic 1972.

Next page is blank.

DISTRIBUTION LIST

NO. OF COPIES	ORGANIZATION
12	Commander Defense Technical Information Center ATTN: TCA Cameron Station Alexandria, VA 22314
1	Commander US Army Materiel Development & Readiness Command ATTN: DRCCP DRCPA-S DRCDE-R DRCDE-D DRCBSI-L DRCBSI-D 5001 Eisenhower Avenue Alexandria, VA 22333
2	Commander US Army Armament Research & Development Command ATTN: DRDAR-SEA Technical Library
1	ATTN: DRDAR-SCF-DD (W. J. Dzwiak)
1	DRDAR-SCF-CC (Doo J. Lee)
1	DRDAR-SCF-CC (J. Schmitz)
1	DRDAR-SEA (Richard Moore) Dover, NJ 07801
1	Commander Rock Island Arsenal ATTN: Tech Lib Rock Island, IL 61299
1	Commander Harry Diamond Laboratories ATTN: DELHD-SAB 2800 Powder Mill Road Adelphi, MD 20783
1	Commander US Army Test & Evaluation Command ATTN: STEDP-MT-L Dugway Proving Ground, UT 84222

NO. OF COPIES	ORGANIZATION
1	Commander US Army Aviation R&D Command ATTN: DRDAV-BC PO Box 209 St Louis, MO 63166
1	Commander US Army Electronics R&D Command ATTN: DRDEL-SA Fort Monmouth, NJ 07703
1	Commander US Army Electronics R&D Command ATTN: DRDEL-AP-OA 2800 Powder Mill Road Adelphi, MD 20783
2	Director US Army TRADOC Systems Analysis Activity ATTN: ATAA-SL ATAA-T White Sands Missile Range, NM 88002
1	Commander US Army Missile Command ATTN: DRSMI-C (R&D)
1	DRSMI-RGN (Dr. H. L. Pastrick)
1	DRSMI-RGN (Dr. W. C. Kelly)
1	Redstone Arsenal, AL 35809
1	Commander US Army Troop Support & Aviation Materiel Readiness Command ATTN: DRSTS-BA 4300 Goodfellow Blvd St Louis, MO 63120
1	Commander US Army Tank-Automotive Research and Development Command ATTN: DRDTA-UL (Tech Lib) DRDTA-V Warren, MI 48990

NO. OF COPIES	ORGANIZATION
1	Commander US Army Mobility Equipment R&D Command ATTN: DRDME-O Fort Belvoir, VA 22060
1	Commander US Army Natick R&D Command ATTN: DRDNA-O Natick, MA 01760
2	Chief Defense Logistics Studies Information Exchange US Army Logistics Management Center ATTN: DRXMC-D Fort Lee, VA 23801
1	Commander US Army Concepts Analysis Agency 8120 Woodmont Avenue Bethesda, MD 20014
1	Reliability Analysis Center ATTN: Mr. I. L. Krulac Griffiss AFB, NY 13441
	Aberdeen Proving Ground
2	Cdr, USATECOM ATTN: DRSTE DRSTE-CS-A Bldg 314
	Dir, BRL, Bldg 328
	Dir, BRL ATTN: DRDAR-TSB-S (STINFO Branch) Bldg 305
1	Dir, HEL, Bldg 520 ATTN: DRXHE-AM (Seymour Steinberg)
1	Dir. AMSAA ATTN: DRXSY-G (John Kramar)
1	DRXSY-GA (Richard M. Norman)
1	DRXSY-C (Keith Myers)
1	DRXSY-CS (James Brown)
1	DRXSY-CS (Harold H. Burke)

NO. OF COPIES	ORGANIZATION
	Dir, AMSAA (cont'd)
1	ATTN: DRXSY-CS (Toney Perkins)
1	DRXSY-A (Daniel O'Neill)
1	DRXSY-AD (Jack Meredith)
1	DRXSY-AD (John Foulkes)
1	DRXSY-AD (Denise Phillips)
1	DRXSY-AS (Joseph Wald)
1	DRXSY-AA (Gary Drake)
1	DRXSY-AA (William J. Nicholson, Jr)
1	DRXSY-MP (Herbert Cohen)